Wind Power Variability, Its Cost, and Effect on Power Plant Emissions

A Dissertation
Submitted in partial fulfillment of the requirements for the degree of

Doctor of Philosophy

Warren Katzenstein
July 2010

Advisor
Jay Apt

Thesis Committee:
Jay Apt
Lester B. Lave
M. Granger Morgan
Gregory Reed
Allen Robinson

Carnegie Mellon University
Department of Engineering and Public Policy
Pittsburgh, Pennsylvania 15213 USA

Abstract

The recent growth in wind power is transforming the operation of electricity systems by introducing variability into utilities' generator assets. System operators are not experienced in utilizing significant sources of variable power to meet their loads and have struggled at times to keep their systems stable. As a result, system operators are learning in real-time how to incorporate wind power and its variability. This thesis is meant to help system operators have a better understanding of wind power variability and its implications for their electricity system.

Characterizing Wind Power Variability

We present the first frequency-dependent analyses of the geographic smoothing of wind power's variability, analyzing the interconnected measured output of 20 wind plants in Texas. Reductions in variability occur at frequencies corresponding to times shorter than ~24 hours and are quantified by measuring the departure from a Kolmogorov spectrum. At a frequency of 2.8×10^{-4} Hz (corresponding to 1 hour), an 87% reduction of the variability of a single wind plant is obtained by interconnecting 4 wind plants. Interconnecting the remaining 16 wind plants produces only an additional 8% reduction. We use step-change analyses and correlation coefficients to compare our results with previous studies, finding that wind power ramps up faster than it ramps down for each of the step change intervals analyzed and that correlation between the power output of wind plants 200 km away is half that of co-located wind plants. To examine variability at very low frequencies, we estimate yearly wind energy production in the Great Plains region of the United States from automated wind observations at airports covering 36 years. The estimated wind power has significant inter-annual variability and the severity of wind drought years is estimated to be about half that observed nationally for hydroelectric power.

Estimating the Cost of Wind Power Variability

We develop a metric to quantify the sub-hourly variability cost of individual wind plants and show its use in valuing reductions in wind power variability. Our method partitions wind energy into hourly and sub-hourly components and uses corresponding market prices to determine the cost of variability. The metric is applicable to variability at all time scales faster than hourly, and can be applied to long-period forecast errors. We use publically available data at 15 minute time resolution to apply the method to ERCOT, the largest wind power production region in the United States. The range of variability costs arising from 15 minute to 1 hour variations (termed load following) for 20 wind plants in ERCOT was \$6.79 to 11.5 per MWh (mean of \$8.73 ±\$1.26 per MWh) in 2008 and \$3.16 to 5.12 per MWh (mean of \$3.90 ±\$0.52 per MWh) in 2009. Load following variability costs decrease as wind plant capacity factors increase, indicating wind plants sited in locations with good wind resources cost a system less to integrate. Twenty interconnected wind plants have a variability cost of \$4.35 per MWh in 2008. The marginal benefit of interconnecting another wind plant diminishes rapidly: it is less than \$3.43 per MWh for systems with 2 wind plants already interconnected, less than \$0.7 per MWh for 4-7 wind plants, and less than \$0.2 per MWh for 8 or more wind plants. This method can be used to value the installation of storage and other techniques to mitigate wind variability.

Estimating How Wind Power Variability Affects Power Plant Emissions

Renewables portfolio standards (RPS) encourage large scale deployment of wind and solar electric power, whose power output varies rapidly even when several sites are added together. In many locations, natural gas generators are the lowest cost resource available to compensate for this variability, and must ramp up and down quickly to keep the grid stable, affecting their emissions of NO_x and CO_2. We model a wind or solar photovoltaic plus gas system using measured 1-minute time resolved emissions and heat rate data from two types of natural

gas generators, and power data from four wind plants and one solar plant. Over a wide range of renewable penetration, we find CO_2 emissions achieve ~80% of the emissions reductions expected if the power fluctuations caused no additional emissions. Pairing multiple turbines with a wind plant achieves ~77 to 95% of the emissions reductions expected. Using steam injection, gas generators achieve only 30-50% of expected NO_x emissions reductions, and with dry control NO_x emissions increase substantially. We quantify the interaction between state RPSs and constraints such as the NO_x Clean Air Interstate Rule (CAIR), finding that states with substantial RPSs could see upward pressure on CAIR NO_x permit prices, if the gas turbines we modeled are representative of the plants used to mitigate wind and solar power variability.

Acknowledgements

I would like to thank the Alfred P. Sloan Foundation, the Electric Power Research Institute, the US National Science Foundation (under NSF Cooperative Agreement No. SES-0345798), the Doris Duke Charitable Foundation, the Department of Energy National Energy Technology Laboratory, the Heinz Endowments, the Pennsylvania Technology Assistance Alliance, and the RenewElec program and Electricity Industry Center at Carnegie Mellon University for supporting this work.

I could not have accomplished the research contained within this thesis without the guidance and support of my advisor Jay Apt or my thesis committee of Lester Lave, Granger Morgan, Gregory Reed, and Allen Robinson.

I would also like to thank Brett Bissinger, Jack Ellis, Emily Fertig, Elisabeth Gilmore, Lee Gresham, Eric Hittinger, Lester B. Lave, Ralph Masiello, Hannes Pfeifenberger, Steve Rose, Mitchell Small, Kathleen Spees, Samuel Tanenbaum, Rahul Walawalkar for their helpful discussions and guidance. I am grateful to Tom Hansen of Tucson Electric Power for supplying the solar PV data, the Electricity Reliability Council of Texas (ERCOT) for their publicly available wind data, and the companies that supplied the wind and gas generator data, who wish to remain anonymous. I would also like to express my gratitude for the help and support Patti Steranchak, Patty Porter, Victoria Finney, Barbara Bugosh, and the rest of EPP's administrative staff have given me.

Finally, I would like to thank my parents William and Patricia Katzenstein for their never-ending support and love, my brothers Aaron and Wesley, my sister Julie, and good friends Andres Del Campo, Ben Nahir, Shelby Suckow, Ryan and Kym Hallahan, Lee Gresham, and Brett Bissinger for their moral support.

Table of Contents

List of Figures

List of Tables

Chapter 1 - Introduction

1.1 Overview and Motivation

The recent growth in wind power is transforming the operation of electricity systems by introducing variability into utilities' generator assets. Due to a lack of cost-effective storage solutions, utilities must continually produce the amount of electricity consumed by their customers. Utilities have traditionally relied on dispatchable generators[1] to serve their customers' ever changing demand for electricity. Wind plants, on the other hand, are not dispatchable assets and system operators are currently learning how to incorporate significant quantities of wind energy.

Wind was one of the first power sources harnessed by civilizations. The earliest known sailing vessels date back to 4000 BC and the earliest known windmills (to pump water or grind grain) date back to 2000 BC (Anderson, 2003; Hinrichs and Kleinbach, 2002). Windmills became prevalent throughout civilized societies numbering over 8,000 in Holland and 10,000 in England in 1750. In the United States, rural farmers used them extensively to pump water for their crops, grind flour, and later provide electricity for their farms. Yet windmills were made obsolete with the development of the steam engine and the Rural Electrification Act of 1936 (Hinrichs and Kleinbach, 2002).

The modern era of wind power started with the oil embargo of 1973 and the subsequent energy crisis. It was during the high fuel prices of the 1970s that the United States and Europe were suddenly aware of their dependence on foreign fuel supplies and they began efforts for energy independence. The United States and Europe immediately responded by pouring tens of millions of

[1] Generators such as fossil-fuel, nuclear, or hydro power plants that system operators can dispatch to provide a certain amount of power at a certain amount of time.

dollars into the research and development of wind turbines to generate electricity (Righter, 1996). Hindsight has shown the governments' R&D effort was not a primary driver of innovation and that federal subsidies were a better mechanism to spur innovation in wind turbine design (Samaras, 2006).

The United States needed to do more than just fund R&D if wind power was going to have a chance. During the late 1970s, the Carter administration realized electric utilities in the United States would not pursue renewable energy projects even if mature technology existed (Graves et al., 2006). As a result, the United States enacted the Public Utilities Regulatory Policies Act of 1978 (PURPA)[2] to encourage the development and deployment of cogeneration and green energy technologies. PURPA enabled third parties to develop and operate power plants but restricted the types of power plants to small (<80 MW) renewable energy and cogeneration projects. Today, approximately 83% of the wind projects developed between 1980 and 2008 are owned by third party power producers (Wiser and Bolinger, 2009). PURPA, thus, was a significant policy act that was vital to the future build out of wind power.

Yet even with the R&D efforts and the implementation of PURPA, wind power was still in its infancy during the 1970s and 1980s because it was not cost-competitive with conventional dispatchable generators. The United States realized wind power needed subsidies to encourage large-scale deployment. This was first observed in the early 1980s when the United States shifted its focus from funding wind turbine R&D to providing wind power subsidies. Approximately 1.5 GW of wind power was installed between 1980 and 1985 as a result (figure 1-1). The early federal subsidies were allowed to expire as soon as the price of oil fell substantially in 1986 (Hinrichs and Kleinbach, 2002). Federal subsidies for wind power were absent until 1994 when Congress

[2] It was also designed to increase the efficiency of our electricity use.

implemented the Production Tax Credit (PTC). The PTC was a sizable subsidy and as seen in figure 1-1, the wind power industry in the United States was dependent on the PTC. The US wind power industry grew significantly when the PTC was in effect and much more slowly when the PTC expired briefly in 2000, 2002, and 2004. Thus, the PTC was the final piece the US wind industry needed to spur the modern increase in wind power in the United States.

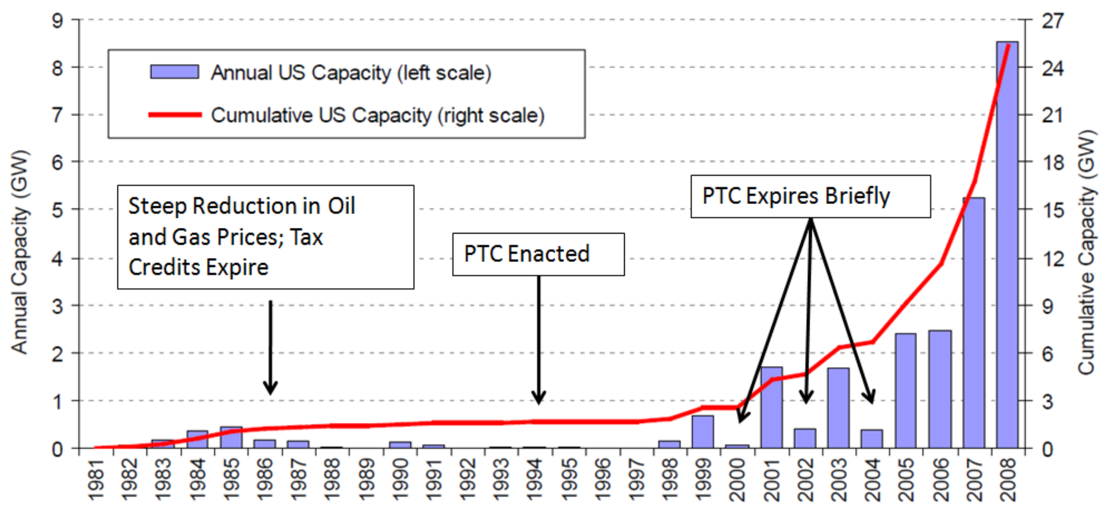

Figure 1-1 - Recent development of wind power in the United States (Wiser and Bolinger, 2009)

As a result of the PTC and PURPA, wind grew at an average rate of 28% from 1998 to 2008 (EIA, 2009). Wind power penetration, in terms of energy, has gone from << 1% in 1997 to ~2% in 2009 in the United States (Wiser and Bolinger, 2009). The individual states in wind rich regions have higher penetration rates. Lawrence Berkeley Laboratory estimates 15 states have wind energy penetration rates > 2% with Iowa (13.3%), Minnesota (10.4%), and South Dakota (8.8%) as the three states with the highest penetration levels (Wiser and Bolinger, 2009). Aggressive renewables portfolio standards (RPS) enacted by 29 states and new federal and state subsidies are helping ensure wind power maintains its aggressive growth for the next decade.

System operators are not experienced in utilizing significant quantities of variable power to meet their loads. As a result, system operators have struggled at times to keep their systems stable. The Electricity Reliability Council of Texas (ERCOT), for example, worked hard to keep their system stable when it lost ~1.7 GW of wind power over a 4 hour period on February 26, 2008. The sudden die-off of wind adversely coupled with an unanticipated rise in ERCOT's load and forced ERCOT to implement their Emergency Electric Curtailment Plant (EECP) to curtail 1200 MW of interruptible load (ERCOT, 2008)[3]. In another example, the wind in Bonneville Power Authority's (BPA) territory unexpectedly calmed for 12 days in January 2009 (BPA, 2009). As a result, BPA lost 1 GW of wind power for a week and a half and was forced to use its hydro reserves in wind's place.

System operators are learning in real-time how to incorporate wind power and its variability. This thesis is meant to help system operators have a better understanding of wind power variability and its implications for their electricity system. In Chapter 2, I present methods to characterize large penetrations of wind power and measure reductions in wind power variability as wind plants are interconnected in ERCOT. In Chapter 3, I present methods to estimate the cost of wind power variability and value reductions in wind power variability. Finally, in Chapter 4, I estimate what effect wind variability has on the emissions of fossil fuel generators and what implications this has for emissions displacement calculations.

1.2 References

Anderson, R.C., 2003. A Short History of the Sailing Ship. Courier Dover, Mineola.

BPA, 2009. Integrating Wind Power and Other Renewable Resources into the Electricity Grid. Bonneville Power Authority, September. Available: http://www.bpa.gov/corporate/windpower/docs/Wind-WIT_generic_slide_set_Sep_2009_customer.pdf

[3] During the ERCOT incident 150 MW of conventional generation tripped offline and was a contributing factor although a minor one compared to the loss of 1.7 GW of wind power and the addition of 4 GW of load.

EIA, 2009. Annual Energy Review – Table 8.2a Electricity Net Generation: Total (All Sectors), 1949-2008. US Energy Information Agency. Available: http://www.eia.doe.gov/emeu/aer/txt/stb0802a.xls

ERCOT, 2008. ERCOT Operations Report on the EECP Event of February 26, 2008. Electricity Reliability Council of Texas. Available: http://www.ercot.com/meetings/ros/keydocs/2008/0313/07._ERCOT_OPERATIONS_REPORT_EECP022608_public.doc

Graves, F., Hanser, P., Basheda, G., 2006. PURPA: Making the Sequel Better than the Original. Edison Electric Institute. Available: http://www.eei.org/whatwedo/PublicPolicyAdvocacy/StateRegulation/Documents/purpa.pdf

Hinrichs, R., Kleinback, M., 2002. Energy: Its Use and the Environment. Harcourt, Orlando.

Righter, R., 1996. Wind Energy in America: A History. University of Oklahoma Press, Norman.

Samaras, C., 2006. Learning from Wind: A Framework for Effective Low-Carbon Energy Diffusion. Carnegie Mellon Electricity Industry Center, Working Paper CEIC-06-05. Available: http://wpweb2.tepper.cmu.edu/ceic/publications.htm

Wiser, R., Bolinger, M., 2009. 2008 Wind Technologies Market Report. Energy Efficiency and Renewable Energy, US Department of Energy. Available: http://eetd.lbl.gov/ea/emp/reports/2008-wind-technologies.pdf

Chapter 2 - The Variability of Interconnected Wind Plants

2.1 Chapter Information

Authors: Warren Katzenstein, Emily Fertig, and Jay Apt

Published: Aug 2010 in *Energy Policy*.

Citation: Katzenstein, W., Fertig, E., Apt, J., 2010. The Variability of Interconnected Wind Plants. *Energy Policy*, 38(8), p.4400-4410.

2.2 Abstract

We present the first frequency-dependent analyses of the geographic smoothing of wind power's variability, analyzing the interconnected measured output of 20 wind plants in Texas. Reductions in variability occur at frequencies corresponding to times shorter than ~24 hours and are quantified by measuring the departure from a Kolmogorov spectrum. At a frequency of 2.8×10^{-4} Hz (corresponding to 1 hour), an 87% reduction of the variability of a single wind plant is obtained by interconnecting 4 wind plants. Interconnecting the remaining 16 wind plants produces only an additional 8% reduction. We use step-change analyses and correlation coefficients to compare our results with previous studies, finding that wind power ramps up faster than it ramps down for each of the step change intervals analyzed and that correlation between the power output of wind plants 200 km away is half that of co-located wind plants. To examine variability at very low frequencies, we estimate yearly wind energy production in the Great Plains region of the United States from automated wind observations at airports covering 36 years. The estimated wind power has significant inter-annual variability and the severity of wind drought years is estimated to be about half that observed nationally for hydroelectric power.

2.3 Introduction

Currently 29 of the United States of America have renewables portfolio standards (RPS) that mandate increasing their percentage of renewable energy, and the US House of Representatives has enacted a federal renewable electricity standard (Database of State Incentives for Renewables and Efficiency, 2009; Waxman and Markey, 2009). Major electricity markets such as California, New York, and Texas expect wind to play a large role in meeting their RPS. As a result of the state RPS requirements and a federal production tax credit equivalent to a carbon dioxide price of approximately $20/metric ton (Dobesova et al., 2005), wind power net generation is currently experiencing very high growth rates (51% in 2008, 28% average annual growth rate over the past decade) in the United States (EIA, 2009).

Wind power's variability and fast growth rate have led areas including Cal-ISO, PJM, NY-ISO, MISO, and Bonneville power to undertake wind integration studies to assess whether their systems can accommodate significant (5-20%) penetrations of wind power (CAISO, 2007; DOE, 2008; EnerNex, 2009; GE, 2008; Hirst, 2002). Included in each integration study is how wind power variability can be mitigated with options such as storage, demand response, or fast-ramping gas plants. Some system operators are beginning to charge wind operators for costs arising from the integration of high wind penetration in their system. In 2009, the Bonneville Power Authority (BPA) introduced a wind integration charge of $1.29 per kW per month (~0.6¢/kWh assuming a 30% capacity factor), citing reliability risks and substantial costs encountered in fulfilling 7% of their energy needs with wind power (BPA, 2009).

Previous studies have shown that interconnecting wind plants with transmission lines reduces the variability of their summed output power as the number of installed wind plants and the distance between wind plants increases (Archer and Jacobson, 2007; Czisch and Ernst, 2001;

Giebel, 2000; IEA, 2005; Kahn, 1979; Milligan and Porter, 2005; Wan, 2001). Kahn (1979) estimates the increased reliability of spatially separated wind plants, writing that "wind generators can displace conventional capacity with the reliability that has been traditional in power systems." Kahn (1979) calculates the loss of load probability (LOLP) and the effective load carrying capability (ELCC) of up to 13 interconnected California wind plants.

Czisch and Ernst (2001) and Giebel (2000), in separate studies, show the correlation between wind plants decreases with distance. Each concludes wind power variability is reduced by summing the output power from spatially separated wind plants. Czisch and Ernst (2001) and Giebel (2000) both find that wind plant outputs are correlated even over great distances (correlation coefficient > 0).

Milborrow (2001) shows a smoothing effect by calculating the output power change over a certain time interval (step-change) of wind plants. He finds the one-hour power swing of 1,860 MW of wind power in Western Denmark over a three month period in 2001 was at most 18% of installed capacity compared with 100% for a single wind plant. In contrast, Bonneville Power Authority in the U.S. Pacific Northwest experienced a maximum one-hour step-change of 63% in 2008 for their 1,670 MW of wind power.

Archer and Jacobsen (2007) write that interconnected wind plants would produce "steady deliverable power." Using hourly and daily averaged wind speed measurements taken at 19 airports located in Texas, New Mexico, Oklahoma, and Kansas, they estimate generation duration curves and operational statistics of wind power arrays. They find that "an average of 33% and a maximum of 47% of yearly averaged wind power from interconnected plants can be used as reliable, baseload electric power" (Archer and Jacobson, 2007).

The previous studies analyze wind's variability primarily in the time domain, using metrics such as 10-minute step-change histograms, correlation coefficients and LOLP.

Frequency domain analysis is a powerful complementary method that can be used to characterize variability and evaluate whether and at what frequencies smoothing occurs as more wind plants are introduced into a system. We use Fourier transform techniques to estimate the power spectral density of wind generated power (PSD) (Apt, 2007; Cha and Molinder, 2006; Press et al., 1992) and characterize the variability of actual wind plant output within ERCOT, the electricity market serving most of Texas. We also use step-change analyses and correlation coefficients to characterize the variability of ERCOT wind plants and wind plants modeled from wind monitoring stations located throughout the Midwest and Great Plains and compare our results with previous studies.

To characterize the year-to-year variations of wind power production, we calculate the yearly output of wind power by modeling wind plants over a span of 36 years. We examine the existence and likely severity of wind drought years as compared to hydroelectric power reduction by rainfall droughts.

2.4 Data

We use both ERCOT wind plant power output data and National Oceanic and Atmospheric Administration (NOAA) wind speed data for our analyses. We use 15-minute time resolution real power output data from 20 wind plants within ERCOT (figure 2-1)[4]. The ERCOT data were obtained from ERCOT's website and contained no dropouts. If necessary, data from each wind plant are scaled to the end-of-the-year capacity of the wind plant to adjust for mid-year capacity additions.

[4] Electric Reliability Council of Texas (2009) Entity-Specific Resource Output. Retrieved Feb. 18, 2009 from ERCOT's Planning and Market Reports. Available: http://www.ercot.com/gridinfo/sysplan/

We use 2008 wind power data from Bonneville Power Authority to examine whether results similar to our ERCOT results are seen in another system. BPA provides 5-minute system wind power data on its website[5]. There were 0.04% of the data missing from BPA's 2008 wind data set.

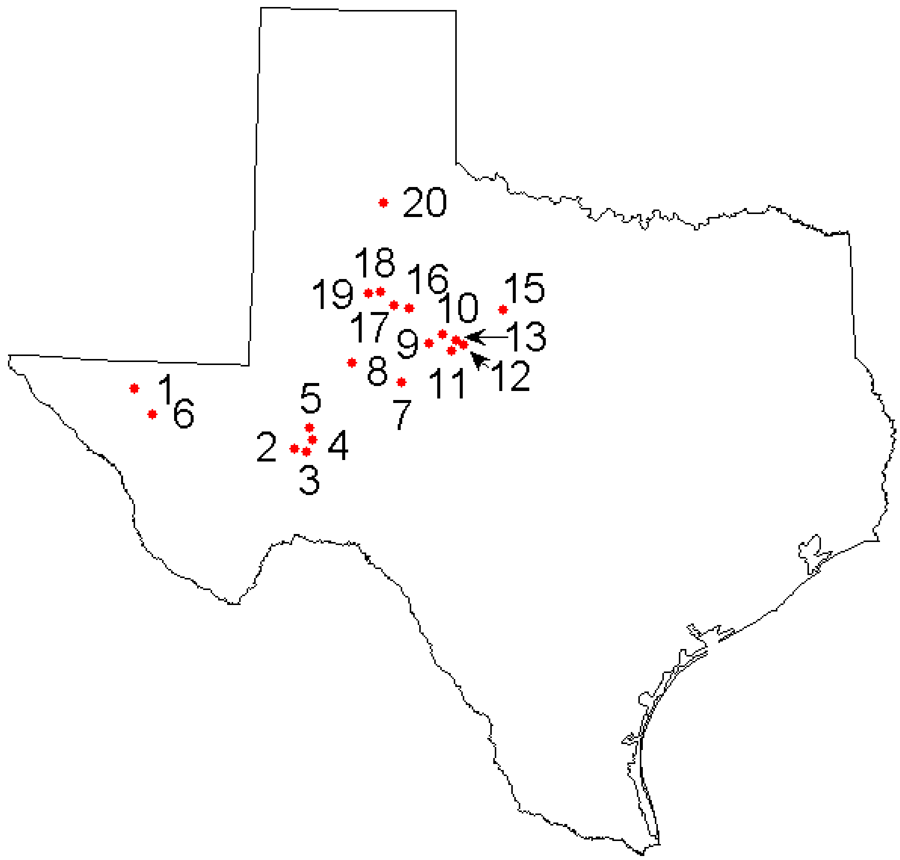

Figure 2-1 - Locations of the ERCOT wind plants from which data were obtained.

When examined in the frequency domain, ERCOT's data exhibit the Kolmogorov spectrum of wind plants as found by Apt (2007). The Nyquist frequency, the highest frequency the data can represent without aliasing, is 5.6 x 10^{-4} Hz (corresponding to 30 minutes) for ERCOT's 15-minute wind power output data.

---

[5] Bonneville Power Authority wind generation in balancing authority. Retrieved May 6, 2009. Available at http://www.transmission.bpa.gov/business/operations/wind/

We use NOAA ASOS two-minute resolution wind speed data to estimate the effect of interconnecting up to 40 wind plants throughout 7 states located in the Midwest, Southwest, and Great Plains regions[6]. ASOS is a joint project among NOAA, the Department of Defense, the Federal Aviation Administration, and the US Navy with ~ 1000 stations that automatically record surface weather conditions (NOAA et al., 1998). We selected 40 stations to represent the high wind energy locations of the Great Plains region where wind plants are currently being developed; Archer and Jacobson (2007) analyzed a subset of this region. Each minute, ASOS stations record wind speed and direction averaged over the previous two minutes to the neared nautical mile per hour. Table 2-1 in appendix A lists the 40 ASOS sites we use and figure 2-2 plots their location. The average distance between the 40 ASOS sites we use is 785 km and the median distance is 725 km.

[6] See table 2-1 in the Appendix for a list of specific sites. Data are available at ftp://ftp.ncdc.noaa.gov/pub/data/asos-onemin/

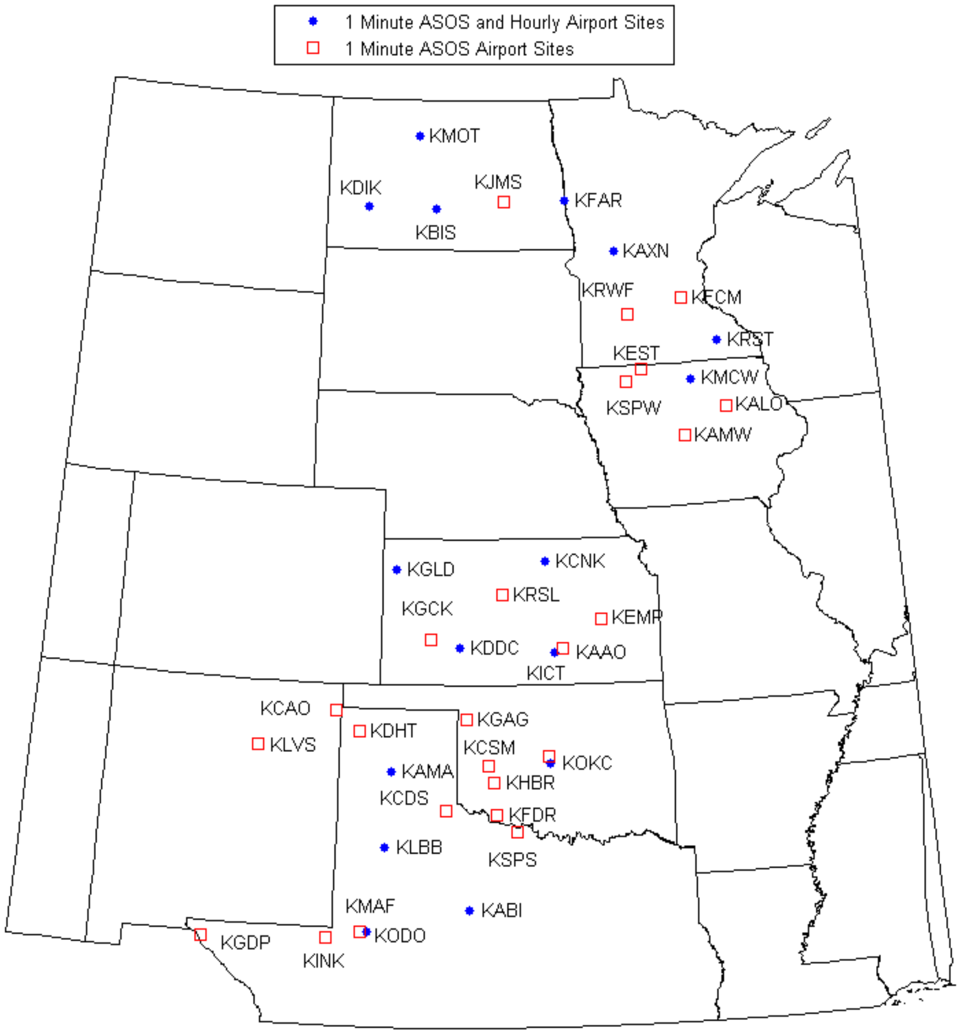

Figure 2-2 – Locations of the airports from which data were obtained.

There are three limitations to using ASOS wind speed data to model wind plants. The first is that the data are reported as integer knots (NOAA et al., 1998). The second is that the data are a running 2-minute average. Both reduce the high frequencies we can resolve in the frequency domain (Over and D'Odorico, 2002). A noise floor is evident in the power spectral density, caused by the one knot amplitude resolution of the data. The effect of averaging is a departure from the Kolmogorov spectrum at frequencies greater than approximately $2x10^{-4}$ Hz (periods of 90 minutes or shorter) that we do not observe in non-ASOS anemometer data. The third limitation of the ASOS data set is prevalence of bad data[7]. In 2007, our selected ASOS sites had an average bad data rate of 7.7%. Spencer Municipal Airport, Iowa (KSPW) had the best data collection in our sample with a bad data rate of 4.6% and Theodore Roosevelt Regional Airport in Dickinson North Dakota (KDIK) had the worst with a bad data rate of 16.5%.

We use NOAA hourly data obtained from airport sites (squares in figure 2-2) to study how the energy output of wind plants varies over many years. There is significant variation in the historical hourly data sets of the 40 airports prior to ASOS deployment in the 1990s. Some airports recorded wind speeds every third hour and only during the day. Data dropouts of months to years are present in the majority of the data sets. We used only the 16 airports out of the 40 that had hourly wind speed data from 1973 to 2008 and did not have a data dropout greater than 5 days. The 16 sites are listed in table 2-2 in appendix A and had an average missing data rate of 13%.

2.5 Methods

2.5.1 Interconnecting Wind Plants

We simulate wind plants interconnected with uncongested transmission capacity (sometimes called the copper plate assumption) by summing together either ERCOT wind plant power output data or NOAA airport wind speed data (taken at 8 or 10 meters, depending on the station) scaled up to a height of 80 meters using a method outlined in section 2.5.3 and transformed to power using a cubic curve (equation 2-1) that provides a good match to observed data from 1.5 MW turbines and turbine-mounted anemometer data.

[7] Bad ASOS data were data dropout where periods of time were missing from the data set.

Equation 2-1

$$P(t) = \begin{cases} 341 - 277v_{wind} + 62v_{wind}^2 - 2.5v_{wind}^3 & \text{if} \quad v_{wind} \geq 2.9 \text{ m/s and } v_{wind} < 14 \text{ m/s} \\ 1500 & \quad v_{wind} \geq 14 \text{ m/s} \\ 0 & \quad v_{wind} < 2.9 \text{ m/s} \end{cases}$$

Previous work indicates that wind power variability can be reduced by either increasing the number of wind plants or increasing the distance between wind plants. For our step change and frequency analyses, we add stations together according to their location. We select an ERCOT wind plant as the starting point, calculate the distance to each of the other stations using a WGS-84 ellipsoidal Earth, and sort the results from closest to farthest wind plant (Vincenty, 1975). We simulate interconnected wind plants by adding the closest wind plant's power to the system, perform step change and PSD analyses, and repeat until all wind plants have been interconnected. The same method is used to add ASOS stations together by distance.

2.5.2 Missing Data

The 1-minute ASOS and hourly NOAA data sets are incomplete. For the ASOS data, we treat missing data as follows. If the length of the missing data segment is less than 3 minutes, then the missing data are filled in by interpolating between the 2 closest points. Any missing data segments longer than 3 minutes are excluded from the summed result.

For the NOAA hourly data set used for the wind drought analysis, any missing data segments with a length of 3 hours or less are filled in by interpolating between the 2 closest points. Any missing data segments with a length greater than 3 hours but less than 120 hours are filled in using average wind speeds calculated from the previous four weeks for each hour of the day. We then take the time of day average segment that coincides with the missing data segment and scale it to match its boundaries with the boundaries of the surrounding good data segments. Any data set that has a missing data segment longer than 120 hours is excluded.

2.5.3 Scaling Wind Data to Hub Height

The airport wind speed measurements were taken at heights of 8 to 10 meters and are scaled up to 80 meters before being transformed to power data. We use a logarithmic velocity profile to estimate wind speeds at a hub height of 80 meters (equation 2-2) (Seinfeld and Pandis, 2006). The logarithmic velocity profile assumes the surface layer is adiabatic. The logarithmic velocity profile depends on a surface roughness length that characterizes the boundary layer near the ASOS station; we use $z_0 = 0.03$ meters.

Equation 2-2

$$\overline{u_*}(80m) = \frac{u_*}{\kappa} \ln \frac{80}{z_0}$$

where

$$u_* = \frac{\kappa \bar{u}_*(h_r)}{\ln \frac{h_r}{z_0}}$$

$$h_r = \text{reference height}$$

$$z_0 = \text{surface roughness length}$$

κ ~ 0.4 (von Karman constant)

2.5.4 Correlation Analysis

Correlation between power output time series of two wind plants can be quantified by Pearson's correlation coefficient:

Equation 2-3

$$\rho = \frac{\sum_i (x_i - \bar{x})(y_i - \bar{y})}{\sigma_x \sigma_y \sqrt{\sum_i (x_i - \bar{x})^2} \sqrt{\sum_i (y_i - \bar{y})^2}}; \ (-1 \leq \rho \leq 1).$$

Power outputs of two wind plants that rise and fall in relative unison have ρ near one, and little smoothing takes place. A correlation coefficient near zero indicates that wind power outputs vary independently of each other. A negative correlation coefficient, although not seen in the data, would indicate anticorrelation between wind power outputs such that high power output from one wind plant is associated with low power output from the other; maximum smoothing would occur if ρ = -1. Previous studies have shown that as the distance between wind plants increases, the correlation between their outputs decreases. The standard deviation of summed time series signals is dependent on the correlation between each individual time series signal (equation 2-4) (Giebel, 2000).

Equation 2-4

$$\sigma_{sum}^2 = \frac{1}{N^2}\sum_i \sum_j \sigma_i \sigma_j corr_{ij}$$

2.5.5 Step Change Analysis

The most common time domain method used in wind power studies is a step change analysis (see for example Wan, 2004, 2007) where the change in power for a given time step is calculated and either reported as power (e.g. MW) or as a percentage of the rated capacity of a wind plant (equation 2-5). We calculate step changes as a percentage of the maximum power produced by a wind plant or summed plants (equation 2-6).

Equation 2-5

$$\Delta P = P(t+\tau) - P(t) \text{ or } \Delta P = \frac{P(t+\tau)-P(t)}{P_{NameplateCapacity}} \times 100$$

Equation 2-6

$$\Delta P = \frac{P(t+\tau)-P(t)}{\max(P)} \times 100$$

We calculate step changes at 30-minute, 60-minute and 1-day time intervals because they are important to ancillary services and day-ahead electricity markets. We plot the maximum step change observed versus the distance from the original starting wind plant to the next wind plant interconnected.

2.5.6 Frequency domain

To characterize the smoothing of wind power's variability as a function of frequency as wind plants are interconnected, we analyze wind power in the frequency domain. Our results can be used to help determine the most economical generation portfolio to compensate for wind's variability. For the Texas wind plant data, we compute the discrete Fourier transform of the time series of output in order to estimate the power spectrum (sometimes termed the power spectral density or PSD) of the power output of a wind plant.

One of the attributes of power spectrum estimation is that increasing the number of time samples does not decrease the standard deviation of the PSD at any given frequency f_k. In order to take advantage of a large number of data points in a data set to reduce the variance at f_k, the data set may be partitioned into K time segments. The Fourier transform of each segment is taken and a PSD constructed. The PSDs are then averaged at each frequency, reducing the variance of the final estimate by the number of segments (and reducing the standard deviation by $1/\sqrt{K}$. The length of a data set determines the lowest frequency that can be resolved and segmenting increases the lowest frequency we are able to resolve in a signal by a factor of K (Apt, 2007; Press et al., 1992). Since we wish to characterize wind power variability in the time range of current market operations (24 hours to 15 minutes), the decreased ability to examine frequencies corresponding to very long times is a small price to pay for the decreased variance.

A Fourier transform requires evenly sampled data points to transform a signal from the time domain to the frequency domain. The Texas wind plant output data is complete for the time period (2008) examined. However, the ASOS data has significant gaps. For example, the longest continuous data segment for one ASOS station was 42 days and the longest coincident continuous data segment of the 40 summed ASOS stations was 12 hours. The high percentage of missing data would limit our frequency analysis in two ways. First, we would be able to use only the 12 hours of coincident continuous good wind speed data. Second, we wouldn't be able to use segmenting to reduce the variability of the ASOS PSDs because the length of the coincident continuous good data is so short. To overcome the limitations imposed by the high percentage of missing ASOS data we calculate PSDs by using a Lomb periodogram instead of a periodogram estimated using a Fourier transform. The Lomb periodogram (Lomb, 1976) was developed for use in intermittent astrophysics data (equation 2-7) and does not require evenly sampled data points to calculate the PSD of a signal. Instead of calculating the Fourier frequencies of a signal, it applies a least-squares fit of sinusoids to the data to obtain the frequency components. The time delay component τ in equation 2-7 ensures the frequencies produced by the Lomb periodogram are orthogonal to one another. We implement the Lomb periodogram by using the algorithm of Press et al. (1992).

Equation 2-7 - Lomb Periodogram

$$P_N(\omega) = \frac{1}{2\sigma^2}\left\{\frac{\left[\sum_j (h_j - \bar{h})\cos\omega(t_j - \tau)\right]^2}{\sum_j \cos^2\omega(t_j - \tau)} + \frac{\left[\sum_j (h_j - \bar{h})\sin\omega(t_j - \tau)\right]^2}{\sum_j \sin^2\omega(t_j - \tau)}\right\}$$

Subject to the constraint:

$$\tan(2\omega\tau) = \frac{\sum_j \sin 2\omega t_j}{\sum_j \cos 2\omega t_j}$$

In computing the PSDs, we use 8 segments for the ERCOT data and 32 segments for the ASOS data to reduce the variability of using a year's worth of data. The algorithm used to implement the Lomb periodogram requires two factors, ofac and hifac, to be defined for each signal. The first factor, ofac, is an oversampling factor that we set to 6 for ASOS data and 1 for ERCOT data. The second factor, hifac, determines the highest frequency the algorithm is able to resolve. We calculate hifac for each signal to produce the correct Nyquist frequency.

Kolmogorov (1941) proposed that the energy contained in turbulent fluids is proportional to the frequency of the turbulent eddies present in the fluid, $E \propto f^{\beta}$, with $\beta = -5/3$, and this result has been widely verified in subsequent empirical studies (for example, Grant et al., 1961; Monin, 1967). Apt (2007) has shown the power spectrum of a wind plant's power output follows a Kolmogorov spectrum between frequencies of 30 seconds and 2.6 days. We expect departures from Kolmogorov of $\beta < -5/3$ if any smoothing occurs when wind plants are interconnected. As wind plants are interconnected we estimate β by linearly regressing the log of the PSD of the summed wind power between the frequencies of 1.2×10^{-5} to 5.6×10^{-4} Hz (24 hours to 30 minutes).

Kolmogorov's relationship is valid for wind only for frequencies corresponding to times of approximately 24 hours or less. It has been shown the spectra of wind speed turbulence flatten for longer frequencies, indicating wind has constant energy in its lower frequencies (longer than a few days) (Jang and Lee, 1998). We use a modified von Karman formulation (equation 2-8) for wind speed turbulence spectrum to model the power spectrum of one wind plant over the frequency range of 43 days to 30 minutes (Kaimal, 1972).

To estimate the smoothing arising from interconnecting wind plants, we determine if departures from a Kolmogorov spectrum occur in the following manner. We fit equation 2-8 to the PSD of a single wind plant to determine a value for *B*.

Equation 2-8

$$PSD(f) = \frac{A}{1 + Bf^{-5/3}}$$

As we add wind plants to the single wind plant, we fit equation 2-8 to the resulting summed PSD to determine a value for A and produce an appropriately scaled single wind plant model PSD. We then compare the slope of the log of the summed PSD to the -5/3 slope of the single wind plant model in the Kolmogorov region between frequencies corresponding to 30 minutes and 24 hours. We measure deviations from the spectrum of equation 2-8 by dividing the power contained in each frequency of the summed PSD by the power estimated in each frequency of the single wind plant model. If no smoothing occurs when wind plants are interconnected the result should be close to 1 for all frequencies. If there is a reduction in variability then there will be frequencies for which the fraction is less than 1. Finally, we use a linear regression on the log of the fractions to display the mean fraction response versus frequency.

2.5.7 Wind Drought Analysis

Analyzing long-term variations in wind power production is important for system planning. If significant drought periods occur, system planners must ensure adequate resources and renewable energy credits (RECs) are available to cover the wind power underproduction. Similarly, wind production that is significantly above the long-term average may depress the market price for RECs and increase the requirements for compensating power sources.

We use hourly NOAA data to estimate the yearly energy production of wind turbines from 1973 to 2008. We scale the wind speed measurements to 80 meter hub heights (see section 2.5.3) and transform it to hourly power data with a power curve (see section 2.5.1). A surface roughness of

0.03 meters is assumed for all of the airports. For each year the hourly power data from all 16 turbines is summed and compared to the mean yearly power production for the 35 year period.

2.6 Results

2.6.1 Frequency Domain

In figure 2-3, we show the ERCOT PSD results for 1, 4, and 20 wind plants using 15 minute time resolution data for 2008. A single wind plant follows a Kolmogorov spectrum ($f^{-5/3}$) from 1.2×10^{-5} to 5.6×10^{-4} Hz (corresponding to times of 24 hours to 30 minutes). When 4 wind plants are added together, the power contained in this region decreases with frequency at a faster rate ($f^{-2.49}$ instead of $f^{-1.67}$). For 20 wind plants the power decreases even more rapidly with increasing frequency ($f^{-2.56}$). Adding wind plants together does not appreciably reduce the 24 hour peak. BPA's summed wind power ($f^{-2.2}$) shows less smoothing than ERCOT's wind power, very likely because 17 of BPA's 19 wind plants are located within 170 km of each other in the Columbia River gorge and the maximum distance between BPA wind plants is 290 km.

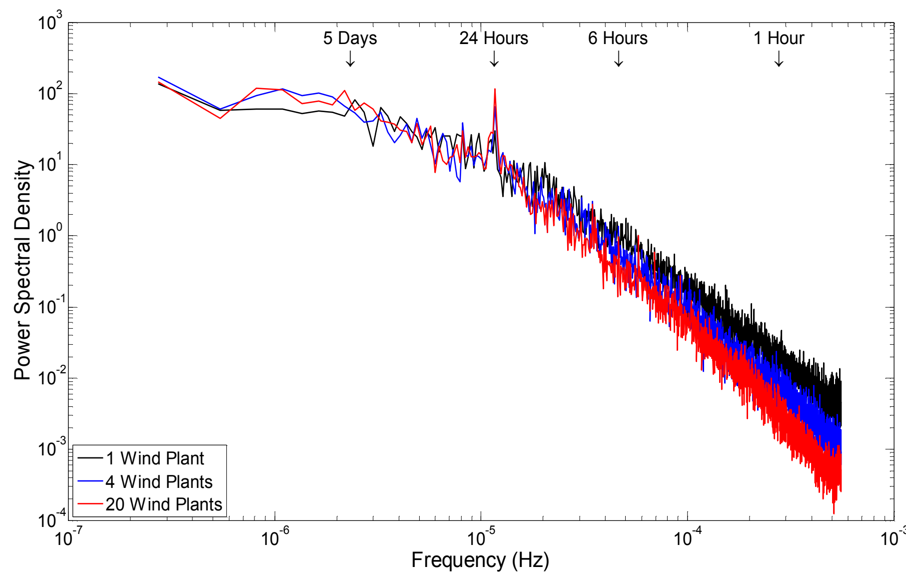

Figure 2-3 – Power spectral density (with 8 segment averaging, K = 8) for 1 wind plant, 4 interconnected wind plants, and 20 interconnected wind plants in ERCOT. Wind power variability is reduced as more wind plants are interconnected, with diminishing returns to scale.

The amplitude of variability of twenty interconnected wind plants has ~95% less power at a frequency of $2.8\text{x}10^{-4}$ Hz (corresponding to 1 hour) than that of a single wind plant (figure 2-4). The reduction in variability has very rapidly diminishing returns to scale, as interconnecting 4 wind plants gives an 87% reduction in variability at this frequency and interconnecting the remaining 16 wind plants produces the remaining 8% reduction. The maximum reductions in variability occur at the higher frequencies and dimish as the frequency decreases until at 24 hours there is no reduction in variability (figure 2-3). Figure 2-5 shows the reduction in variability achieved as a function of the number of interconnected wind plants for frequencies corresponding to 1, 6, and 12 hours.

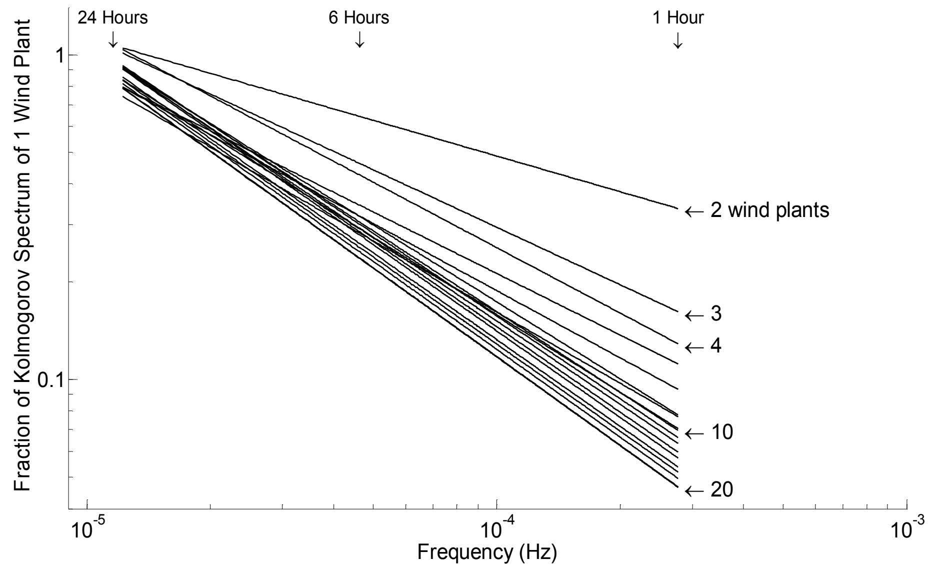

Figure 2-4 – Fraction of a Kolmogorov spectrum of 1 wind plant for interconnected wind plants over a frequency range of 1.2×10^{-5} to 5.6×10^{-4} Hz. As more wind plants are interconnected less power is contained in this frequency range.

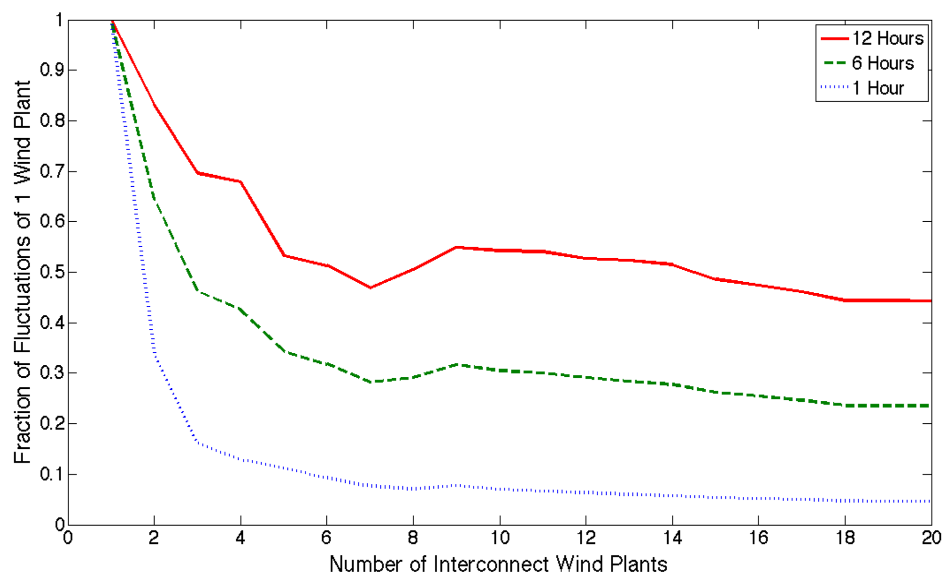

Figure 2-5 - Fraction of a Kolmogorov spectrum of different time scales versus the number of interconnected wind plants. Interconnecting four or five wind plants achieves the majority of the reduction of wind power's variability. We note that reductions in wind power variability are dependent on more than just the number of wind plants interconnected (e.g. size, location, and the order in which the wind plants are connected; see equation 2-9).

We calculate β (f^{β}) for simulations where each of ERCOT's 20 wind plants is used as the starting location and the remaining 19 wind plants are interconnected to it in order of their distance (closest to farthest). We use the resulting 400 data points to model the change in β due to three factors: ρ, the correlation coefficient between the interconnected wind plants and the next wind plant to be interconnected; $P_{Nameplate\ Ratio}$, the ratio between the nameplate capacity of the wind plant to be interconnected and the nameplate capacity of the interconnected wind plants; and N, the number of wind plants interconnected. Equation 2-9 is the result of linearly regressing the log of the change in β with the three variables (R^2 is 0.77 and all variables are significant to a 99% level).

Equation 2-9

$$\log \Delta\beta = 7.6\rho + 0.91P_{Nameplate\ Ratio} - 0.1N - 8.9$$

The PSD of forty interconnected modeled 1.5 MW GE turbines located throughout the Great Plains and Midwest did not depart from a Kolmogorov spectrum. We have eliminated as a possible cause the different time resolutions by averaging the ASOS data at 15 minute intervals (the ERCOT sampling rate). It is possible that the discrepancy between the ASOS simulated power output and the observed ERCOT power output spectra may arise from intra-wind-plant aerodynamic effects, but further analysis is required, including the determination of the frequency dependence of the smoothing as a function of wind plant size.

2.6.2 Generation Duration Curves

We have computed normalized generation duration curves for a single ERCOT wind plant, twenty interconnected ERCOT wind plants, and all of BPA's wind plants (figure 2-6). Also shown is the average normalized generation duration curve of ERCOT's 20 wind plants interconnected with their nearest three neighbors and the area encompassed by +/- 1 standard deviation. One wind plant has a higher probability of achieving close to its nameplate capacity than interconnected wind plants but an increased probability of no wind or low wind power events.

Archer and Jacobson (2007) concluded on the basis of meteorological data that interconnected wind plants spread throughout Texas, Oklahoma, Kansas, and New Mexico would produce at least 21% of their rated capacity 79% of the time and 11% of their rated capacity 92% of the time. The ERCOT and BPA data from operating wind turbines do not support that conclusion. ERCOT's twenty interconnected wind plants produced at least 10% of their rated power capacity 79% of the time and at least 3% of their rated capacity 92% of the time. BPA's nineteen interconnected wind plants produced at least 3% of their rated capacity 79% of the time and 0.5% of their rated capacity 92% of the time. Hereinafter we define "firm power" for a generator as an availability range of 79 to 92%.

Archer and Jacobson's (2007) simulations produce baseload capacity equivalents for wind power that are 2 to 20 times greater than those observed in the ERCOT and BPA data. Two effects may be responsible for the discrepancy between our results and Archer and Jacobson's results. The first is that Archer and Jacobson analyze a larger geographical area than that encompassed by ERCOT or BPA. The second is that Archer and Jacobson use individual model wind turbines while we use data from operating wind plants.

The average generation duration curve of four interconnected ERCOT wind plants shows that a small number of interconnected wind plants achieves the majority of the smoothing of wind power's variability and corresponds to the result obtained from our power spectral density analysis. 19 BPA and 20 ERCOT interconnected wind plants similarly achieve only 70% to 88% of their nameplate capacities but BPA's wind power has a higher probability of low to no wind power occurances. The higher probability of low to no wind events in BPA's system is likely because of the limited geographic dispersion of BPA's wind plants noted in the preceding section.

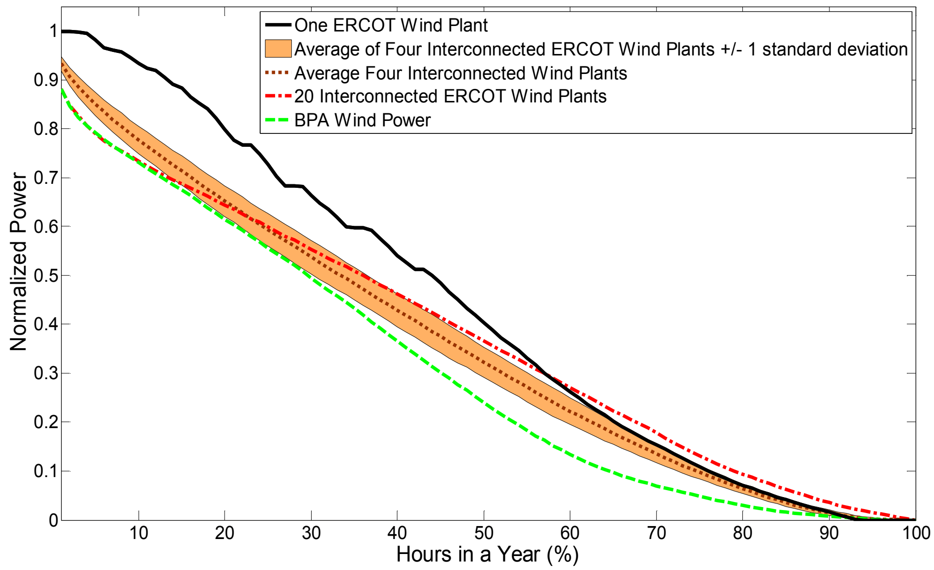

Figure 2-6 – Normalized generation duration curves for ERCOT interconnected wind plants and BPA's total wind power for 2008. The average normalized generation duration curve of ERCOT's 20 wind plants interconnected with their nearest three neighbors is plotted (dotted line) with the area encompassed by one standard deviation (tan area).

2.6.3 Pairwise Correlations of Wind Power Output

In figure 2-7 we show the correlation coefficients between pairs of wind plants versus the geographical distance between the wind plants, using measured 15-minute wind power averages from 20 wind plants in Texas for 2008. Wind plants that are located less than 50 kilometers apart tend to have highly correlated power outputs ($0.7 < \rho < 0.9$), while wind plants located more than 500 kilometers apart show lower correlation ($\rho < 0.3$). All of the correlation coefficients were greater than zero at the 99% significance level (t-test).

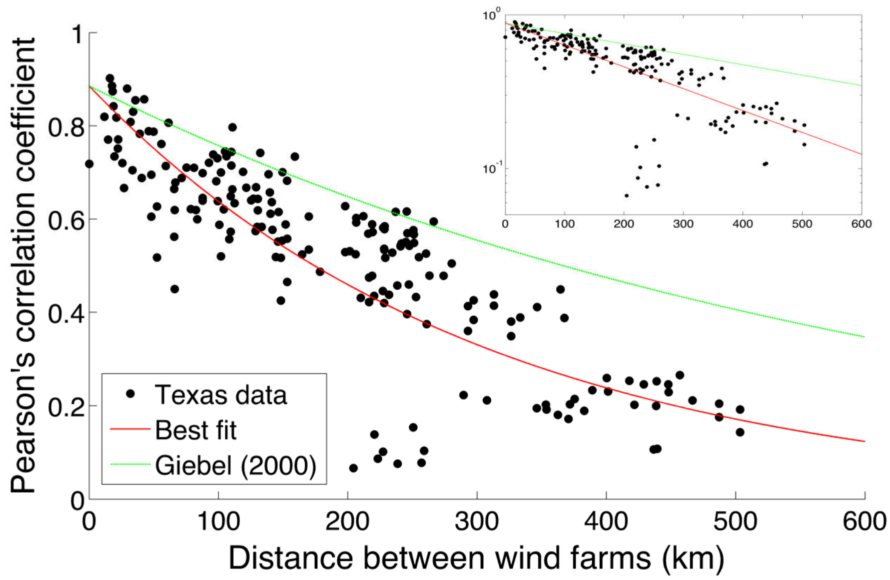

Figure 2-7 - Correlation coefficients vs. distance between pairs of wind plants (inset shows the data on a semi-log plot).

The exponential fit shown in figure 2-7, $\rho \propto \exp(-distance/D)$, has a decay parameter *D* of 305 kilometers and an intercept of ρ = 0.89 at zero separation distance. A linear regression of log-transformed correlation coefficients against distance has an R^2 of 0.55 (i.e. the exponential model explains about half of the variation in the correlation coefficients).

Eight pairs of wind plants, between 200 and 300 kilometers apart, have correlation coefficients lower than 0.2 that lie below the overall trend. These eight pairs are Delaware Mountain and Kunitz paired with each of Woodward Mountain, Indian Mesa, Southwest Mesa, and King Mountain (table 2-2 – appendix A). This probably reflects the influence of local topography and climate patterns and demonstrates that geographical proximity does not necessarily imply high correlation. Removing these eight points increases *D* to 320 kilometers; the difference between this value and that of the full data set is not statistically significant (t-test, 95% significance level), so the cluster of 8 points does not exert strong leverage on the model.

Giebel (2000) performed a similar analysis for wind power in Europe and found *D* to be 641 kilometers (green line in figure 2-7). While the current study analyzes 15-minute wind energy data sampled constantly for 2008, Giebel (2000) acquired data by applying a power curve to 10-minute wind speed averages sampled every 3 hours, thus obtaining 10-minute wind power averages at 3-hour intervals. To assess the distortion in cross-correlations that this difference introduces, one week of 10-second wind power data for two wind plants in Texas and Oklahoma was processed to mimic Giebel's data as well as that of the current study. The correlation coefficient for 10-minute averages taken every three hours was 0.31, and for consecutive 15-minute averages was also 0.31. The similarity of these values suggests that the difference in data sampling frequencies between the current study and Giebel (2000) does not introduce distortions that prohibit comparison.

Fixing the best-fit intercept for the Texas data in figure 2-7, the decay parameter of the European model (641 km) differs from that of the best-fit Texas model (305 km) at the 99% significance level (t-test). The R^2 of Giebel's model applied to the Texas data is 0.05, which reflects the poor fit of the European model to the Texas data.

A significantly higher decay parameter for wind power in Texas would imply that more smoothing occurs over a given distance in Texas than in Europe; however, large variation in correlation coefficients for the European data prohibits a firm comparison. European wind speed cross-correlation data for December 1990 – December 1991 has an exponential best fit with *D* = 723 kilometers (Giebel, 2000). The correlation coefficients show a large degree of scatter, especially in the 0 – 500 kilometer region that overlaps with the data of the current study; between 400 and 500 kilometers, ρ for the European wind speed data ranges from approximately 0.1 to 0.7, while ρ for the Texas wind power data ranges from 0.1 to 0.3. Assuming a similar degree of scatter in ρ for the resulting European wind power time series, no significant difference between cross-correlations of

Texas and European wind power data can be determined by comparing the current study and Giebel (2000); the European exponential model is a poor fit for the Texas data, but the Texas model could fit the European data comparably to the best fit model of Giebel (2000), especially at distances below 500 kilometers.

2.6.4 Step Change Analysis

Figure 2-8 shows the maximum ASOS 30-minute, 60-minute and 1-day percent step changes in power as a function of distance when KCNK (Concordia, Kansas), a station close to the geographic centroid of the ASOS airports, is used as the starting station, and additional stations are added based on their distance from the starting station. Figure 2-9 is constructed using KMOT (Minot, North Dakota), the station farthest from the geographical center of mass, as the starting station.

Adding together wind plants reduces the substantial step changes in power experienced by individual wind plants. As more distant wind plants are interconnected, the maximum step change in power relative to the maximum power produced reaches an asymptote of 15%-30% for step changes of an hour or less. The reductions in variability are approximately equal to those observed by Milborrow (2001) (a maximum hourly step-change of 18%) and are less than what BPA experienced in 2008 (a maximum hourly step-change of 63%). BPA's control area is significantly smaller than the geographic region spanned by the 40 ASOS sites. The largest 30-minute increase or decrease in power estimated from 40 interconnected ASOS wind plants was 15% of the maximum wind power produced. The maximum 1-day step changes are also reduced as more distant wind plants are interconnected although a reduction of at most 20% is achieved.

The reductions are obtained over relatively short distances with ~50% of the reductions occurring within 400 km. In figure 2-8, 93% of the reductions occur in the first 600 km and 7%

occurs between distances of 600 to 1200 km. If the reference wind plant is at a geographic extreme rather than the centroid (figure 2-9), 93% of the reductions occur in the first 1000 km.

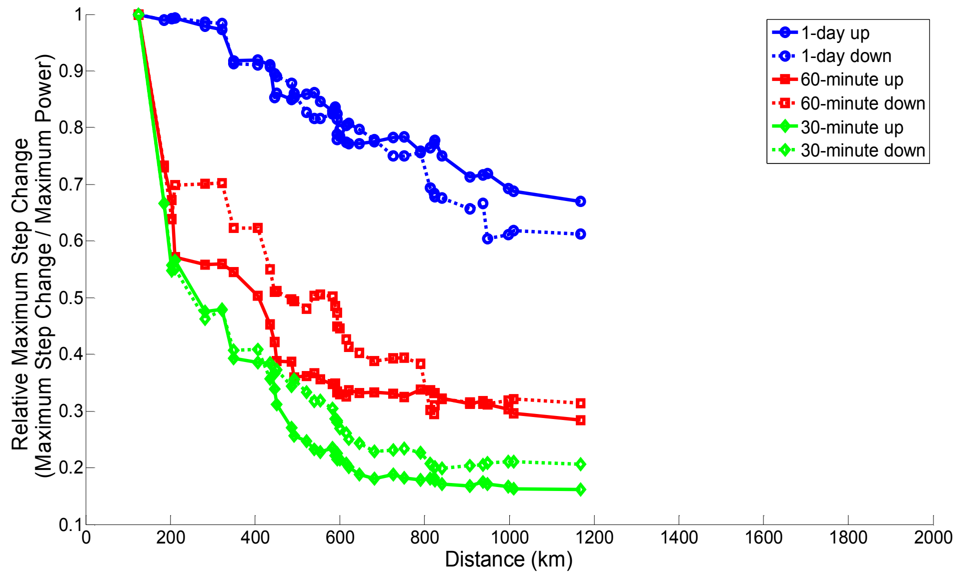

Figure 2-8 – ASOS step change analysis using KCNK (Concordia, Kansas) as the starting location. Each point represents an additional interconnected station. The relative maximum step change, measured as the maximum step change divided by the maximum power, decreases with distance as more wind plants are interconnected.

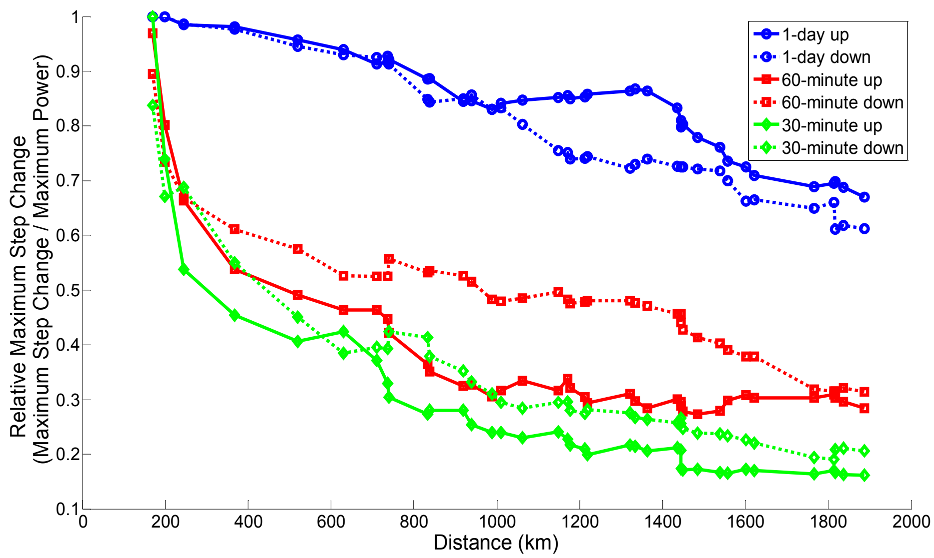

Figure 2-9 – ASOS step change analysis using KMOT (Minot, North Dakota) as the starting location. Each point represents an additional interconnected station. The relative maximum step change, measured as the maximum step change divided by the maximum power, decreases with distance as more wind plants are interconnected.

Figure 2-10 shows the maximum ERCOT 30-minute, 60-minute, and 1-day percent step changes in power when ERCOT wind plant 1 (Delaware Mountain), the wind plant farthest from the geographic centroid of ERCOT's wind plants, is used as the starting wind plant. Similar reductions in variability to those simulated from ASOS data are produced when ERCOT wind plants are interconnected. Reductions of 42% for 30-minute step changes, 50% for 60-minute step changes, and 16% for 1-day step changes are achieved when wind plants within 500 km are interconnected. The reductions for ERCOT are observed over shorter distances than predicted by the ASOS results. In ERCOT's system, wind power ramps up faster than it ramps down for each of the step change intervals analyzed. If system operators are to match wind's fluctuations exactly, they will need to have a larger capacity from generators and demand response to ramp down their power than they will require from them to ramp up.

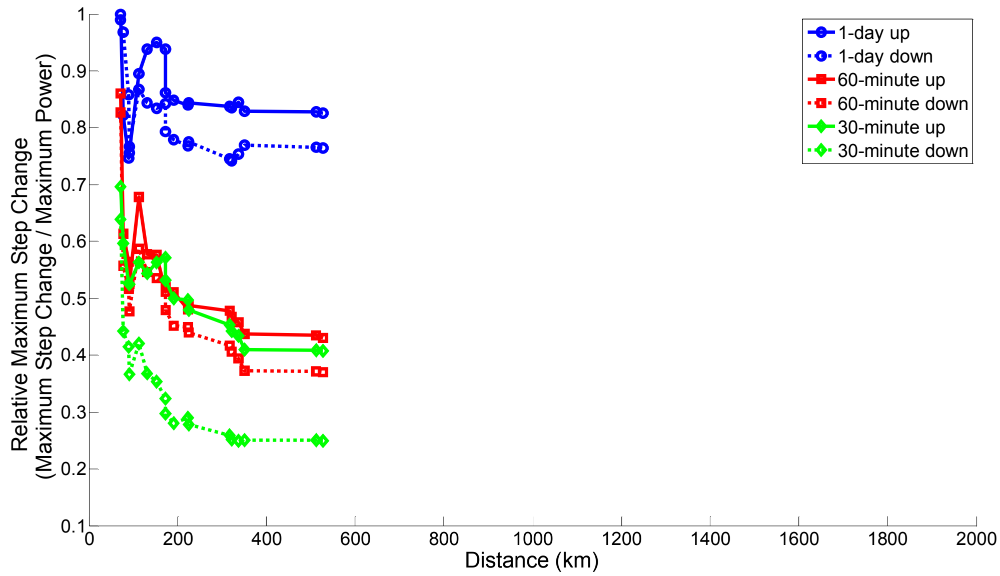

Figure 2-10 – ERCOT step change analysis when wind plant 1 (Delaware Mountain, TX) is used as the starting location. The relative maximum step change, measured as the maximum step change divided by the maximum power, decreases with distance as more wind plants are interconnected.

2.6.5 Are There Wind Droughts?

We estimated yearly variation in wind energy production from modeled 1.5 MW turbines at 16 locations over the years 1973 to 2008 (figure 2-11). Also plotted is the annual energy produced from hydroelectric power in the United States for the same time span. We normalized each of the results by their mean. The standard deviation for the estimated wind production was 6% of the mean energy produced per year. The largest deviation from the mean occurred in 1988 when the estimated wind energy production was 14% more than the mean annual production. The largest negative deviation from the mean occurred in 1998 when estimated wind energy produced was 10% less than the mean annual production. The standard deviation for the actual hydroelectric production was 12% of the mean energy produced per year for the 36 year period. U.S. hydropower's largest positive deviation from the mean occurred in 1997 when hydropower production was 26% above the mean. The largest negative deviation occurred in 2001 when hydropower production was 23% below average.

Thus, yearly wind energy production from the sample of 16 airports in the central and southern Great Plains is predicted to exhibit long term variations, and these are about half that observed nationally for hydropower (we note that the bulk of hydropower production is regionally concentrated).

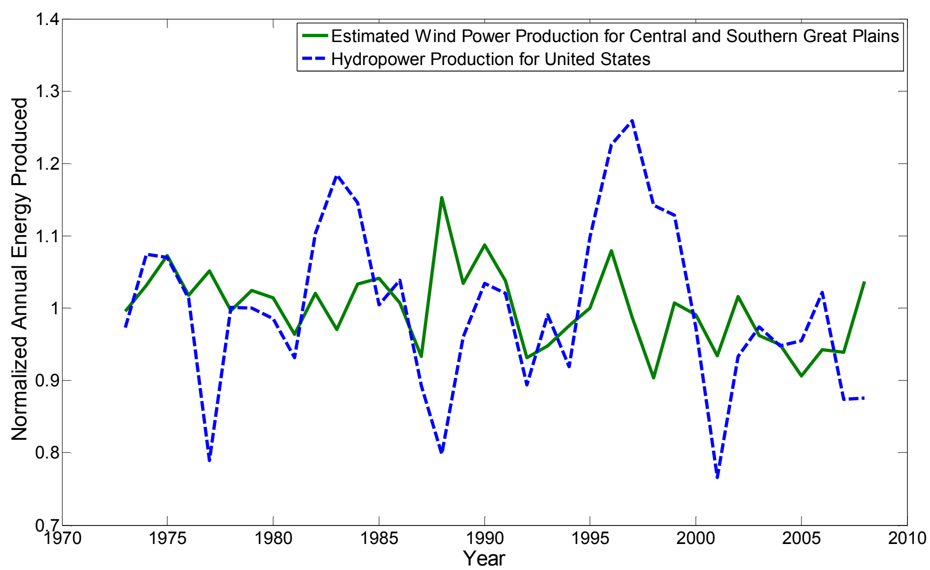

Figure 2-11 – Normalized predicted annual wind energy production from 16 wind turbines located throughout the Central and Southern Great Plains. The normalized annual hydropower production for the United States is also plotted for comparison.

2.7 Analysis

The variability of interconnected wind plants is less than that of individual wind plants when measured in the time domain with step change analyses and in the frequency domain with power spectrum analyses. The amount of smoothing is a predictable function of frequency, correlation coefficient, nameplate capacity ratio, and the number of interconnected wind plants. Reductions in variability diminish as more wind plants are interconnected. Finally, yearly wind power production is likely to vary, and have year-to-year variations about half that observed nationally for hydropower.

These results do not indicate that wind power can provide substantial baseload power simply through interconnecting wind plants. ERCOT's generation duration curve shows wind power reliably provides 3-10% of installed capacity as firm power (as defined above) while BPA's generation duration curve shows 0.5-3% of their wind power is firm power. The frequency domain analyses have shown that the power of interconnected wind plants will vary significantly from day to day and the results of the step change analyses show day-to-day fluctuations can be 75 to 85% of the maximum power produced by a wind plant (figures 2-8 to 2-10).

The benefit of interconnecting wind plants is a significant reduction in the high frequency variability of wind power. Reductions in the relative magnitude of the 30-minute and hourly step changes will reduce the per MWh ancillary service costs of wind energy. The reductions will also improve the root mean square error of wind energy forecasts for a system's total wind energy production but not the forecast error for individual wind plants. Estimating the value of these benefits is difficult due to the proprietary algorithms used by system operators. We have provided system planners with a metric that better characterizes the variability of large penetrations of wind power. System planners can then identify the resources needed to compensate the variability and calculate the associated costs.

2.8 References

Apt, J., 2007. The spectrum of power from wind turbines. Journal of Power Sources, 169, 369-374.

Archer, C.L., Jacobson, M.Z., 2007. Supplying baseload power and reducing transmission requirements by interconnecting wind plants. Journal of Applied Meteorology and Climatology, 46, 1701-1717.

BPA, 2009. BPA announces rate changes. Bonneville Power Authority, News Releases, PR 31 09. Available: http://www.piersystem.com/go/doc/1582/292435/

CAISO, 2007. Draft: integration of renewable resources report. California Independent System Operator, Renewables workgroup. Available: http://www.caiso.com/1c60/1c609a081e8a0.pdf

Cha, P., Molinder, J., 2006. Fundamentals of Signals and Systems: A Building Block Approach. Cambridge, New York.

Czisch, G., Ernst, B., 2001. High wind power penetration by the systematic use of smoothing effects within huge catchment areas shown in a European example. "Windpower 2001" American Wind Energy Association, Washington, DC, 2001. Available: http://www.iset.uni-kassel.de/abt/FB-I/projekte/awea_2001_czisch_ernst.pdf

Dobesova, K., J. Apt, and L.B. Lave, *Are renewables portfolio standards cost-effective emission abatement policy?* Environmental Science & Technology, 2005. 39(22): 8578-8583.

DOE, 2008. 20% wind energy by 2030. U.S. Department of Energy, Office of Energy Efficiency and Renewable Energy. Available: http://www1.eere.energy.gov/windandhydro/pdfs/41869.pdf

DSIRE. Database of State Incentives for Renewables and Efficiency, 2009. www.dsireusa.org.

EIA, 2009. Annual Energy Review - Table 8.2a Electricity Net Generation: Total (All Sectors), 1949-2008. U.S. Energy Information Agency. Available: http://www.eia.doe.gov/emeu/aer/txt/stb0802a.xls

EnerNex, 2006. 2006 Minnesota wind integration study, Volume 1. EnerNex Corporation. Available: http://www.uwig.org/windrpt_vol%201.pdf

ERCOT, 2009. Entity-Specific Resource Output. Retrieved Feb. 18, 2009 from ERCOT's Planning and Market Reports. Available: http://www.ercot.com/gridinfo/sysplan/

GE, 2008. ERCOT wind impact \ integration analysis. General Electric. Available: http://www.ercot.com/meetings/ros/keydocs/2008/0227/ERCOT_final_pres_d1_w-o_backup.pdf

Giebel, G., 2000. On the benefits of distributed generation of wind energy in Europe. Ph.D. dissertation, Carl von Ossietzky University of Oldenburg, 2000, 104 pp. Available: http://www.drgiebel.de/GGiebel_DistributedWindEnergyInEurope.pdf

Grant, H.L., Stewart, R.W., Moilliet, A., 1961. Turbulence spectra from a tidal channel. Journal of Fluid Mechanics, 12, 241-263.

Hirst, E., 2002. Integrating wind energy with the BPA power system: preliminary study. Bonneville Power Authority. Available: http://www.bpa.gov/Power/pgc/wind/Wind_Integration_Study_09-2002.pdf

International Energy Agency, 2005. Variability of Wind Power and Other Renewables – Management Options and Strategies. Available: http://www.iea.org/papers/2005/variability.pdf

Jang, J., Lee, Y., 1998. A study of along wind speed power spectrum for Taiwan area. Journal of Marine Science and Technology, 6.1, 71-77.

Kahn, E., 1979. The reliability of distributed wind generation. Electric Power Systems Research, 2, 1-14.

Kaimal, J.C., 1972. Spectral characteristics of surface layer turbulence. Journal of the Royal Meteorological Society, 98, 563-589.

Kolmogorov, A., 1941. The local structure of turbulence in incompressible viscous fluids at very large Reynolds numbers. Dokl. Akad. Nauk. SSSR, 30, 301-305. Reprinted (1991) R. Soc. Lond. Proceedings: Mathematical and Physical Sciences, 434, 9-13.

Lomb, N.R., 1976. Least-squares frequency analysis of unevenly spaced data. Astrophysics and Space Science, 39, 447-462.

Milborrow, D, 2001. *Penalties for intermittent sources of energy*. Working Paper for U.K. Cabinet Performance and Innovation Unit (PIU) Energy Review. Available: http://www.cabinetoffice.gov.uk/media/cabinetoffice/strategy/assets/milborrow.pdf

Milligan, M., Porter, K., 2005. Determining the capacity value of wind: a survey of methods and implementation. "Windpower 2005" American Wind Energy Association, Denver, 2005, National Renewable Energy Laboratory, Conference Paper, NREL/CP-500-38062. Available: http://www.nrel.gov/docs/fy05osti/38062.pdf

Monin, A.S., 1967. Turbulence in the Atmospheric Boundary Layer. Physics of Fluids, 10 (9P2), S31-S37.

National Oceanic and Atmospheric Administration, Department of Defense, Federal Aviation Administration, United States Navy, 1998. Automated Surface Observing System (ASOS) User's Guide. Available: http://www.nws.noaa.gov/asos/pdfs/aum-toc.pdf

Over, T.M., D'Odorico, P., 2002. Scaling of surface wind speed. In : Lee, Jeffrey A. and Zobeck, Ted M., 2002, Proceedings of ICAR5/GCTE-SEN Joint Conference, International Center for Arid and Semiarid Lands Studies, Texas Tech University, Lubbock, Texas, USA Publication 02-2 p.50. Available: http://www.csrl.ars.usda.gov/wewc/icarv/15a.pdf

Press, W.H., S.A. Teukolsky, W.T. Vetterling, and B.P. Flannery, Numerical Recipes in FORTRAN: The Art of Scientific Computing, second ed., Cambridge University Press, Cambridge, 1992.

Seinfeld, J.H., Pandis, S.N., 2006. Atmospheric Chemistry and Physics: From Air Pollution to Climate Change, second ed. Wiley, Hoboken.

Vincenty, T., 1975. "Direct and Inverse Solutions of Geodesics on the Ellipsoid with Application of Nested Equations." Survey Review, 23, 88-93.

Wan, Y., 2001. Wind Power Plant Monitoring Project Annual Report. National Renewable Energy Laboratory, Technical Report, NREL/TP-500-30032. Available: http://www.nrel.gov/docs/fy01osti/30032.pdf

Wan, Y., 2004. Wind power plant behaviors: analyses of long-term wind power data. National Renewables Energy Laboratory, Technical Report, NREL/TP-500-36551. Available: http://www.nrel.gov/docs/fy04osti/36551.pdf

Waxman, H., Markey, E., 2009. H.R. 2454: American clean energy and security act of 2009. United States House of Representatives, 111th Congress. Available: http://www.govtrack.us/data/us/bills.text/111/h/h2454pcs.pdf

2.9 Appendix A

Table 2-1 - Table of ASOS stations used to obtain wind speed data.

Station	State	Latitude			Longitude			Hourly Data Used?
		Degrees	Minutes	Seconds	Degrees	Minutes	Seconds	
KEST	IA	43	24	29.73	94	44	47.94	
KSPW	IA	43	9	57.64	95	12	20.15	
KMCW	IA	43	9	34.76	93	20	12.56	Yes
KAMW	IA	41	59	59.49	93	37	16.3	
KALO	IA	42	33	22.35	92	23	47.19	
KDDC	KS	37	46	0.28	99	57	58.68	Yes
KGCK	KS	37	55	43.6	100	43	32.48	
KCNK	KS	39	32	57	97	39	8	Yes
KRSL	KS	38	52	16.67	98	48	31.04	
KAAO	KS	37	44	51.3	97	13	16	
KEMP	KS	38	19	55.34	96	11	18.26	
KGLD	KS	39	22	17.239	101	41	56.371	Yes
KICT	KS	37	38	59.8	97	25	59	Yes
KRWF	MN	44	32	48.41	95	5	0.09	
KRST	MN	43	54	31.73	92	29	48.18	Yes
KFCM	MN	44	49	42.71	93	27	37.5	
KAXN	MN	45	51	56.85	95	23	32.27	Yes
KBIS	ND	46	46	23.07	100	44	58.21	Yes

KJMS	ND	46	55	44.34	98	40	41.91	
KDIK	ND	46	47	46.94	102	48	1.33	Yes
KMOT	ND	48	15	33.78	101	16	51.9	Yes
KFAR	ND	46	55	17.62	96	48	49.63	Yes
KCAO	NM	36	26	43.89	103	9	14.13	
KLVS	NM	35	39	15.2	105	8	32.6	
KCSM	OK	35	20	26.74	99	11	55.82	
KFDR	OK	34	21	7.5449	98	59	2.0727	
KGAG	OK	36	17	43.94	99	46	35.125	
KHBR	OK	34	59	28.7	99	3	5	
KPWA	OK	35	32	3	97	38	49	
KOKC	OK	35	23	35.12	97	36	2.64	Yes
KABI	TX	32	24	23.49	99	41	0.66	Yes
KAMA	TX	35	13	8.52	101	42	18.84	Yes
KCDS	TX	34	25	58.79	100	17	35.28	
KDHT	TX	36	1	20.41	102	32	58	
KGDP	TX	31	42	3.6	106	16	34.36	
KLBB	TX	33	39	48.86	101	49	22.18	Yes
KMAF	TX	31	56	42.98	102	12	15.65	Yes
KODO	TX	31	55	18.52	102	23	10.74	
KINK	TX	31	46	46.69	103	12	10.28	
KSPS	TX	33	59	19.666	98	29	30.816	

Table 2-2 - ERCOT wind plants

Number	Name	Latitude	Longitude
1	Delaware Mountain	31.6486	-104.75
2	Woodward	30.9575	-102.377
3	Indian Mesa	30.9333	-102.182
4	Southwest Mesa	31.0844	-102.108
5	King Mountain	31.2213	-102.161
6	Kunitz	31.3478	-104.4723
7	Capricorn Ridge	31.8207	-100.793
8	Airtricity	32.0649	-101.536
9	Sweetwater	32.32	-100.4
10	Trent Mesa	32.429	-100.199
11	Buffalo Gap	32.2287	-100.062
12	Horse Hollow	32.344	-99.9853
13	Callahan Divide	32.299	-99.872
14	Post Oak	32.7234	-99.2963
15	Mesquite	32.7234	-99.2963
16	Camp Springs	32.7556	-100.698
17	ENA Snyder	32.7921	-100.918
18	Brazos	32.9574	-101.128
19	Red Canyon	32.9389	-101.316
20	Whirlwind	34.0862	-101.086

Chapter 3 - The Cost of Wind Power Variability

3.1 Chapter Information

Authors: Warren Katzenstein and Jay Apt

Status: CEIC working paper

3.2 Abstract

We develop a metric to quantify the sub-hourly variability cost of individual wind plants and show its use in valuing reductions in wind power variability. Our method partitions wind energy into hourly and sub-hourly components and uses corresponding market prices to determine the cost of variability. The metric is applicable to variability at all time scales faster than hourly, and can be applied to long-period forecast errors. We use publically available data at 15 minute time resolution to apply the method to ERCOT, the largest wind power production region in the United States. The range of variability costs arising from 15 minute to 1 hour variations (termed load following) for 20 wind plants in ERCOT was \$6.79 to 11.5 per MWh (mean of \$8.73 ±\$1.26 per MWh) in 2008 and \$3.16 to 5.12 per MWh (mean of \$3.90 ±\$0.52 per MWh) in 2009. Load following variability costs decrease as wind plant capacity factors increase, indicating wind plants sited in locations with good wind resources cost a system less to integrate. Twenty interconnected wind plants have a variability cost of \$4.35 per MWh in 2008. The marginal benefit of interconnecting another wind plant diminishes rapidly: it is less than \$3.43 per MWh for systems with 2 wind plants already interconnected, less than \$0.7 per MWh for 4-7 wind plants, and less than \$0.2 per MWh for 8 or more wind plants. This method can be used to value the installation of storage and other techniques to mitigate wind variability.

3.3 Introduction

Wind power is quickly becoming a significant source of energy in the United States. It had an average annual growth rate of 28% over the past decade and supplied 1.3% of United States' energy in 2008 (EIA, 2010). However, wind is a variable source of power and increases the operational costs of electricity systems because system operators are required to "secure additional operating flexibility on several time scales to balance fluctuations and uncertainties in wind output" (Northwest Wind Integration Action Plan, 2007). There is interest in using storage technologies or fast-ramping fossil fuel generators, called flexible resources, to mitigate wind power variability and decrease the costs of integrating wind power into electrical systems (Denholm, 2005; Hittinger et al., 2010; Korpass et al., 2003).

Previous research and wind integration studies performed by Independent System Operators (ISOs) and Regional Transmission Operators (RTOs) have estimated that the cost of integrating wind power ranges from $0.5 to 9.5 per MWh for wind penetration levels ranging from 3.5 to 33% (Wiser and Bolinger, 2008). Traditionally wind integration costs are paid by the end-user, but system operators have begun to recover the integration costs of wind energy from wind plants directly. In 2009, Bonneville Power Authority (BPA) introduced a tariff of $5.7 per MWh for wind plants within its system to recover the costs of integrating wind power (BPA, 2009). BPA was the first system to charge wind generators for the integration costs of wind energy and other systems are considered likely to follow suit (Kirby and Milligan, 2006).

Wind plant owners may implement solutions to mitigate variability if they are charged for integration costs. A wind plant will be willing to pay up to the tariff imposed by the system for a solution that completely eliminated the variability it produces. In BPA this would be $5.7 per MWh. Realistically it is not cost effective to completely firm the power output of a wind plant. The costs of integrating wind power are incurred mainly at hourly and subhourly time scales and wind power is variable over time scales of subminute to weekly (Northwest Wind Integration Action Plan, 2007; Katzenstein et al., 2010; Apt, 2007). Wind plants will seek to use flexible technologies to reduce their variability in the hourly and subhourly time scales.

Here we develop a metric to determine the cost of variability of individual wind plants and then show its use in valuing reductions in wind power variability. Keith and DeCarolis state that it should be "possible…to assess the overall cost of wind's intermittency" by "portioning the cost of wind's variability between various markets…and market participants" (Keith and DeCarolis, 2005). Here we present an unbiased method to partition wind energy between hourly and subhourly markets and use the corresponding market prices to determine the cost of variability from individual wind plants.

The methods used to estimate the integration costs of bulk wind energy are not suitable to evaluate reductions in wind power variability for individual wind plants. First, all of the integration studies have focused on the net wind energy in a system and not the energy produced by individual wind plants. Second, the integration studies use large complex models that are either proprietary or difficult to replicate and are inappropriate to implement on a small scale. Third, the majority of the studies have focused on future large penetrations of wind energy instead of current levels.

There are additional advantages to estimating the variability cost of individual wind plants instead of the net wind power in a system. First, doing so provides a method to determine cost effective solutions to reduce wind power variability. Second, it is important to determine if all wind plants in a system equally contribute to the wind integration costs or if there are a few wind plants sited in poor locations that are causing the majority of the incurred costs. Finally, system operators may be able to prioritize wind plant projects in their interconnection queues to minimize their integration costs for wind energy.

3.4 Data

We use 15-minute time sampled wind power data from 20 ERCOT wind plants in 2008 and 2009. In addition, we use 15-minute ERCOT balancing energy service (BES) price data and hourly load following and regulation capacity price data for years 2004 through 2009. The locations of the 20 ERCOT wind plants are plotted in figure 3-7 in appendix B. Figures 3-8 through 3-13 in appendix B are box plots of the ERCOT ancillary service prices for years 2004 through 2009.

3.5 Methods

Our method partitions all of a wind plant's energy among the suite of markets available. We first describe a generalized formulation of this principle that is representative of the electricity markets in the United States and then present a metric specific to ERCOT. The three types of services a generator in a United States electricity system can provide are energy, capacity, and ancillary. Each service is necessary to maintain a functioning electricity system although each electricity system in the United States does not offer competitive markets for all of the services described.

Providing energy is the primary service of an electricity system, accounting for 70 to 95% of the wholesale cost of electricity (ISO New England, 2009; PJM, 2009; Potomac Economics, 2009). Energy markets are typically operated on an hourly basis and, depending on the ISO, a generator can submit bids for each hourly interval in day-ahead markets, hour-ahead markets, or real time markets. System operators accept enough generator bids to meet the predicted load for a given hour plus a specified reserve margin. Generators whose bids are accepted are required to supply power at the specified level for that hour.

From a system point of view, capacity markets ensure a system has enough generators it can call upon to meet their maximum load plus a reserve margin. From a generator's point of view, energy markets are designed for generators to recover their variable costs while capacity markets are designed for generators to recover their fixed costs. Capacity markets are typically longer term markets that operate on a yearly basis.

Ancillary services are a suite of products designed to handle the variability present in an electrical network. Variability exists in electricity grids due to fluctuations in load, transmission, and generation. The nature of electrical networks and the lack of cost effective storage in electricity systems means that the exact amount of electricity produced must be consumed if the system is to remain stable. Small deviations can be tolerated but need to be corrected according to the standards set by the North American Electricity Reliability Council (NERC). The suite of ancillary services are traditionally defined as load following, regulation, energy imbalance, spinning reserve, supplemental reserve, frequency control, voltage control, nonoperating reserve, and standby service (Hirst and Kirby, 1997).

Renewable energy credit (REC) markets value the additional benefits renewable energy generators add to a system. The primary benefits of renewable energy are that it is a zero emissions source and that it satisfies policy goals mandated by over 29 states. The additional yet less tangible benefits are a decreased dependence on foreign energy sources, an increase in portfolio diversity, and a hedge against future fuel prices. Typically, one renewable energy credit is the environmental and social value of one MWh of renewable energy.

From a system operator's point of view, the value of energy from a wind plant is the sum of the wind plant's energy, capacity, REC, and ancillary service benefits and its ancillary service costs. The costs of incorporating wind power into a system can be classified based on the two defining characteristics of wind power: uncertainty and variability. Systems incur costs due to wind power's uncertainty because system operators can never know with a 100% certainty what the output of a wind plant will be at a given time. The difference between the forecast and the actual output of a given wind plant must be eliminated using either hourly energy markets or ancillary services markets. We do not estimate the cost of forecast errors in this paper but note that the cost of forecast errors can be included in our metric.

Wind power variability, the fact that the output of a wind plant is constantly changing, also causes systems to incur costs. Any change in the power output of a wind plant must be compensated by another source in the system. This source could be other wind plants, loads, conventional generators, or energy storage. If conventional generators are used, the inefficiencies suffered due to changing its power level are costs directly related to wind power. We note that wind power variability also changes the loading of transmission lines and we do not attempt to calculate the resulting changes in transmission profitability.

We estimate the cost of wind power variability in ERCOT by partitioning the power output of a wind plant between hourly energy and ancillary service markets (figure 3-1). For each hour, we determine a constant amount of a wind plant's energy to partition to the hourly energy market. We remove the hourly energy component from the wind signal and then determine the residual ancillary services required. For the example in figure 3-1 we assume a simplified ancillary services market, representative of ERCOT's ancillary services, that consist of load following and regulation markets. Regulation is the ancillary service that handles rapid fluctuations on time scales of minutes and load following is the ancillary service that handles larger fluctuations on time scales of 15 minutes. We first determine the amount of load following capacity and energy needed and then determine the amount of regulation capacity and energy required. We do not attempt to calculate the capacity or REC benefits of wind plants because they do not affect the variability costs of wind plants. Only the energy portioned to the hourly energy market affects the estimated variability cost.

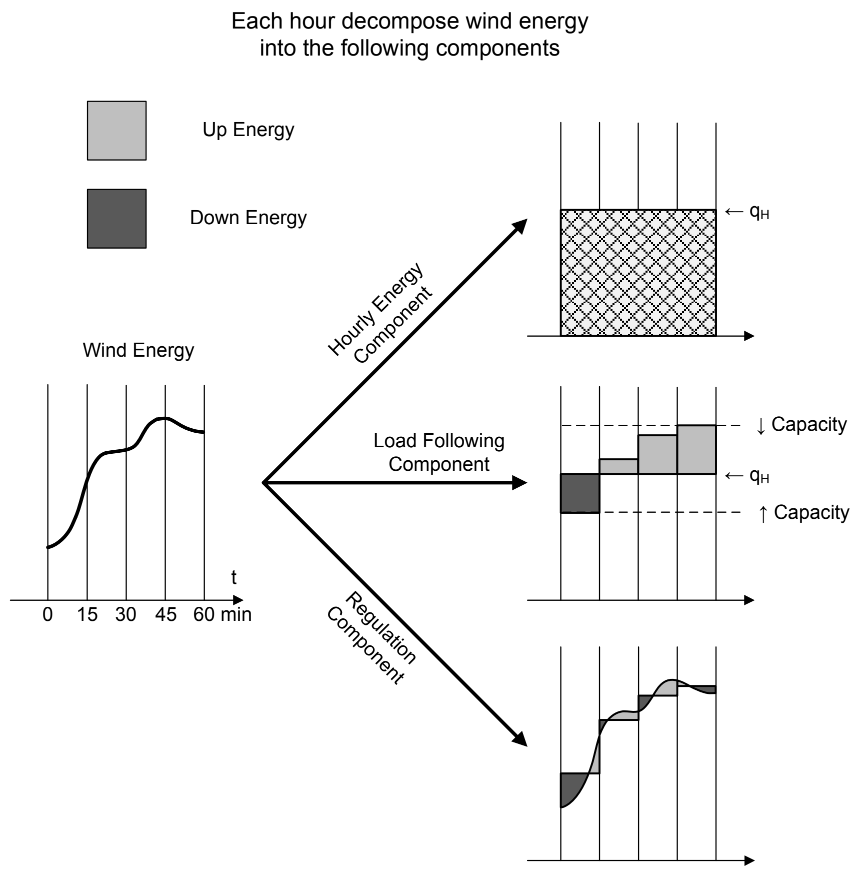

Figure 3-1 - Conceptual diagram of how we partition wind energy into hourly energy, load following, and regulation components.

Equation 3-1 is the simplified formulation of the variability cost of wind energy for wind plants in ERCOT. We calculate only the load following component of the ancillary service cost of wind energy because we were able to obtain only 15-minute time-resolved wind energy data for 20 ERCOT wind plants. The yearly variability cost of energy from a wind plant is the sum of its hourly costs.

$$Variability\ Cost = \sum_{k=1}^{4} \varepsilon_k P_k + P_{UP} \min(\varepsilon_k) + P_{DN} \max(\varepsilon_k) \qquad (3\text{-}1)$$

and

$$\text{Yearly Cost} = \sum_{i=1}^{8760} \text{Hourly Cost}_i$$

Where P_k is the subhourly price of energy

P_{UP} is the subhourly price for up regulation capacity

P_{DN} is the subhourly price for down regulation capacity

q_H is the amount of firm hourly energy partitioned

$\varepsilon_k = W_k - q_H$, the amount of subhourly energy per time period k

In formulating equation 3-1, we make two key assumptions. The first is that each wind plant is a price taker and does not affect market prices for energy or ancillary services. The second is that deviations from the hourly energy level are costs and are to be avoided.

The variability cost of wind energy, as calculated from equation 3-1, is dependent on what value is chosen for q_H (the hourly energy component). In order to create an unbiased cost metric, each hour we use the set of energy and ancillary services prices and wind power data to determine the q_H that minimizes the variability cost. Thus, we are estimating what the variability cost of wind plant's in ERCOT was in a given year, and not attempting to predict what it will be. Equation 3-2 is the formulation of the optimization problem for ERCOT. Constraints on the optimization problem are:

1. The sum of energy components in each 15-minute interval must equal the energy produced by the wind plant in the 15-minute interval.
2. The maximum ancillary services capacity during the hour plus the hourly energy component is equal to the maximum wind power produced during the hour.

3. The hourly energy component plus the minimum ancillary services capacity (assumed to be negative) during the hour is equal to the minimum wind power produced during the hour.

We determine q_H, ε_k, $\max(\varepsilon_k)$, and $\min(\varepsilon_k)$ for each hour (using the Matlab fmincon function).

Minimize	$f(q_H, \varepsilon_1, \varepsilon_2, \dots, \varepsilon_4)\colon \sum_{k=1}^{4} \varepsilon_k P_k + P_{UP} \max(\varepsilon_k) + P_{DN} \min(\varepsilon_k)$	(3-2)
Where	$\varepsilon_k = W_k - q_H$	k = 1:4
Subject to	1) $h_k(q_H, \varepsilon_k)\colon q_H + \varepsilon_k = W_k,$	k = 1:4
	2) $g(q_h, \max(\varepsilon_k))\colon q_h + \max(\varepsilon_k) = \max(W_k)$	k = 1:4
	3) $d(q_h, \min(\varepsilon_k))\colon q_h + \min(\varepsilon_k) = \min(W_k)$	k = 1:4

We use ERCOT's balancing energy service (BES) as the prices for P_k. Each hour for P_{UP} we use the minimum of ERCOT's up-regulation price for capacity and responsive reserve price for capacity. Each hour for P_{DN} we use the minimum of ERCOT's down-regulation price for capacity and responsive reserve price for capacity. We use the minimum of the prices because we are trying to find the minimum variability cost of each wind plant in ERCOT.

3.6 Results

Figure 3-2 displays the estimated variability costs of 20 ERCOT wind plants sorted by their capacity factors for 2008. The mean variability cost was $8.73 per MWh (16% of the mean BES price of electricity in ERCOT in 2008) with a standard deviation of $1.26 per MWh. As the capacity factor increases, the variability cost decreases, indicating wind plants sited in locations with good wind resources cost a system less. In 2008, the range of costs for wind plant variability was $6.79 to 11.5 per MWh. We do not observe a dependence of variability costs on the nameplate capacity of a wind plant, although a larger data set with a larger range of nameplate capacities is needed to make a conclusive statement.

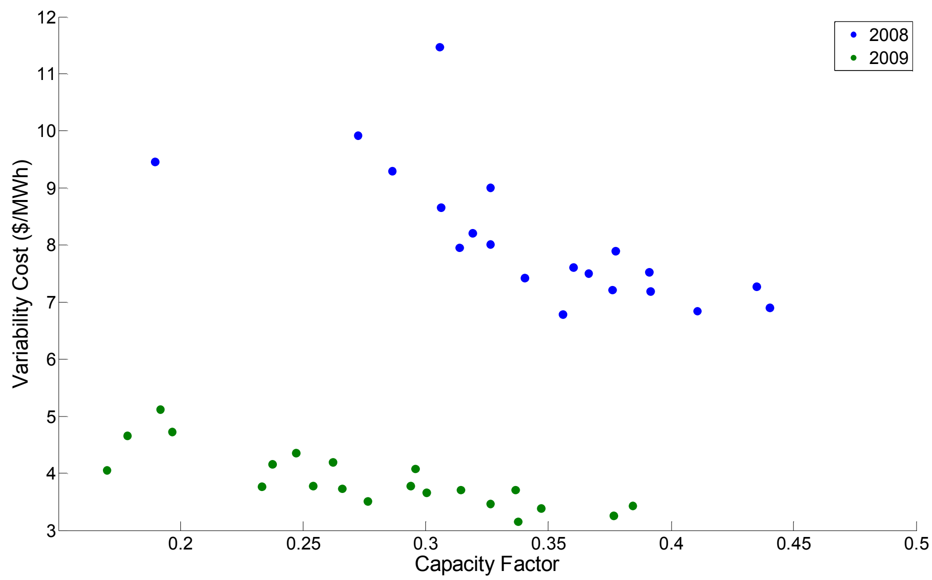

Figure 3-2 - Estimated variability costs for 20 ERCOT wind plants versus their capacity factors for 2008. The variability cost of wind power decreases as the capacity factor of a wind plant increases.

Figure 3-2 also displays the estimated variability costs of 20 ERCOT wind plants sorted by their capacity factors for 2009. The mean variability cost in 2009 was $3.90 per MWh (12% of the mean BES price of electricity in ERCOT in 2009) with a standard deviation of $0.52 per MWh. The same relationship of declining variability costs versus capacity factor is present. In 2009, the range of costs for wind plant variability was $3.16 to 5.12 per MWh. The estimated variability costs for 2009 were substantially lower than the variability costs estimated for 2008 and are a direct result of lower ancillary service prices in 2009 compared to 2008 (see figures 3-14 and 3-15 in appendix B).

Variability costs decline as the capacity factor increases for two reasons. First, we measure variability costs per MWh of wind energy produced and the amount of energy partitioned to ancillary services does not grow as fast as the amount of energy produced by the wind plant. Second, wind turbines produce power from wind based on a cubic power curve (see figure 3-16 in appendix B). As the capacity factor of a wind plant increases, it produces more of its power in region 3 where the turbines produce their maximum power. Actual power curves are not as smooth as the one depicted but nonetheless in region 3 there is less of a chance for significant changes in power output from one minute to the next compared with regions 1 and 2.

We use this cost metric to value the reductions in wind plant variability when wind plants are interconnected to each other. Previous research has shown that wind power variability is reduced as wind plants are interconnected to each other with transmission lines (Katzenstein et al., 2010). We compare the variability costs of individual wind plants to the variability cost of 20 interconnected wind plants. Figure 3-3 shows how the variability costs of wind energy are reduced as wind plants are interconnected. In figure 3-3, we selected the wind plants with the highest, median, and lowest variability costs and then interconnected the remaining 19 wind plants to them based on distance (closest to farthest) and calculated the variability cost after each interconnection.

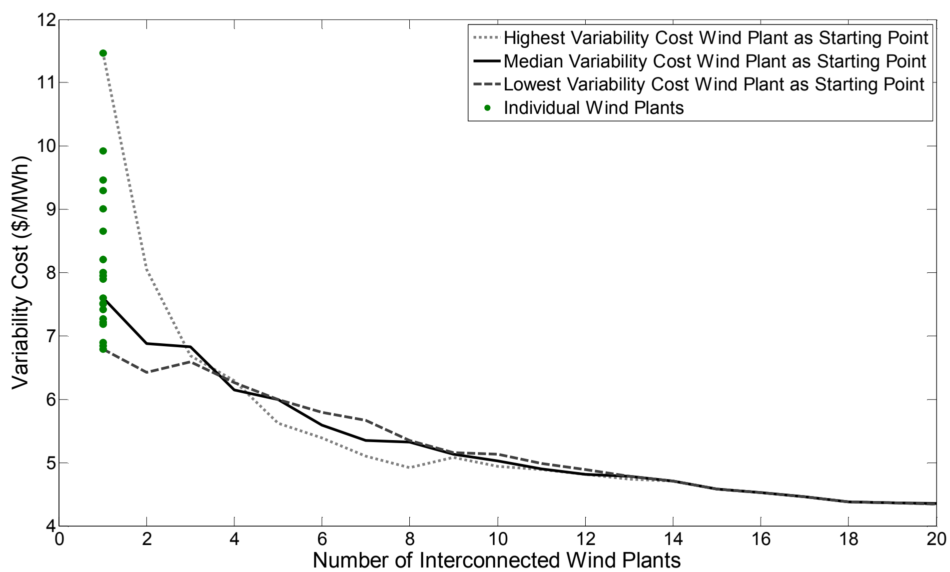

Figure 3-3 - Variability costs of wind energy decrease as wind plants are interconnected. Interconnecting 20 wind plants together produces a mean savings of $3.76 per MWh compared to the 20 individual ERCOT wind plants (green dots). Only 8 wind plants need to be interconnected to achieve 74% of the reduction in variability cost. Three cases are shown where the highest, median, and lowest variability cost wind plants were used as starting points and the remaining 19 wind plants were interconnected to them based on distance (closest to farthest).

In 2008, twenty wind plants interconnected to each other with transmission lines of infinite capacity (sometimes referred to as a copper plate interconnection) have a variability cost of $4.35 per MWh (8.1% of the mean BES price of electricity in ERCOT). Interconnecting twenty wind plants produces a mean savings of $3.76 per MWh compared to the variability costs of individual ERCOT wind plants. A minimum savings of $2.44 per MWh and a maximum savings of $7.15 per MWh are achieved. The majority of the reductions in variability cost are achieved quickly as only 8 wind plants need to be interconnected to obtain the maximum reductions in variability costs. Our estimated load following variability costs for interconnected wind plants are comparable to the load following costs previously determined in integration studies and BPA's integration tariff (Acker, 2007; BPA, 2009; EnerNex Corp., 2007; EnerNex Corp. and Idaho Power Co., 2007; PacificCorp, 2007; Puget Sound Energy, 2007).

As seen in figure 3-4, the marginal benefit of interconnecting another wind plant decreases rapidly as more wind plants are interconnected. The marginal benefit of interconnecting another wind plant is less than $3.43 per MWh for 1 wind plant already interconnected, less than $1.36 per MWh for 2 wind plants, less than $0.7 per MWh for 3-7 wind plants, and less than $0.19 per MWh for 8 or more wind plants. If the worst case (Highest Variability Cost Wind Plant as Starting Point) is excluded, the marginal benefit of interconnecting another wind plant is less than $0.72 per MWh for 1 wind plant already interconnected, less than $0.05 per MWh for 2 wind plants, less than $0.68 per MWh for 3-7 wind plants, and less than $0.19 per MWh for 8 or more wind plants.

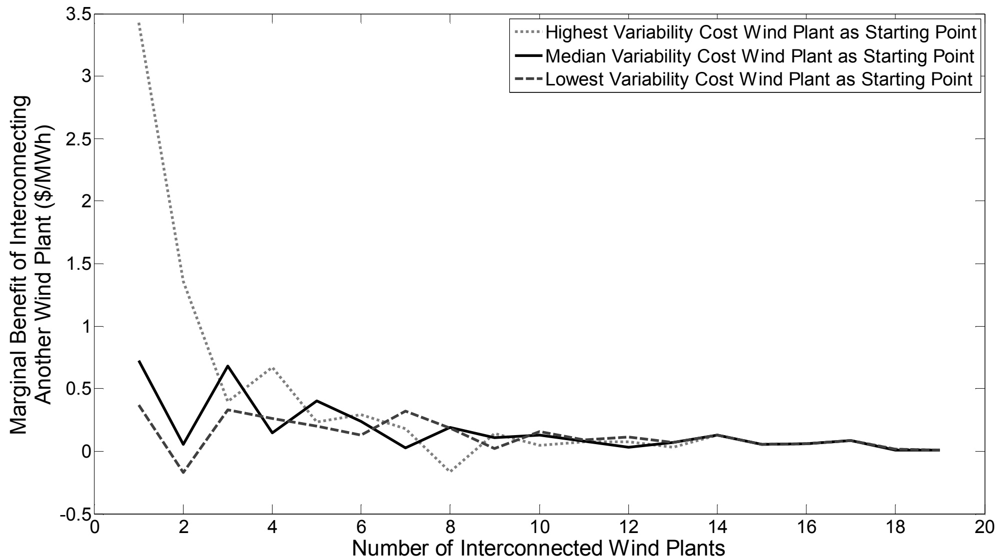

Figure 3-4 - Marginal benefit of interconnecting an additional wind plant in reducing variability costs. For example, with one wind plant interconnected to a system, the maximum marginal benefit of interconnecting another wind plant is $3.43 per MWh.

The reduction in integration costs is sometimes used as a reason for building large transmission lines to remote locations (for example, see EnerNex, 2010). We estimate how much farther a system would be willing to build a transmission line to interconnect a wind plant based on how much it reduces wind variability costs. We modeled the cost of transmission lines based on data from Fertig and Apt (2010) and found a quadratic equation, with input variables distance and transmission line capacity, produced the best fit (adj. R^2 of 0.84) (equation 3-3). In order to estimate how many additional miles a system would be willing to extend their transmission line, we first calculated the cost of a transmission line to a location 100 miles away. We then calculate the present value of a wind plant's interconnection benefit using a discount rate of 0.1, a transmission line capacity of 2000 MW, and lifetime of 30 years for the transmission line. We add the resulting PV benefit to the cost of the transmission line and calculate how long the new transmission line is. The difference in distance between the old and new transmission line distances is the maximum distance a system would be willing to build a transmission line to interconnect the wind plant solely to recapture the reduction in variability costs.

$$C_{Transmission} = \$1{,}000{,}000 + P * D(840 - 0.62D) \qquad (3\text{-}3)$$

Where $C_{Transmission}$ = the cost of transmission line

P = the capacity of transmission line

D = the distance of transmission line.

A system should not be willing to build transmission lines to interconnect wind plants to reduce their load following variability costs (figure 3-5). A system with less than 10 wind plants would initially be willing to build a transmission line an additional 2-5 miles to interconnected wind plants and reduce their variability costs. When more than 10 wind plants are interconnected, a system would be willing to extend a transmission line at most 2 mile to reduce their wind integration costs.

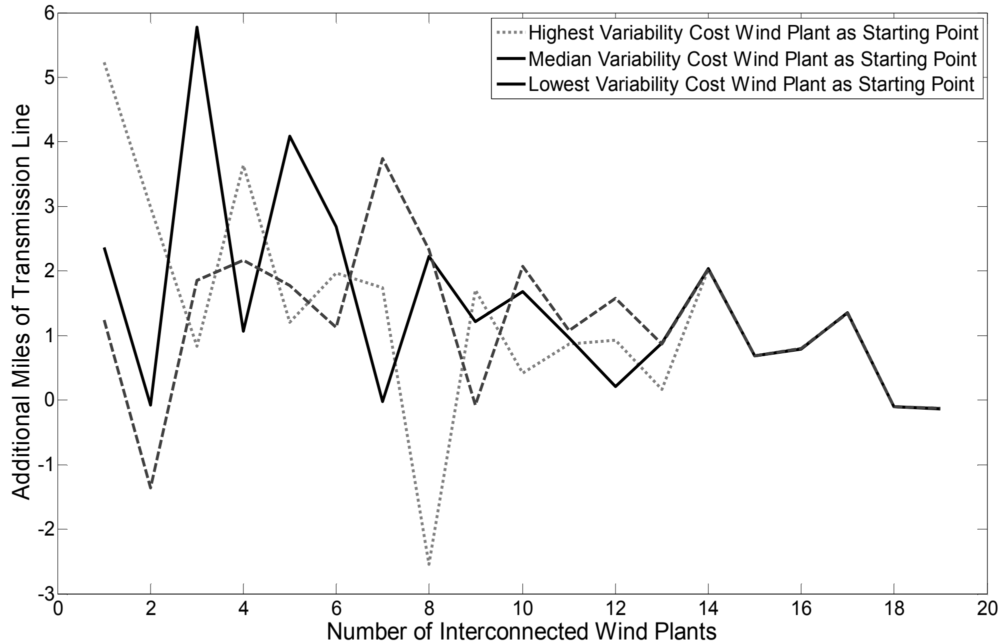

Figure 3-5 - Marginal benefit of interconnecting an additional wind plant valued in terms of miles ERCOT would be willing to extend a 2GW, 100 mile transmission line.

Figure 3-6 displays how the rankings of wind plants based on their variability costs change from 2008 to 2009. For 2008, we ranked the 20 ERCOT wind plants based on their estimated variability costs and assigned the labels A through T to the 20 wind plants, with A being the wind plant with the highest variability cost and T being the wind plant with the lowest variability cost. For 2009, we reordered the wind plants based on their variability costs. The labels were kept the same in order to track how the rankings changed. The grey lines are visual guides to help the reader track the changes.

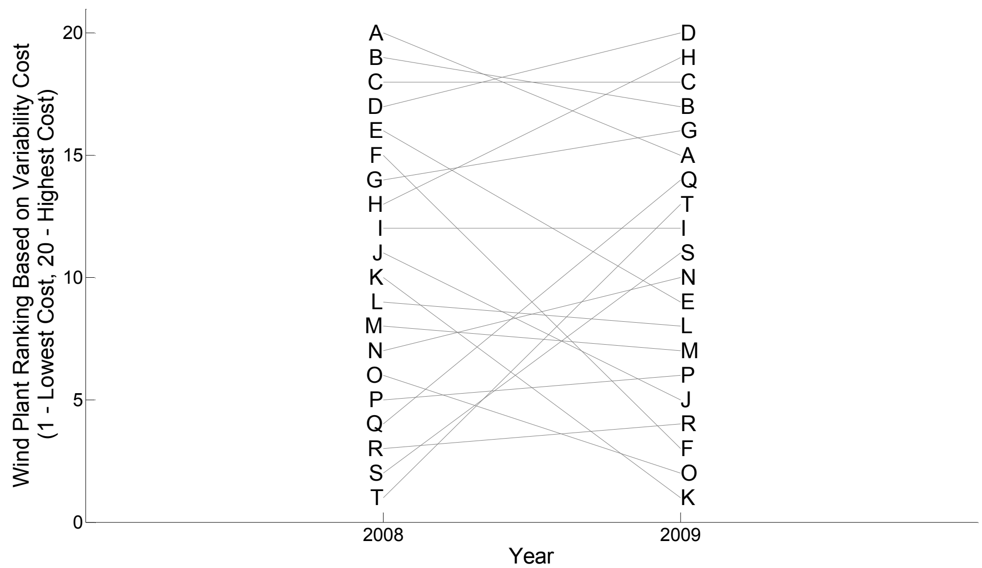

Figure 3-6 - The change in wind plant ranking of variability cost from 2008 to 2009. For 2008 (left side), we ranked the 20 ERCOT wind plants based on their estimated variability costs and assigned the labels A through T to the 20 wind plants, with A being the wind plant with the highest variability cost and T being the wind plant with the lowest variabilty cost. For 2009 (right side), we reordered the wind plants based on their variability costs but kept the labels the same.

As seen in figure 3-6, ERCOT wind plants significantly change their rankings from 2008 to 2009. Three of the 4 least cost wind plants in 2008 become 3 of the 10 wind plants with the highest variability cost. Eight of the 20 wind plants change their rank by two spots or less. This indicates some wind plants are persistent in their variability costs while others vary significantly year to year. A longer data set is required to determine conclusively if there are wind plants that have consistent variability costs. The significant reordering of wind plants from 2008 to 2009 is because of the change in power output of the wind plants from 2008 to 2009. Our results are insensitive to yearly changes in ancillary service prices (see appendix B).

3.7 Conclusions

We have developed a cost metric capable of estimating the variability cost of individual wind plants from observed 15-minute power output data and found it produces results similar to integration studies produced by the major electricity market operators in the United States. Wind plants with higher capacity factors have lower variability costs and cost a system less to integrate. We find that the relative ranking of wind plants based on variability costs is dependent on the wind power produced from the wind plants and not on ancillary service prices.

We have also provided a method to value reductions in wind power variability. Interconnecting 20 wind plants produced a mean savings of $3.76 per MWh. Our cost metric can be used to evaluate the cost-effectiveness of storage solutions[8] to mitigate wind power variability. Systems can use the methods we developed to determine if building long transmission lines to good wind sites is cost-effective. Our estimates for wind power variability costs do not include the regulation costs of wind. Future work should extend our analysis to examine how much regulation adds to wind power variability costs. In addition, future work should examine how variability costs plus uncertainty (forecast error) costs compare to wind integration costs.

System operators need to determine if the cost of variability from wind plants should be socialized or assigned to wind plants. Currently in most systems rate payers are providing a subsidy to the wind industry by paying for the integration costs of wind energy. BPA, on the other hand, determined the wind plants in their system should pay for the cost of integrating their power and is recovering wind integration costs ex-ante with a flat tariff applied equally to all wind plants in its system. If other systems follow BPA's example, system operators will have to decide if they want to recover wind integration costs ex-ante or ex-poste. By recovering integration costs ex-ante, systems can provide wind plants with more certainty on how much they will have to pay over the course of a year, however wind plants may then pay more (or less) than what it actually cost to integrate their power into a system. By recovering costs ex-poste, wind plants will pay each year what it actually

[8] Batteries in preproduction development scale currently have projected costs of less than $10 per MWh for greater than 10,000 cycles. How much lower than $10 per MWh their costs are is to be determined as well as whether they are cost effective solutions for mitigating wind power variability.

cost to integrate their power into a system. Ex-poste recovery would inject a significant amount of uncertainty into wind plant financial pro formas and would make it more difficult for wind plants to obtain financing.

System operators must also determine whether a flat tariff (such as BPA's tariff) or a capacity factor based tariff indexed to the price of electricity is appropriate to recover integration costs. Figure 3-2 supports a capacity factor based tariff indexed to the price of electricity. Variability costs decline as the capacity factor of a wind plant increases so wind plants with higher capacity factors should pay less than wind plants with lower capacity factors. In addition, wind integration costs vary significantly year to year (figures 3-14 and 3-15) and any tariff should be indexed to the price of electricity to capture this variation. Yet, as figure 3-4 shows, the variability cost of 20 interconnected wind plants is less than the sum of the 20 individual wind plant variability costs, so even lower capacity factor plants contribute to reduced integration costs (although the marginal benefit of smoothing by interconnection of more than a few plants is minimal). Additionally, systems should offer a reduced tariff to wind plants that actively mitigate their variability to encourage the development of market based solutions to minimize wind power variability.

Finally, if system planners can identify wind plants in their interconnection queues with the highest capacity factors they could take an active approach to decrease their integration costs by giving priority to these projects. While the benefit a wind plant adds to a system is more complicated than just its projected variability cost (for example, transmission costs are important) system planners should have the ability to prioritize projects within their queue based on the benefits they provide. Wind plants should also be given priority in the interconnection process if they implement flexible technologies to mitigate their variability costs.

3.8 References

Acker, T., 2007. Arizona Public Service Wind Integration Cost Impact Study. Arizona Public Service Company.

Apt, J., 2007. The Spectrum of Power from Wind Turbines. *J. of Power Sources*, 169(2): 369-374.

BPA, 2009. "BPA announces rate changes." Bonneville Power Authority, News Releases, PR 31 09. Available: http://www.piersystem.com/go/doc/1582/292435/

DeCarolis, J., Keith, D., 2005. The Costs of Wind's Variability: Is There a Threshold? *The Electricity Journal*, 18: 69-77. Available: http://people.ucalgary.ca/~keith/papers/72.Decarolis.2005.Threshold.e.pdf

Denholm, P., 2005. Emissions and Energy Efficiency Assessment of Baseload Wind Energy Systems. *Environ. Sci. Technol.*, 39(6): 1903-1911.

EIA, 2010. Annual Energy Review. US Energy Information Agency.

EnerNex Corporation, 2010. Eastern Wind Integration and Transmission Study: Executive Summary and Project Overview. EnerNex Corporation, NREL/SR-550-47086. Available: http://www.nrel.gov/wind/systemsintegration/pdfs/2010/ewits_executive_summary.pdf

EnerNex Corporation, 2007. Final Report Avista Corporation Wind Integration Study. EnerNex Corporation.

EnerNex Corporation, Idaho Power Company, 2007. Operational Impacts of Integrating Wind Generation into Idaho Power's Existing Resource Portfolio: Report Addendum. Idaho Power Company.

Fertig, E., Apt, J., 2010. Compensating for Wind Variability Using Co-Located Natural Gas Generation and Energy Storage. Carnegie Mellon Electricity Industry Center Working Paper CEIC-10-01.

Hirst, E., Kirby, B., 1997. Creating Competitive Markets for Ancillary Services. Oak Ridge National Laboratory, ORNL/CON-448. Available: http://www.ornl.gov/sci/btc/apps/Restructuring/con448.pdf

Hittinger, E., Whitacre, J.F., Apt, J., 2010. Compensating for Wind Variability Using Co-Located Natural Gas Generation and Energy Storage. Carnegie Mellon Electricity Industry Center, Working Paper.

ISO New England, 2009. 2008 Annual Market Report. Internal Market Monitoring Unit of ISO New England.

Katzenstein, W., Fertig, E., Apt, J., 2010. The Variability of Interconnected Wind Plants. *Energy Policy*, 38(8): 4400-4410.

Katzenstein, W., Apt, J., 2009. Air Emissions Due to Wind and Solar Power. *Environmental Science and Technology*, 43(2):253-258.

Kirby, B., Milligan, M., 2006. Cost-Causation-Based Tariffs for Wind Ancillary Service Impacts. WINDPOWER 2006, June 4-7, Pittsburgh, PA. Available: http://www.nrel.gov/wind/pdfs/40073.pdf

Korpass, M., Holen, A.T., Hildrum, R., 2003. Operation and Sizing of Energy Storage for Wind Power Plants in a Market System. *Electrical Power and Energy Systems*, 25(8): 599-606.

Northwest Power and Conservation Council, 2007. The Northwest Wind Integration Action Plan. Available: http://www.nwcouncil.org/energy/wind/library/2007-1.pdf

NWCC, 2008. Transmission Update. National Wind Coordinating Collaborative, April.

PacifiCorp, 2007. Technical Appendix for the 2007 Integrated Resource Plan. PacifiCorp.

PJM, 2009. A Review of Generation Compensation and Cost Elements in the PJM Markets. PJM RTO.

Potomac Economics, 2009. 2008 State of the Market Report for the ERCOT Wholesale Electricity Markets.

Puget Sound Energy, 2007. 2007 Integrated Resource Plan, Appendix G – Wind Integration Studies. Puget Sound Energy.

Wiser, R., Bolinger, M., 2008. *2008 Wind Technologies Market Report.* US DOE. Available: http://eetd.lbl.gov/ea/emp/reports/2008-wind-technologies.pdf

Smith, J., Parson, B., Acker, T., Milligan, M., Zavadil, R., Schuerger, M., DeMeo, E., 2007. Best Practices in Grid Integration of Variable Wind Power: Summary of Recent US Case Study Results and Mitigation Measures. EWEC, Milan, Italy, May 2007.

3.9 Appendix B

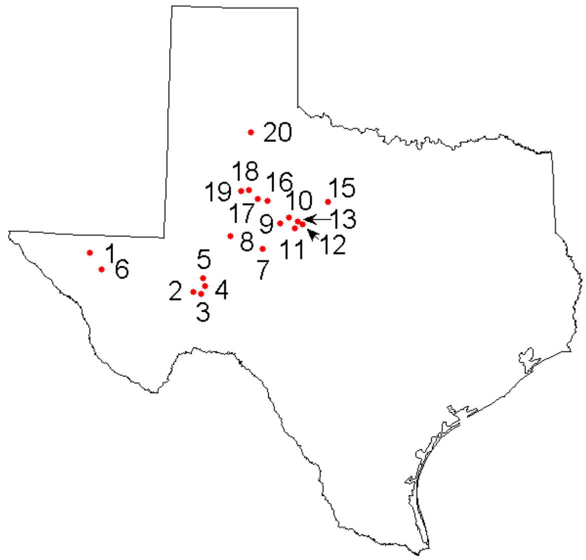

Figure 3-7 - Location of the 20 ERCOT wind plants in Texas

Table 3-1 - Mean and Median values for ERCOT's Down Regulation (DR), Up Regulation (UR), and Balancing Energy Service (BES)

Year	*2004*	*2005*	*2006*	*2007*	*2008*	*2009*
Mean DR ($/MW)	11.09481	19.60145	7.961669	8.297936	19.51802	7.251425
Mean UR ($/MW)	11.47404	18.94291	15.24432	13.13814	22.70802	9.701911
Mean BES ($/MW)	41.79429	66.37815	51.35951	52.21617	53.53612	25.77374
Median DR ($/MW)	7.98	13.5	6.19	7.26	16.8	5.01
Median UR ($/MW)	9	14.425	11.555	9.89	15.265	6.03
Median BES ($/MWh)	39.06	55.29	45.02	48.13	49.39	23.08

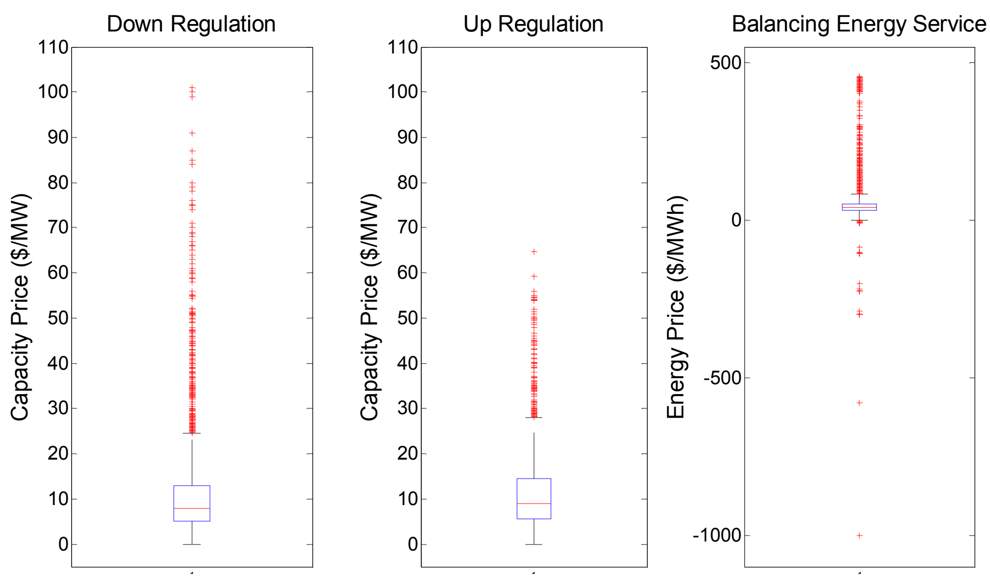

Figure 3-8 - Box plots for 2004 ERCOT ancillary service prices

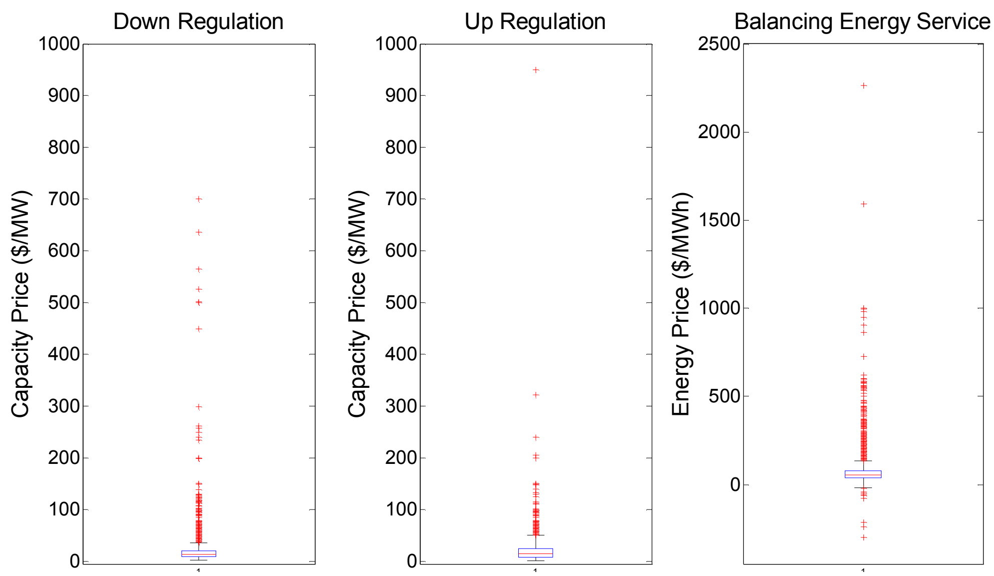

Figure 3-9 - Box plots for 2005 ERCOT ancillary service prices

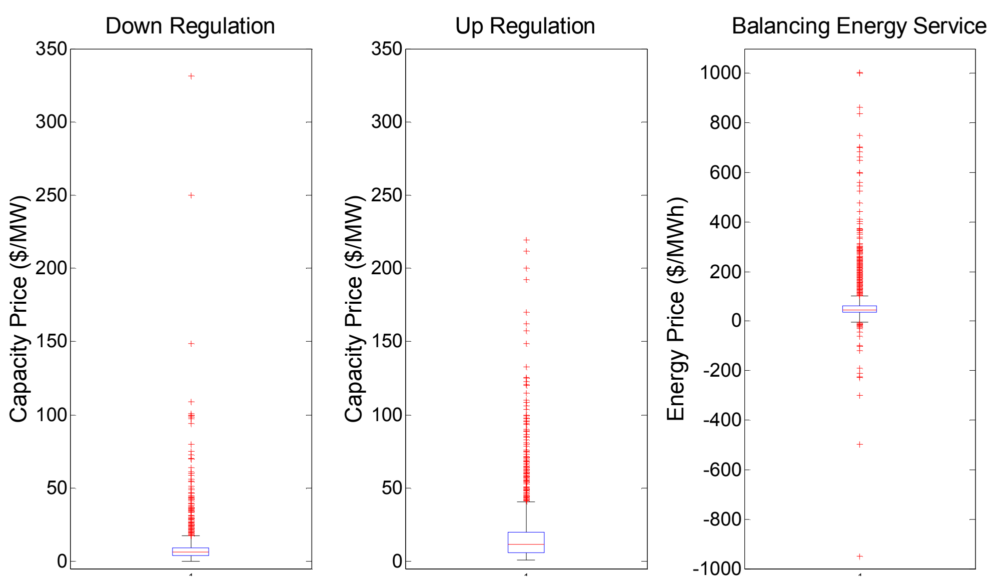

Figure 3-10 - Box plots for 2006 ERCOT ancillary service prices

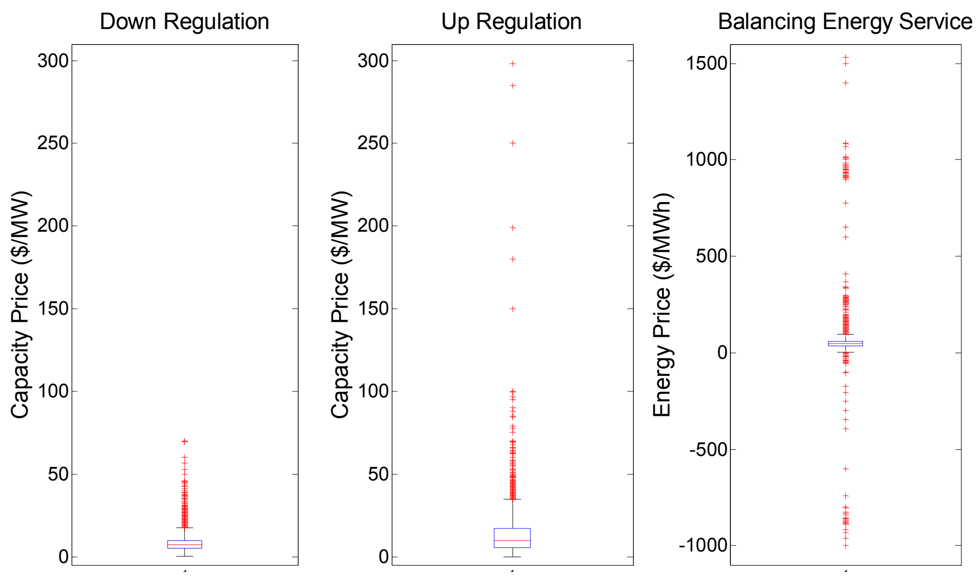

Figure 3-11 - Box plots for 2007 ERCOT ancillary service prices

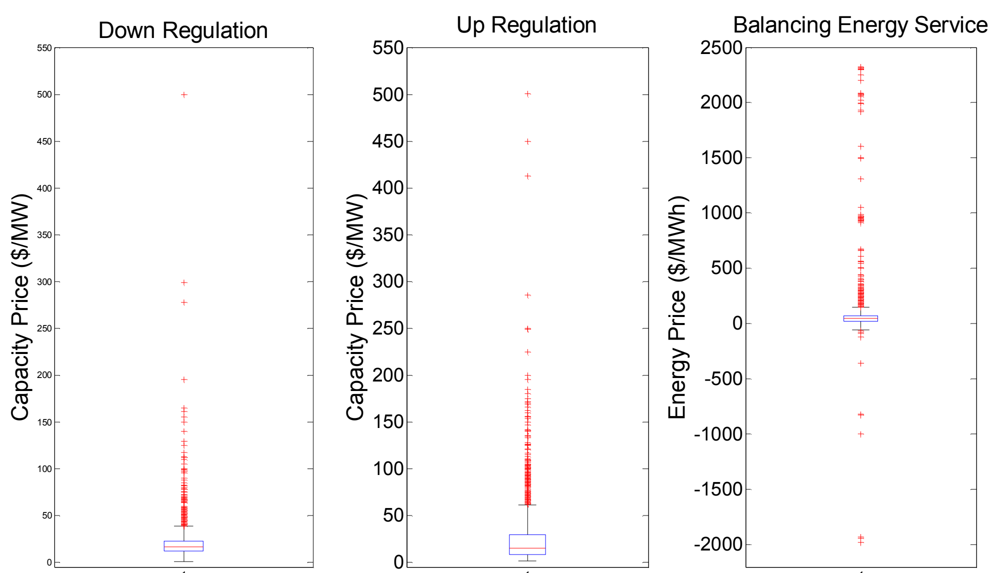

Figure 3-12 - Box plots for 2008 ERCOT ancillary service prices

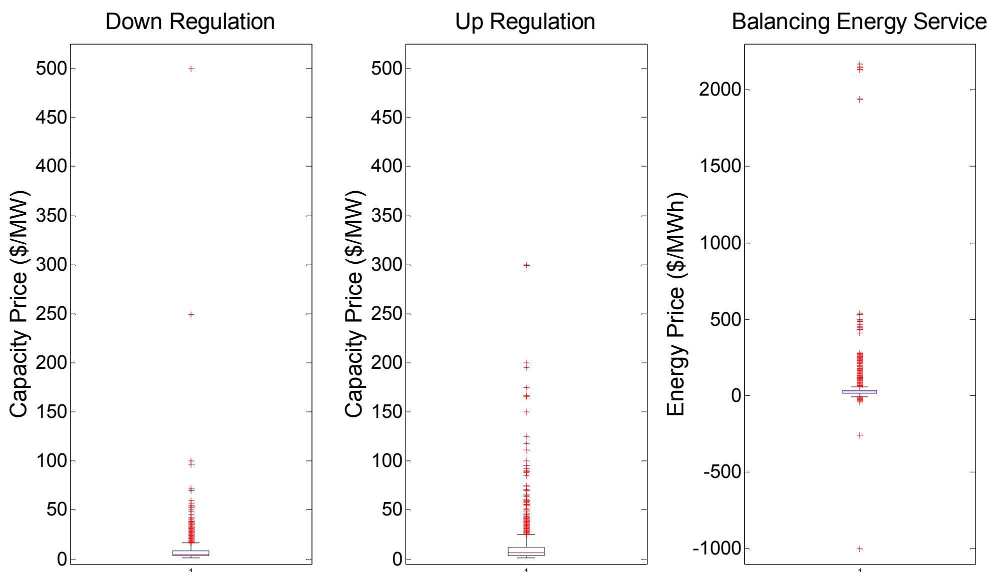

Figure 3-13 - Box plots for 2009 ERCOT ancillary service prices

The wind power data for the 20 ERCOT wind plants spanned 2008 and 2009 yet the ancillary service prices spanned 2004 through 2009. Each subplot in figure 3-14 displays the estimated variability costs when the 20 ERCOT wind plants in 2008 and the displayed year of ancillary service prices are used as inputs to the cost metric. Figure 3-14 shows the sensitivity of our metric to six years of varying price signals. Each year the same relationship of declining variability costs as capacity factors increase is seen. The range of results is dependent on the price of the ancillary services each year. Years 2005 and 2008 had the highest ancillary service prices and as a result, our metric estimates the highest variability cost for the 20 ERCOT wind plants for 2005 and 2008. The converse is true for 2009 ancillary service prices. Similar results were obtained using 2009 ERCOT wind data (figure 3-15).

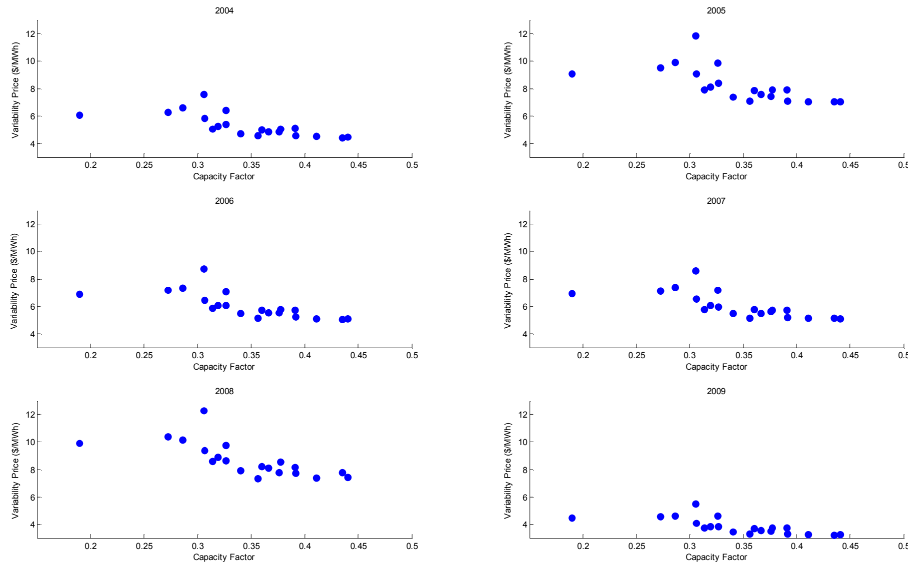

Figure 3-14 - Sensitivity of our 2008 wind power results to different years of ancillary price data

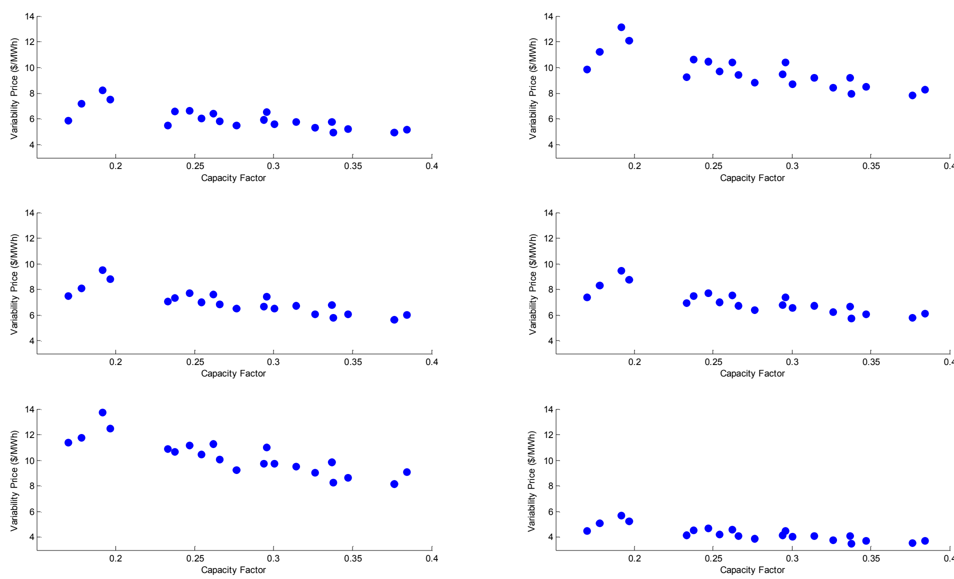

Figure 3-15 - Sensitivity of our 2009 wind power results to different years of ancillary price data

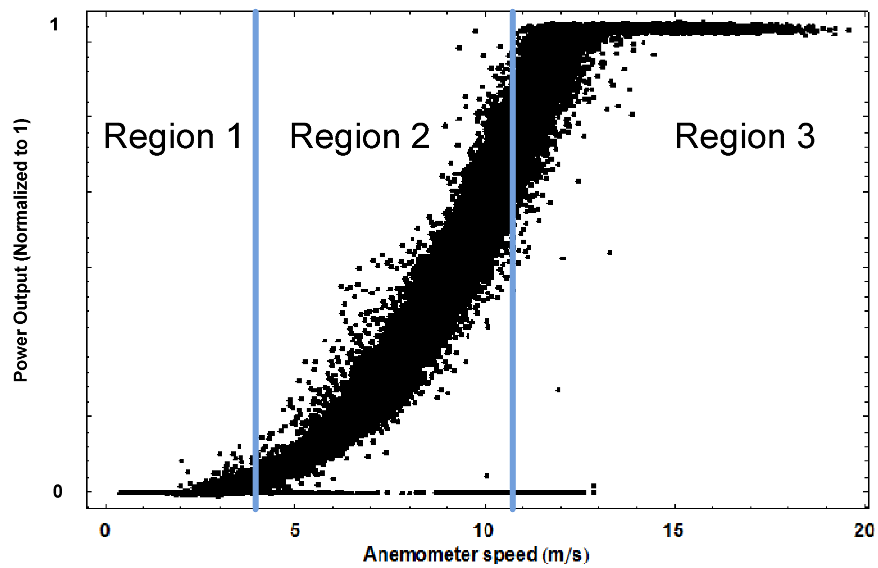

Figure 3-16 - Actual power curve for a wind turbine

As seen in figure 3-17, a wind plant's rank is insensitive to ancillary price data. In other words, wind plant A, the wind plant with the highest estimated variability cost using 2004 ancillary price data and 2008 wind power data, had the highest variability cost in all six years. Fourteen of the twenty wind plants change their rank by two spots or less over a six year span. The greatest change is by wind plant T when from 2006 to 2008 it changed 5 spots then returned to its original rank in 2009. This indicates our results are sensitive to the energy output of the wind plants rather than ancillary service prices. Similar results were obtained using 2009 ERCOT wind data (figure 3-18).

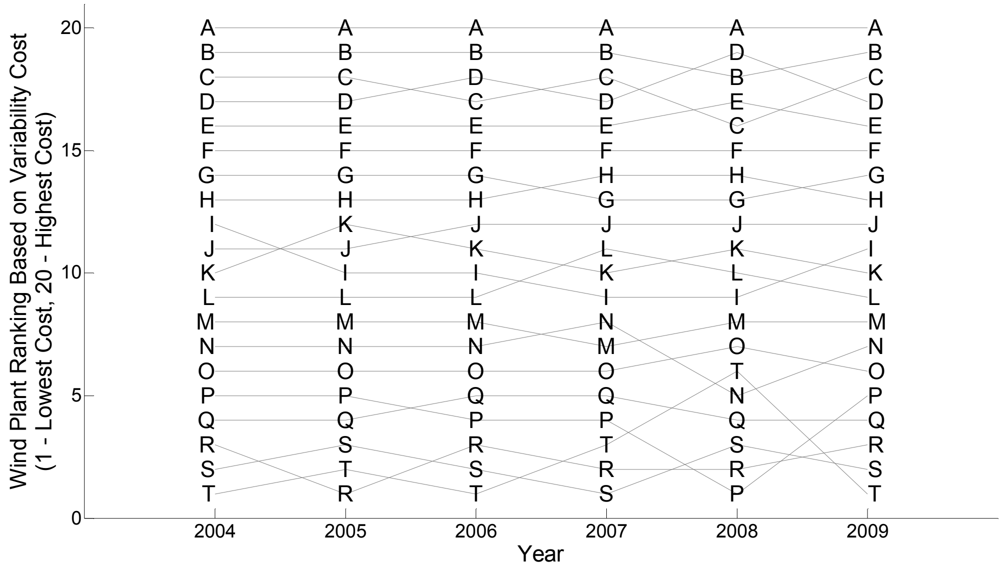

Figure 3-17 - Change in 2008 wind plant rankings based on variability cost for six different years of ancillary service prices

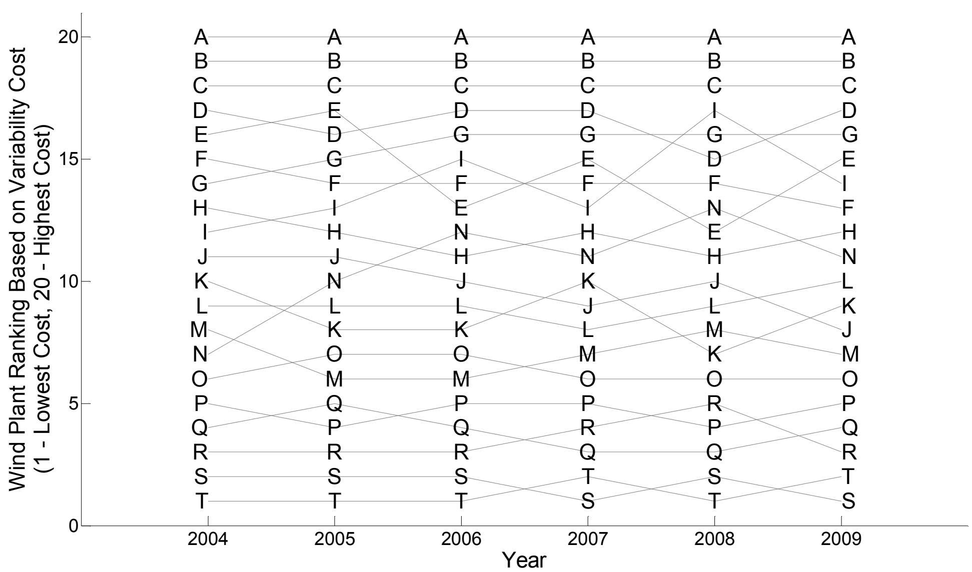

Figure 3-18 - Change in 2009 wind plant rankings based on variability cost for six different years of ancillary service prices

Figure 3-19 displays the results if the ancillary service prices are kept constant and the ERCOT wind energy data set is varied. Figure 3-19 is the sorted variability costs of 2008 ERCOT wind and ancillary price data on the left and 2009 ERCOT wind and ancillary price data on the right. Similar to figure 3-17, the 2008 ERCOT wind data results were sorted by variability costs and labeled

A through T with A being the wind plant with the highest variability cost and T being the wind plant with the lowest variability cost. The labels were kept the same for the 2009 wind data but reordered based on the 2009 variability costs.

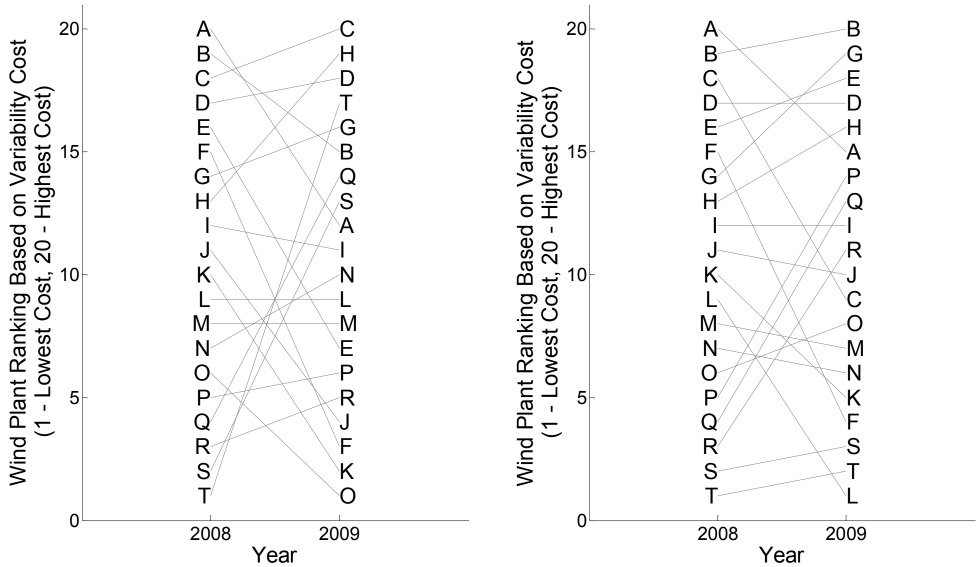

Figure 3-19 - Change in wind plant rankings when the ancillary price data is held constant. In the left subplot, 2008 ancillary price data was used with 2008 and 2009 wind power data. In the right subplot, 2009 ancillary service prices were used with 2008 and 2009

Compared to figures 3-17 and 3-18, the ranking of wind plants based on variability costs in figure 3-19 significantly changes order indicating the relative variability costs of wind plants are dependent on the wind data and not the ancillary service price data. In other words, some wind plants produce wind power that costs a system more to integrate than other wind plants and the set of wind plants that do change from year to year. The implications of this result is that a flat tariff, such as the one BPA imposed, is not an unreasonable method to recoup the integration costs of wind energy. Interestingly, about half of the ERCOT wind plants significantly change their rank from 2008 to 2009 while others do not. This indicates some wind plants are persistent in their variability costs while others vary significantly year to year although a longer wind data set is required to determine anything conclusively.

Chapter 4 - Air Emissions Due to Wind and Solar Power

4.1 Chapter Information

Authors: Warren Katzenstein and Jay Apt

Published Jan 2009 in *Environmental Science and Technology*.

Citation: Katzenstein, W., Apt, J., 2009. Air Emissions Due to Wind and Solar Power. *Environ. Sci. Technol.*, 43(2), p.253-258.

Section 4.8 was published July 2009 in *Environmental Science and Technology.*

Citation: Katzenstein, W., Apt, J., 2009. Response to "Comment on 'Air Emissions Due to Wind and Solar Power.'" *Environ. Sci. Technol.*, 43(15), p.6108-6109.

4.2 Abstract

Renewables portfolio standards (RPS) encourage large scale deployment of wind and solar electric power, whose power output varies rapidly even when several sites are added together. In many locations, natural gas generators are the lowest cost resource available to compensate for this variability, and must ramp up and down quickly to keep the grid stable, affecting their emissions of NO_x and CO_2. We model a wind or solar photovoltaic plus gas system using measured 1-minute time resolved emissions and heat rate data from two types of natural gas generators, and power data from four wind plants and one solar plant. Over a wide range of renewable penetration, we find CO_2 emissions achieve ~80% of the emissions reductions expected if the power fluctuations caused no additional emissions. Pairing multiple turbines with a wind plant achieves ~77 to 95% of the emissions reductions expected. Using steam injection, gas generators achieve only 30-50% of expected NO_x emissions reductions, and with dry control NO_x emissions increase substantially. We quantify the interaction between state RPSs and constraints such as the NO_x Clean Air Interstate Rule (CAIR), finding that states with substantial RPSs could see upward pressure on CAIR NO_x permit prices, if the gas turbines we modeled are representative of the plants used to mitigate wind and solar power variability.

4.3 Introduction

Renewable electricity generated by sources whose output varies rapidly – wind and solar photovoltaic – provided 0.65% of the United States' 2006 net electricity generation (DOE, 2007), but these sources are growing. Renewables portfolio standards (RPSs), enacted by 25 states, along with federal subsidies, have encouraged renewable energy sources (DSIRE, 2008; Rabe, 2006; Wiser and Bolinger, 2007). California requires that 20% of its electric power be generated from renewables by 2010, New Jersey 12% by 2012, and Texas ~ 3% by 2015 (California State Senate, 2002; Fraser, 2005; NJ Board of Public Utilities, 2006).

When these sources provide a significant fraction of electricity, other generators or rapid demand response must compensate when their output drops (Apt, 2007; Curtright and Apt, 2008). Renewable energy emissions studies (Keith et al., 2003; National Research Council of the National Academies, 2007; UNFCCC, 2007) have not accounted for the change in emissions from power sources that must be paired with variable renewable generators such as wind and solar. In many locations, natural gas turbines will be used to compensate for variable renewables. When turbines are quickly ramped up and down, their fuel use (and thus CO_2 emissions) may be larger than when they are operated at a steady power level. Systems that mitigate other emissions such as NO_x may not operate optimally when the turbines' power level is rapidly changed.

Renewables that substitute for fossil generators avoid emissions (emissions displacement). Life cycle assessments (LCAs) estimate the emissions attributed to producing, constructing, operating, maintaining, and decommissioning a given technology (Weisser, 2007). Although integration studies have discussed increased reserve requirements for variable renewable sources, Weisser notes the resulting ancillary emissions are not typically included in LCAs (Weisser, 2007).

Two methods used to identify the displaced generators are economic dispatch analysis and generation portfolio analysis (Keith et al., 2003). Economic dispatch analysis assumes the displaced generators are those with the highest marginal costs of operation (transmission constraints are considered in a few studies). Typically these generators are natural gas and oil fired turbines, although coal plants are on the margin at times (PJM-MMU, 2008). In portfolio analysis the emissions displaced are the differences in a system's generation portfolio before and after variable renewable power is added. That approach assumes a renewable plant displaces generation equally from all assets, not solely from the generators operating on the margin (National Research Council of the National Academies, 2007).

LCAs and emissions displacement studies use emissions factors (kg of pollutant per MWh) to calculate produced or displaced emissions. When fossil-fuel generators are used to compensate for renewables' variability, their emissions are likely to be underestimated by emissions factors calculated for full-power steady-state operations.

Denny and O'Malley (2006) modeled emissions reductions from wind power penetration using an economic dispatch model for Ireland and an emissions factor that varies with turbine power for a natural gas combined-cycle turbine (NGCC) and a simple-cycle natural gas combustion turbine (CT), concluding that CO_2 would be reduced 9% for a wind penetration factor of 11% (82% of the expected reduction for that penetration of wind) and NO_x emission reductions would be 90% of the expected reductions. Their model uses hourly data sets that are not able to capture a portion of the rapid fluctuations of wind (Apt, 2007) and does not depend on ramp rate; they did not examine the effects of different NO_x mitigation methods.

4.4 Model

To estimate emissions from fossil fuel generators used to compensate for variable wind and solar power, we model the combination of variable renewable power with a fast-ramping natural gas turbine to provide baseload power. We use a regression analysis of measured emissions and heat rate data taken at one minute resolution from two types of gas turbines to model emissions and heat rate as a function of power and ramp rate (appendix C). The required gas turbine power and ramp rate to fill in the variations in one minute data from four wind plants and one large solar photovoltaic (PV) plant are determined, then the emissions are computed from the regression model. The system emissions are compared to the emissions of a natural gas plant of the same size, and to the emissions reductions expected from displacement analysis.

4.5 Data

We obtained 1-minute resolution emissions data for seven General Electric LM6000 natural gas combustion turbines and two Siemens-Westinghouse 501FDs natural gas combined-cycle turbines. The LM6000 CTs have a nameplate power limit of 45 MW and utilize steam injection to mitigate NO_x emissions. A total of 145 days of LM6000 emissions data was used in the regression analysis. The Siemens-Westinghouse 501FD NGCC turbines have a nameplate power limit of 200 MW with GE's Dry Low NO_x system (lean premixed burn) and an ammonia selective catalytic reduction system for NO_x control. Emissions data for 11 days were obtained for the 501FD NGCC.

The renewables data includes 1-second, 10-second, and 1-minute resolution and is from four wind plants and one large solar photovoltaic facility located in the following regions in the United States: Eastern Mid-Atlantic, Southern Great Plains, Central Great Plains, Northern Great Plains, and Southwest (table 4-8 in appendix C).

4.6 Approach

The objective of the model plants is to maintain a constant power output by minimizing the error ε between the expected output and the realized output of the model plant at time *i* (equation 4-1). The gas turbine model is subject to physical operating constraints: the upper and lower power limits (equation 4-6) and how quickly the turbine can change its power output (equation 4-7). As discussed in appendix C, the emission and heat rate data we obtained for the gas turbines did not cover all combinations of power and ramp rate. We therefore further constrain the model to operate only in regions of the power-ramp rate space for which we have data. Here we focus on estimating the additional emissions caused by variability, and caution that we have made no attempt to ensure the stability of an electrical grid. Grid dynamic response may somewhat change our results.

$$Min\ \varepsilon_{P,i} = Min\left|P_{GT,i} - P_{\mathrm{I},i} - \varepsilon_{P,i-1}\right| \tag{4-1}$$

where:

$$\begin{aligned} \varepsilon_{P,i} &\equiv Error\ in\ Power\ Plant\ Output \\ P_{\mathrm{I},i} &\equiv Ideal\ Power\ Plant\ Output \\ P_{A,i} &\equiv P_{W,i} + n \cdot P_{GT,i} \\ &= Wind\ Power + Natural\ Gas\ Power \\ &\equiv Actual\ Power\ Generated \\ i &\equiv time\ index \\ n &\equiv Number\ of\ Gas\ Turbines \end{aligned} \tag{4-2}$$

$$\dot{P}_{GT} \equiv \frac{dP_{GT}}{dt} \equiv Ramp\ rate\ of\ Gas\ Turbine \tag{4-3}$$

Subject to:

$$P_A = \text{Constant} \tag{4-4}$$

$$Max\ (P_W) = Max\ (n \cdot P_{GT}) \tag{4-5}$$

$$P_{Min} < P_{GT} \leq P_{Max} \tag{4-6}$$

$$\dot{P}_{Min} \leq \dot{P}_{GT} \leq \dot{P}_{Max} \tag{4-7}$$

We average the wind data to 1-minute resolution to match the time resolution of the natural gas generator emissions data and scale each wind or PV data set's maximum observed power generated during the data set to the nameplate capacity of the paired natural gas turbine. From each renewable data set we calculate the required power levels and ramp rates of the natural gas turbine needed to keep the output of the baseload power plant constant. The operating and data constraints of the natural gas turbine are applied, causing the model gas generator's output power to differ slightly from this ideal power profile, as it would in practice.

The power level and ramp rate of the turbine are used as inputs for an emissions model based on a multiple regression analysis of the measured emissions of two types of natural gas turbines. We model only NO_x and CO_2 emissions from the turbine. Power plant CO emissions account for less than one percent of CO emissions in the United States and are not considered in our analysis (Masters, 1997).

We calculate CO_2 emissions from the measured heat rate of the generator and the type of fuel used. Assuming complete combustion, the CO_2 emission rate can be derived from the heat rate by multiplying by EIA's natural gas conversion factor of 0.053 metric tons of CO_2 per MMBTU (DOE, 2001a). Although operating a turbine at low or medium power loads generally results in incomplete combustion, assuming complete combustion is a reasonable approximation for calculating CO_2

emissions, since most CO and hydrocarbon radicals are oxidized to CO_2 in the atmosphere (Seinfeld and Pandis, 2006). Using one-minute resolution emissions data obtained from an electric generation company for two types of gas turbines, we modeled CO_2 emission rates as a function of power level and ramp rate. We use the emissions models to calculate the mass emitted during a given time interval and sum over all time intervals to obtain the mass emitted during a simulation:

$$M = \sum_{t=1}^{T} \frac{dM_t}{dt} \Delta t \qquad (4\text{-}8)$$

where:

$$M = \text{Total Mass of Pollutant Emitted}$$

$$\frac{dM_t}{dt} = f(P_{GT,t}, \dot{P}_{GT,t}) \qquad (4\text{-}9)$$
$$= \text{Mass Emission Rate of Gas Turbine for Time Period } t$$

$$\Delta t = \text{Time Interval of Data Set}$$

$$T = \text{Time Length of Data Set}$$

4.7 Results

If a given level of penetration α of wind or solar energy causes no additional emissions from gas generators, we can define the mass of expected emissions (ϕ) in terms of the mass of emissions from the gas units (M_{GT}) as

$$\phi = M_{GT} * (1-\alpha) \qquad (4\text{-}10)$$

The expected emissions reductions are $M_{GT} * \alpha$. That is, emissions are expected to be displaced linearly according to the penetration factor of the renewables, an assumption we refer to as equivalent displacement. Dividing equation 4-10 by the energy produced, we define the emissions expected predicted by an equivalent displacement model:

$$\varphi_F = \frac{\varphi}{\sum_{time} P} \qquad (4\text{-}11)$$

If the actual system mass emissions are M_A then the fraction of expected emissions reductions (η) that are achieved is

$$\eta = \frac{(M_{GT} - M_A)}{(M_{GT} - \varphi)} \qquad (4\text{-}12)$$

We define the difference between the expected emissions and the actual emissions of a system as

$$M_V = M_A - \varphi \qquad (4\text{-}13)$$

Consider a system with generators that emit 2 tons of CO_2 per MWh without renewables in the system. Suppose with 10% variable renewables in the system, system emissions are 1.8 tons per MWh. Then η would be (2-1.8)/0.2 = 100% and M_V would be 0. On the other hand, if the emissions were 1.9 tons per MWh with 10% renewables, η would be 50% and M_V would be 0.1 tons per MWh. This framing allows an assessment of the degree to which the introduction of variable renewables displaces emissions from fossil generators, and of the equivalent displacement assumption.

Table 4-1 summarizes results for the five variable power data sets when used in their entirety (without nights, for the solar data). A system with renewables that uses LM6000 turbines for fill-in power achieves 76 - 79% of the expected CO_2 emissions reductions and 20 - 45% of the expected NO_x emissions reductions. An emissions displacement analysis would have overestimated emissions reductions by ~ 23% for CO_2 emissions and by 55% - 80% for NO_x emissions. Similar penalties of 24% are incurred for 501FD CO_2 emissions reductions, but NO_x emissions increase by factors of 2 to 6 times the amount emissions were expected to be reduced, because of the un-optimized NO_x performance of the 501FD system below 50% power.

Table 4-1 - Baseload power plant model results for 5 variable renewable power plant data sets. Note that with night periods removed, the day-only capacity factor for the solar PV plant was 45%. The 95% prediction intervals are shown for a least squares multiple regression analysis (Mendenhall, 1994).

	Energy Produced			**NO_x**		**CO_2**	
	Renewable (MWh)	*Natural gas (MWh)*	*Baseload Total (MWh)*	*Percent of expected emissions reduction* (η)	*Variability emissions (M_V, in kg)*	*Percent of expected emissions reduction* (η)	*Variability emissions (M_V, in tonnes)*
LM6000							
Eastern Wind	1,300	9,600	10,900	45% ± 4	270	79% ± 1	160
Northern Great Plains Wind	660	450	1,100	20% ± 3	350	76% ± 1	88
Central Great Plains Wind	3,400	2,800	6,200	33% ± 4	820	76% ± 1	440
Southern Great Plains Wind	7,700	9,000	16,700	22% ± 3	2,300	77% ± 1	1,000
Southwest PV (days)	170,000	210,000	380,000	23% ± 3	36,000	78% ± 1	15,000
501FD							
Eastern Wind	6,000	42,000	48,000	-220 (+300, -120)	1,000	76% ± 1	770
Northern Great Plains Wind	2,940	1,950	4,890	-620% ± 100	1,100	76% ± 1	400
Central Great Plains Wind	15,000	12,500	27,500	-500% (+150, - 10)	4,500	76% ± 1	1,900
Southern Great Plains Wind	34,000	38,000	72,000	-600% ± 100	13,000	76% ± 1	4,800
Southwest PV (days)	730,000	930,000	1,660,000	-640% ± 100	230,000	77% ± 1	70,000

To investigate the dependence of system emissions on the penetration of renewable energy, we select time periods in our long data sets that have different capacity factors. For wind power data, a sliding window of 1,000 minutes was used. We note the high correlation between the *n*th data subset and the *n*+1 data subset, which differ by only 2 data points, but this method allows us to explore a wide range of penetration of renewable power. For solar data, each day was treated as a data subset (night periods are removed from the data). The solar data set was 732 days in length, yielding 732 different capacity factor results. We combined the results from each analysis and in penetration factor intervals of 1% plot the mean and area encompassed by two standard deviations in figures 4-1a to 4-1d.

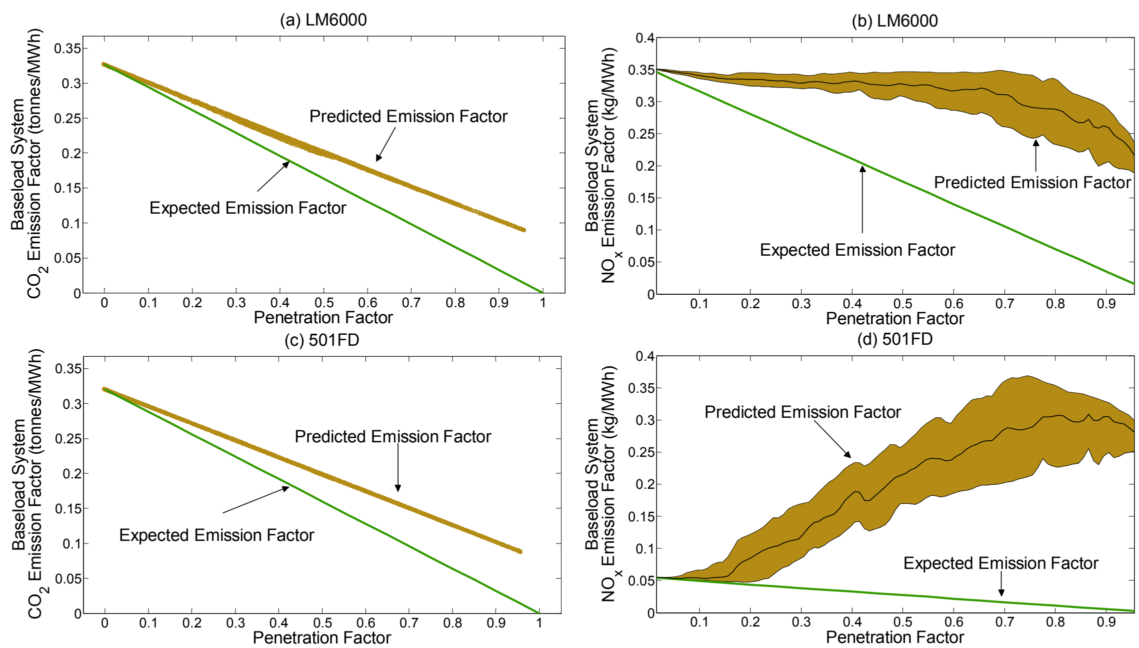

Figure 4-1 - Mean renewable plus natural gas emission factors vs. renewable energy penetration levels (α) (solid black line); area shown represents 2 standard deviations of all five data sets (shaded brown area); see figure 4-2 for representative single data set variability. The expected emissions factor (green, lower line in each figure) is shown for comparison. (a) LM6000 CO2. (b) LM6000 NOx. (c) 501FD CO2. (d) 501FD NOx.

Our model predicts that CO_2 emission factors decrease linearly with renewable penetration at a slope of -0.5 (compared to the expected -0.65, the negative of the emissions factor, equation 4-11) for LM6000s and -0.48 compared to -0.64 (expected) for 501FDs (figures 1a and 1c). At penetration levels of 1, predicted emissions are not eliminated because the natural-gas turbine is modeled as a spinning reserve. Below 65% renewable penetration, the LM6000 NO_x emission factor is roughly constant. Thus, adding renewables is not effective in reducing NO_x for such a system (figure 4-1b).

A threshold effect is observed for the 501FD turbine: for penetration values below ~15%, the predicted NO_x emission factor nearly matches the expected emission factor (figure 4-1d). Since the dry low NO_x control system is optimized for constant high power operations, it is not surprising that this turbine design exhibits high NO_x emissions as the penetration of wind or solar energy increases to the point that the turbine must cycle to low power. Limiting the 501FD's P_{min} limit to >50% nameplate capacity avoids the poor NO_x regions of the DLN system (discussed in appendix C), and results in NO_x emissions reductions. This approach is applicable only if the ratio of energy provided by natural gas generators with DLN to variable power plants is greater than 2:1.

Viewed in terms of η, as the penetration of variable power increases the fraction of expected emissions reductions achieved from a system with LM6000 turbines supplying fill-in power decreases from ~87% to 78% for the Eastern wind data and from 80% to 76% for the Southern and Central Great Plains wind data sets (figure 4-2a). Increasing the penetration factor of variable power effectively reduces the natural gas turbine from steady-state full power conditions to transient-state cycled power conditions and results in higher NO_x emissions. NO_x reductions from a system using LM6000 turbines are roughly half the expected value at 10% penetration, reaching a minimum of 10% to 30% at a penetration of ~50% (figure 4-2b).

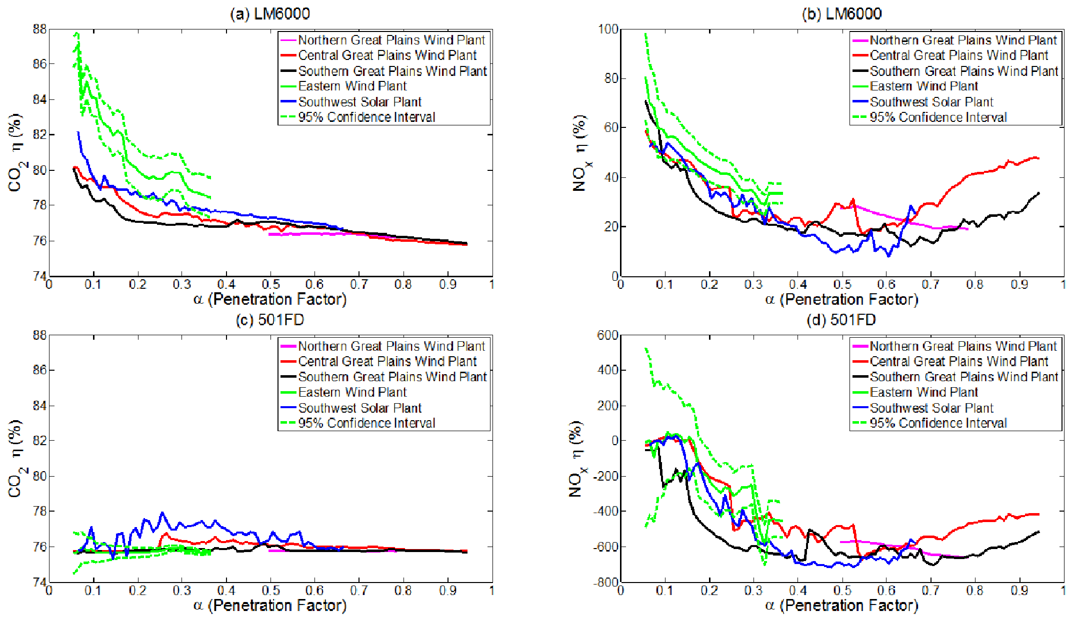

Figure 4-2 - Renewable plus gas generator system mean expected emission reductions (η) vs. variable energy penetration factors (α). 95% prediction intervals (dashed lines) are shown only for the Eastern Wind plant. (a) LM6000 CO_2. (b) LM6000 NO_x. (c) 501FD CO_2. (d) 501FD NO_x.

Emissions of CO_2 from a system with 501FD turbines are ~76% of that expected with no significant dependence on penetration (figure 4-2c). The large inertia of the 501FD combined-cycle plant results in a heat rate that depends only on power (appendix C, figure 4-9), and the deviations from a constant fraction of achieved expected emissions are caused by the constraints we impose on operating the turbine to stay within the limits of the data. As more variable renewable power is added, the NO_x emission factor (figure 4-2d) increases because the 501FD is forced to spend a higher percentage of its time operating in high NO_x emissions regions (as discussed previously).

4.8 Multiple Turbine Analysis for CO_2 Emissions Results

Theoretically, CO_2 emissions are displaced linearly for both the LM6000 case and the 501FD case (Mills et al., 2009). If the fraction of expected emissions reductions for CO_2 achieved is calculated according to equation 4-12, η would be constant for all values of α. For the 501FD results, η ~ 76%. For an LM6000, η ~ 77%. Deviations from η seen in figure 4-2 are due to either ramp rate effects (LM6000) or model error (501FD).

Mills et al. (2009) modeled the fuel use of multiple generators compensating for wind power and determined that multiple generators can increase the efficiency of a wind + gas plant. They assumed that generators are turned on when needed and that there are no spinning reserves. We adapt their model to calculate how η varies with wind penetration (α) and the number of generators in the system. The fundamental equation, assuming no spinning reserves, is

$$\eta = \frac{s\alpha + \frac{f_0}{P_{max}}\left(1 - \frac{\sum_{i=1}^{n} u_i}{n}\right)}{\left(\frac{f_0}{P_{max}} + s\right)\alpha} \qquad (4\text{-}14)$$

where s is the slope of a generator's fuel consumption curve, f_0 is the generator's fuel consumption at zero load, n is the number of identical gas turbines, α is the penetration level of wind energy, P_{max} is the nameplate capacity of each generator, and u_i is the operating status of a each generator (1 if it is on, 0 if it is off). For the results displayed in figure 4-3, 501FD specific data were used. Specifically, P_{max} =200 MW, s = 0.035 MBTU per MW-minute, and f_0 = 2.23 MBTU. The Southern Great Plains wind power data was used to determine what the mean value of η is for a variety of penetration levels. Figure 4-3 displays the results for four cases: 5 generators are paired with one wind plant and no generators are used as a spinning reserve (a); 20 generators are paired with one wind plant and no generators are used as a spinning reserve (b); 5 generators are paired with one wind plant and 1 generator is used as a spinning reserve (c); 20 generators are paired with one wind plant and 1 generator is used as a spinning reserve (d).

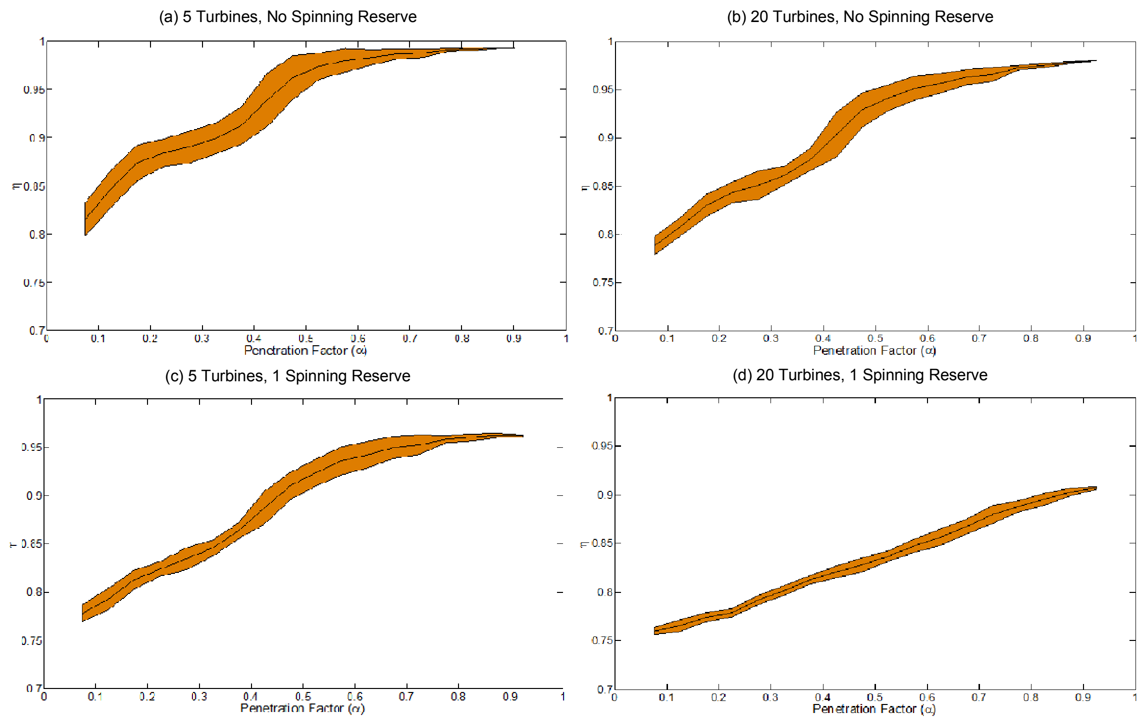

Figure 4-3 - Fraction of expected CO_2 emission reductions achieved (η) when (a) 5 generators are used to compensate for wind's variability, (b) 20 generators are used, (c) 5 generators and one generator is used as a spinning reserve, (d) 20 generators and one generator is used as a spinning reserve. The black line represents the mean η and the area shown (shaded brown area) represents one standard deviation from the mean when the Southern Great Plains wind data set is used.

These results show that a higher fraction of expected CO_2 emission reductions can be achieved when multiple turbines are used to compensate wind power, but still only 77-87% of the expected CO_2 emission reductions are achieved for wind penetration of 20%. Increasing the number of turbines used to backup wind power increases the efficiency of the wind plus gas system. At 20% wind penetration and no generators used as a spinning reserve, approximately 83% of expected CO_2 emission reductions are achieved when 20 generators are used to provide ancillary service, as opposed to 77% when 5 generators provide ancillary service. Realistically, spinning reserves will be necessary to compensate for wind's variability and ensure a stable system. Adding one spinning reserve generator reduces the system's CO_2 emission efficiency versus the wind penetration level.

4.9 Interactions between RPSs and CAIR

We examine the implications of our results by analyzing the potential interaction between state RPSs and the Clean Air Interstate Rule (CAIR). The District of Columbia Circuit Court of Appeals vacated CAIR in July 2008 (US Court of Appeals, 2008), but here we examine the interactions between an RPS and CAIR, under the assumption that a similar NO_x emission rule will come into force in the future. CAIR was designed to reduce annual NO_x emissions 60% by 2015 (EPA, 2008). States with large RPSs may experience NO_x emissions from gas turbines used to fill in the variable renewable power that can make it more difficult to meet CAIR requirements. We estimate what percentage these ancillary emissions could consume of a state's CAIR annual NO_x emissions allocation in 2020 (EPA, 2005) (most RPSs are fully phased in by 2020; here we assume that the 2020 NO_x limits are the same as in 2015).

We assume all RPSs in CAIR states are fulfilled and that all RPS targets that can be, are met with wind. We convert RPSs that are specified by a percentage to MWh of wind generation in 2020 by using the EIA assumption that load will grow linearly to 3% above 2008 load (DOE, 2001b). We also assume all displaced and fill-in generators are similar to either LM6000s or 501FDs. We estimate the expected emission reductions (M_{GT} - ϕ) by using NO_x emission factors of 0.2 kg/MWh for LM6000s and 0.15 kg/MWh for 501FDs obtained from EPA's AP-42 database (EPA, 1995). For each state, we average the estimated η for the four wind plant data subsets and use equation 4-12 to estimate M_A. Finally, we use equation 4-13 to derive the mass of NO_x emissions attributed to variability that are not currently included in most emissions displacement studies.

Table 4-2 summarizes the CAIR analysis.   When LM6000 turbines are used, the potential emissions associated with variability are significant for Illinois, Minnesota, and New Jersey: countering wind's variability could consume 2 to 3% of each state's annual CAIR allocations. If 501FDs are used, 7 of the 12 states could have 2 to 8% of their annual CAIR allocations used to provide fill-in power for wind or PV power plants.

In states like New Jersey, careful selection of the NO_x controls used for wind compensation may be warranted to avoid upward pressure on NO_x permit prices, similar to when the NO_x budget was first implemented (Farrell, 2000). Using the emissions from table 4-2 and assuming an annual NOx emission permit price of $2,800 per ton, the costs associated with degraded emissions performance can be as high as 0.24 cents per kWh of renewable energy for NO_x emissions. With a carbon price of $50 per ton carbon dioxide, the costs can be as high as 0.50 cents/kWh for CO_2 emissions. We caution that these costs do not include the additional maintenance costs that may arise from cycling the gas turbines to compensate for the renewables' variability.

As part of their NO_x control strategy, states may choose to award NO_x allowances to eligible renewable energy and energy efficiency projects. These awards range from a few percent of the NO_x allowances to as much as 15%. New Jersey's set-aside is 5%, and Minnesota has proposed a 15% renewable set-aside (EPA, 2006). Our results caution that annual average emissions factors may not be appropriate for the summer ozone control months, since the character of the variability of both wind and solar PV is dependent on the season. We note that the awards are based on the equivalent displacement assumption, and states that use gas generators to compensate for wind or solar PV variability may find that assumption is not warranted.

Table 4-2 - Summary results of CAIR analysis for the 12 CAIR states with a renewables portfolio standard. The wind penetration fraction is the larger of the fraction of the state's 2020 RPS requirement that could be fulfilled by wind, or currently installed wind. The CAIR allowance is the 2015 allowance. Note: fractions may not match exactly due to rounding.

State	Wind penetration Fraction (α)	State's annual CAIR NO_x allowance (thousand tonnes)	LM6000 with steam injection		501FD with DLN	
			M_V annual (tonnes)	% M_V of state's CAIR allowance	M_V annual (tonnes)	% M_V of state's CAIR allowance
Delaware	0.18	8.6	48	0.56	140	1.6
Illinois	0.18	60	1200	2.0	3400	5.8
Iowa	0.07	43	29	0.07	59	0.13
Maryland	0.075	11	40	0.37	260	2.4
Minnesota	0.25	34	730	2.2	2000	6.0
Missouri	0.11	60	250	0.42	220	0.37
New Jersey	0.16	12	350	3.0	910	7.7
New York	0.077	19	120	0.64	820	4.2
North Carolina	0.11	44	320	0.72	290	0.65
Pennsylvania	0.07	65	180	0.27	1000	1.6
Texas	0.033	150	590	0.04	120	0.08
Wisconsin	0.1	31	140	0.45	120	0.40

The calculations above assume that variability in renewable generation results in similar variability in the natural gas generators used to compensate. There are several reasons this may not be correct, including use of coal and oil generators for compensation and interaction between renewable variability and load variability (Apt, 2007). While we have no data on ramping emissions of coal and oil generators, the estimates in table 4-2 are likely to provide an upper bound on estimates of the emissions increase associated with wind and solar generation's variability. Storage systems other than pumped hydroelectric are presently not cost-effective (Walawalker et al., 2007), but may reduce the need for ramping generators should their costs fall.

4.10 Discussion

Carbon dioxide emissions reductions from a wind (or solar PV) plus natural gas system are likely to be 75-80% of those presently assumed by policy makers. Using multiple generators improves the CO_2 emission efficiency of a wind + gas system by 3-15% for wind penetration levels of 5 to 95%. Nitrous oxide reduction from such a system depends strongly on the type of NO_x control and how it is dispatched. For the best system we examined, NO_x reductions with 20% wind or solar PV penetration are 30-50% of those expected. For the worst, emissions are increased by 2-4 times the expected reductions with a 20% RPS using wind or solar PV.

The fraction of expected emissions reduction, η, is calculated assuming that the emissions predicted to be displaced originate from the same generator type that provides fill-in power: figures 4-2a and 4-2b assume a LM6000 is displaced and a LM6000 is providing compensating power; figures 4-2c and 4-2d assume 501FDs. Realistically, displaced generators will differ from the generators providing fill-in power and would produce different results. We have shown that the conventional method used to calculate displaced emissions is inaccurate, particularly for NO_x emissions. A region-specific analysis can be performed with knowledge of displaced generators, dispatched compensating generators, and the transient emissions performance of the dispatched compensating generators. The results shown here indicate that at large scale variable renewable generators may require that careful attention be paid to the emissions of compensating generators to minimize additional pollution. We note that special emphasis should be placed on the NO_x emissions of compensating generators because natural gas generators are located within load centers.

If system operators recognize the potential for ancillary emissions from gas generators used to fill in variable renewable power, they can take steps to produce a greater displacement of emissions. By limiting generators with GE's DLN system to power levels of 50% or greater, ancillary emissions can be minimized. Operation of DLN controls with existing (but rarely used) firing modes that reduce emissions when ramping may be practical. On a time scale compatible with RPS implementation, design and market introduction of generators that are more appropriate from an emissions viewpoint to pair with variable renewable power plants may be feasible.

4.11 References

Apt, J., 2007. The Spectrum of Power from Wind Turbines. J. of Power Sources 169 (2), 369-374.

California State Senate, 2002. Renewable energy: California Renewables Portfolio Standard Program. Senate Bill No. 1078. Chapter 488. Sponsor: Sher. California State Senate 2001-2002 Session: Sacramento, CA.

Curtright, A., Apt, J., 2008. The Character of Power Output from Utility-Scale Photovoltaic Systems. Progress in Photovoltaics 16 (3), 241-247.

Davis, L.B., Black, S.H., 2000. Dry Low NO_x Combustion Systems for GE Heavy-Duty Gas Turbines. GER-3568G. General Electric Power Systems: Schenectady, NY.

Denny, E., O'Malley, M., 2006. Wind Generation, Power System Operation, and Emissions Reduction. IEEE Trans. on Power Systems 21 (1), 341-347.

DOE, 2001a. Emissions of Greenhouse Gases in the United States 2000; DOE/EIA-0573(2000); Energy Information Administration, US Department of Energy; Appendix B.

DOE, 2001b. Annual Energy Outlook 2001. Energy Information Agency, U.S. Department of Energy.

DOE, 2007. Annual Energy Review 2006. DOE/EIA-0384. Energy Information Administration, US Department of Energy.

DSIRE, 2008. Database of State Incentives for Renewables and Efficiency. http://www.dsireusa.org

EPA, 1993. Alternative Control Techniques Document - NO_x Emissions from Stationary Gas Turbines. EPA-453/R-93-007. Emissions Standards Division, U.S. Environmental Protection Agency: Washington, DC.

EPA, 1995. AP 42; 5th ed.; Office of Air Quality and Standards, U.S. Environmental Protection Agency: Research Triangle Park, NC; Vol. 1, p 3.1-10.

EPA, 2005. CAIR Statewide NO_x Budgets Calculations; OAR-2003-0053; Office of Air and Radiation, U.S. Environmental Protection Agency; Appendix A.

EPA, 2006. State Clean Energy-Environment Technical Forum Roundtable on State NOx Allowance EE/RE Set-Aside Programs June 6, 2006 Call Summary. U.S. Environmental Protection Agency. http://www.keystone.org/spp/documents/6_06_06%20SetAside_summary%20FINAL.doc.

EPA, 2008. Clean Air Interstate Rule Basic Information. U.S. Environmental Protection Agency. http://www.epa.gov/CAIR/index.html.

Farrell, A., 2000. The NO_x Budget: A Look at the First Year. The Electricity J. 13 (2), 83-93.

Fraser, 2005. Relating to this State's Goal for Renewable Energy; S.B. 20; Texas State Legislative Session 79(1): Austin, TX.

Keith, G., Biewald, B., Sommer, A., Henn, P., Breceda, M., 2003. Estimating the Emission Reduction Benefits of Renewable Electricity and Energy Efficiency in North America: Experience and Methods*.* Synapse Energy Economics: Cambridge, MA. http://www.synapse-energy.com/Downloads/SynapseReport.2003-09.CEC.Emission-Reduction-Benefits-Renewables-and-EE-Estimates.03-18.pdf.

Masters, G. M., 1997. Introduction to Environmental Engineering and Science*;* 2nd ed*.*; Prentice Hall: Upper Saddle River, NJ; p 341.

Mendenhall, W.; Sincich, T., 1994. Statistics for Engineering and the Sciences; 4th ed.; Prentice-Hall: Upper Saddle River, NJ.

Mills, A., Wiser, R., Milligan, M., O'Malley, M., 2009. Comment on "Air Emissions Due to Wind and Solar Power." Environ. Sci. Technol. 43(15): 6106-6107.

National Research Council of the National Academies, 2007. Environmental Impacts of Wind-Energy Projects. The National Academies Press: Washington, DC; pp 57-64.

NJ Board of Public Utilities, 2006. Renewable Portfolio Standards (RPS) Rules Adoption*;* N.J.A.C. 14:8-2; NJ Board of Public Utilities: Newark, NJ.

PJM-MMU, 2008. 2007 State of the Market Report. Market Monitoring Unit, PJM Interconnection, Inc.. http://www2.pjm.com/markets/market-monitor/downloads/mmu-reports/2007-som-volume2.pdf.

Rabe, B. G., 2006. Race to the Top: The Expanding Role of U.S. State Renewable Portfolio Standards. Pew Center on Global Climate Change: Arlington, VA. http://www.pewclimate.org/docUploads/RPSReportFinal.pdf.

Seinfeld, J.H.; Pandis, S.N., 2006. Atmospheric Chemistry and Physics; 2nd ed.; Wiley: Hoboken, NJ; chapter 6.

UNFCCC, 2007. Consolidated Baseline Methodology for Grid-Connected Electricity Generation from Renewable Sources*;* ACM0002 / Version 7; United Nations Framework Convention on Climate Change: Nusa Dua, Bali.

US Court of Appeals, D.C. Circuit, 2008. State of N. Carolina v. EPA; No. 05-1244; Argued March 25, 2008; Decided July 11, 2008.

Walawalkar, R., Apt, J., Mancini, R., 2007. Economics of electric energy storage for energy arbitrage and regulation in New York. Energy Poli*cy* 35(4), 2558–2568.Weisser, D., 2007. A Guide to Life-Cycle Greenhouse Gas (GHG) Emissions from Electric Supply Technologies. Energy 32, 1543-1559.

Wiser, R., Bolinger, M., 2007. Annual Report on U.S. Wind Power Installation, Cost, and Performance Trends: 2006. Energy Efficiency and Renewable Energy, U.S. Department of Energy. http://www.nrel.gov/docs/fy07osti/41435.pdf.

4.12 Appendix C

4.12.1 Regression Analyses

4.12.1.1 Data

Each emissions data set contains six variables: date, time, power generated, heat rate, NO_x mass emission, and a calibration flag. We model only NO_x and CO_2 emissions from the turbine. Carbon monoxide is emitted and is regulated for natural gas turbines but we do not consider CO in the present analysis.

4.12.1.2 CO_2 Approach

The LM6000 data (figures 4-4 and 4-5) were divided into four regions corresponding to startup, ramping up to full power, full power, and ramping down to shutdown phases (identified as regions 1, 2, 3, and 4, respectively in figure 4-6).

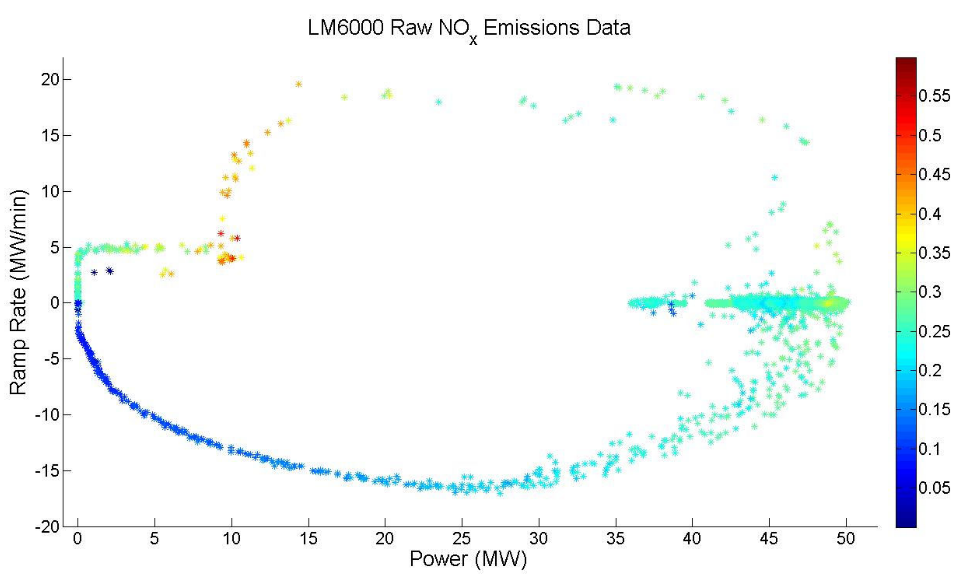

Figure 4-4 - LM6000 raw NO_x emissions data

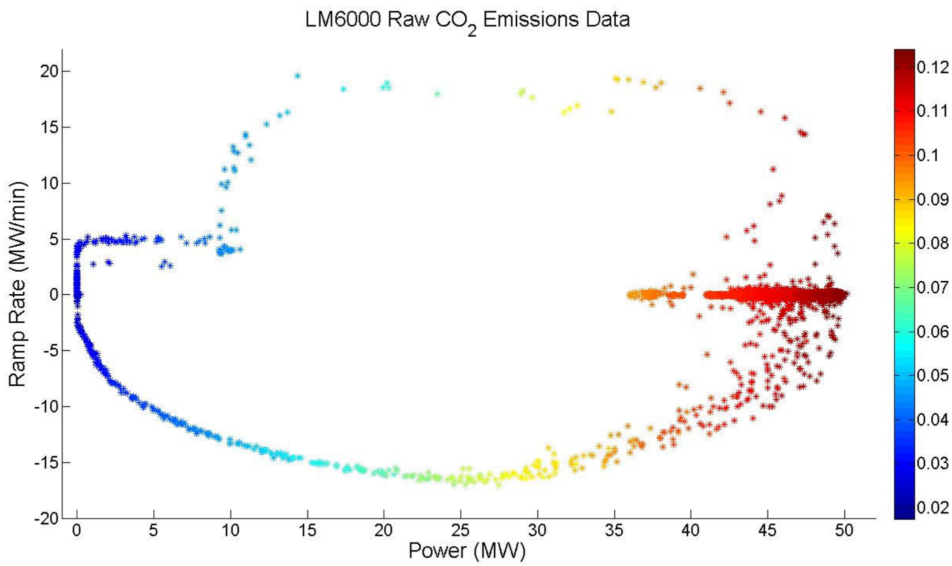

Figure 4-5 - LM6000 raw CO_2 emissions data

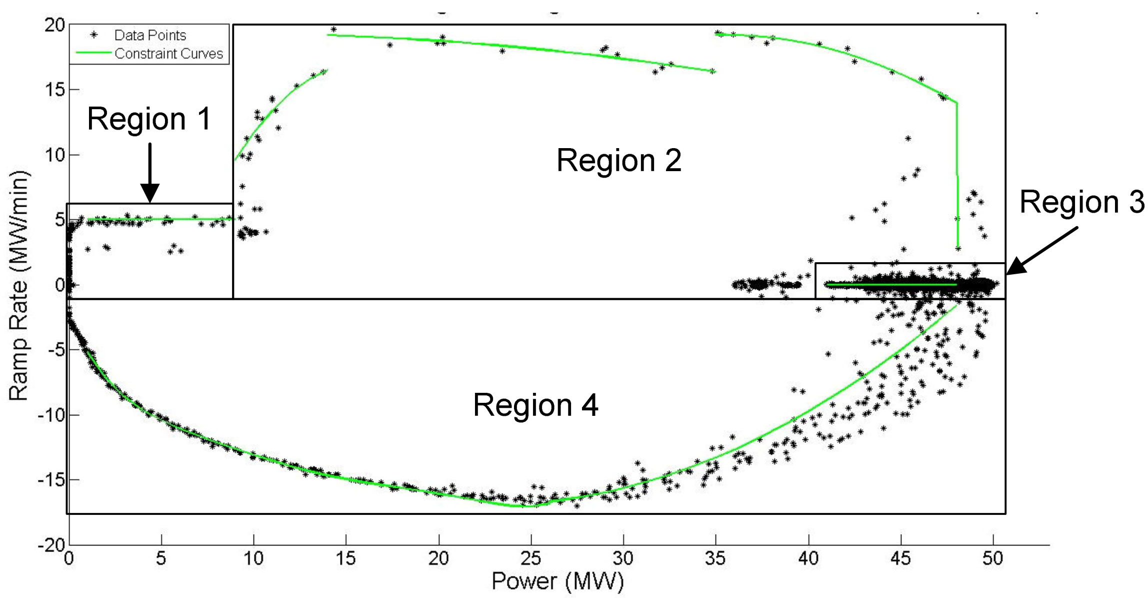

Figure 4-6 - LM6000 emissions data. The emissions data were divided into four regions which were modeled independently. The constraint curves imposed by the populated data are shown for each region.

We performed a multiple regression on each region (equations 4-15 – 4-18); the goodness of fit is shown in figures 4-7 and 4-8, by graphing the absolute percent error between a regression model and the corresponding NO_x emissions data. The 501FD CO_2 data were not divided into multiple regions, as they depend on only the turbine's power level; a linear regression analysis was performed (equation 4-7 and figure 4-9). Adjusted R^2 values are in table 4-3 and detailed statistical information on the regression analyses can be found in tables 4-4 and 4-5.

4.12.1.3 LM6000 CO_2 Regression Results (in tonnes / min)

Region 1

$$\frac{dM_{CO2,LM6000}}{dt} = 2.68x10^{-2} + 1.77x10^{-3} P_{LM6000} \quad (4\text{-}15)$$

Region 2

$$\frac{dM_{CO2,LM6000}}{dt} = 3.18x10^{-2} - 1.54x10^{-3} P_{LM6000} + 5.82x10^{-6} P_{LM6000}^2 - 2.54x10^{-4} \dot{P}_{LM6000} \quad (4\text{-}16)$$

Region 3

$$\frac{dM_{CO2,LM6000}}{dt} = 3.6x10^{-1} + 1.26x10^{-3} P_{LM6000} + 9.27x10^{-6} P_{LM6000}^2 \quad (4\text{-}17)$$

Region 4

$$\frac{dM_{CO2,LM6000}}{dt} = 2.72x10^{-2} + 1.88x10^{-3} P_{LM6000} - 9.207x10^{-6} \dot{P}_{LM6000} \quad (4\text{-}18)$$

4.12.1.4 501FD CO_2 Regression Results (in tonnes / min)

Region 1

$$\frac{dM_{CO2,501FD}}{dt} = 1.18x10^{-1} + 1.84x10^{-3} P_{LM6000} \quad (4\text{-}19)$$

Table 4-3 - Adujsted R^2 values for the regressoins used to model each region of each turbine and pollutant.

Adjusted R^2 Values				
Region	**1**	**2**	**3**	**4**
LM6000				
CO_2	0.85	0.99	0.86	0.99
NO_x	0.85	0.84	-	0.94
501FD				
CO_2	0.99	-	-	-
NO_x	0.72	0.64	0.28	-

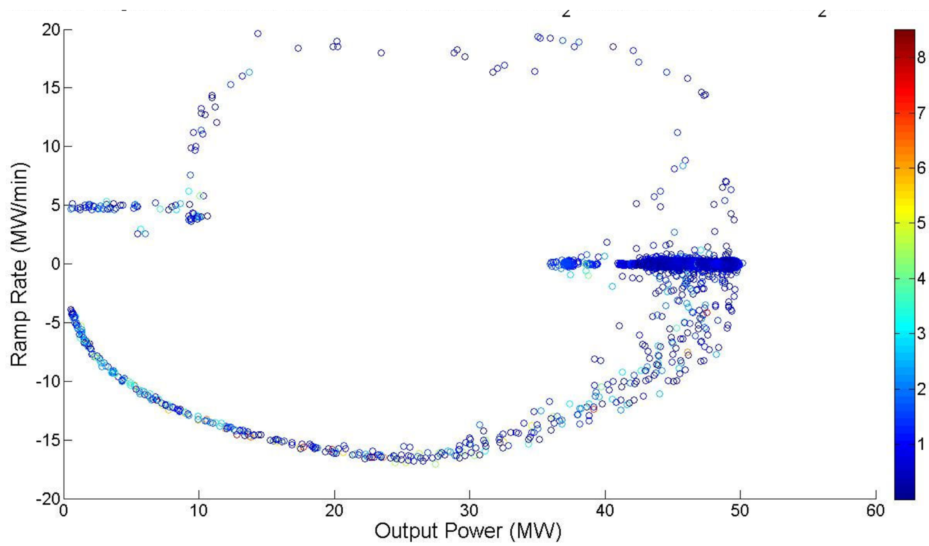

Figure 4-7 - Absolute percent error between calculated CO_2 emissions based on regressions and actual CO_2 emssions from LM6000 data set.

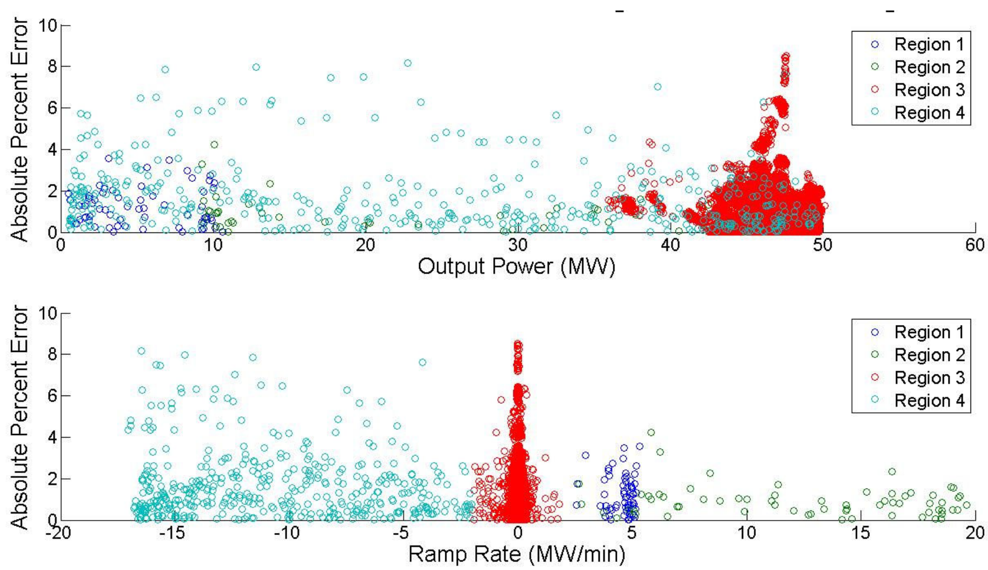

Figure 4-8 - Absolute percent error between calculated CO_2 emissions based on regressions and actual CO_2 emissions from LM6000 data set. Results are colored according to the regions (figure 4-6). Top: absolute percent error for each data point versus power level. Bottom: absolute percent error for each data point versus ramp rate.

Table 4-4 - LM6000 Region CO_2 Regression Results

Region 1

Equation

$$\frac{dM_{CO2,LM6000}}{dt} = 2.68x10^{-2} + 1.77x10^{-3} P_{LM6000} \quad [tonnes / \min]$$

Regression Statistics

Adjusted R^2	0.85
# of Data Points	134
F-value	731.81
Prob>F	<0.0001
Root MSE	$2.63x10^{-3}$

Parameter Statistics

Intercept	Std. Error	$2.84x10^{-4}$		
	t-value	4.34	Prob > |t|	<0.0001
P_{LM6000}	Std. Error	$6.54x10^{-5}$		
	t-value	27.05	Prob > |t|	<0.0001

Region 2

Equation

$$\frac{dM_{CO2,LM6000}}{dt} = 3.18x10^{-2} - 1.54x10^{-3} P_{LM6000} + 5.82x10^{-6} P^2_{LM6000} - 2.54x10^{-4} \dot{P}_{LM6000} \quad [tonnes / \min]$$

Regression Statistics

Adjusted R^2	0.999
# of Data Points	65
F-value	21,893.8
Prob>F	<0.0001
Root MSE	$9.22x10^{-4}$

Parameter Statistics

Intercept	Std. Error	$5.53x10^{-4}$		
	t-value	57.54	Prob > |t|	<0.0001
P_{LM6000}	Std. Error	$7.29x10^{-5}$		
	t-value	21.15	Prob > |t|	<0.0001
P^2_{LM6000}	Std. Error	$1.3x10^{-6}$		
	t-value	4.48	Prob > |t|	<0.0001
R_{LM6000}	Std. Error	$3.44x10^{-5}$		
	t-value	-7.38	Prob > |t|	<0.0001

Region 3

Equation

$$\frac{dM_{CO2,LM6000}}{dt} = 3.6x10^{-1} + 1.26x10^{-3} P_{LM6000} + 9.27x10^{-6} P^2_{LM6000} \quad [tonnes / \min]$$

Regression Statistics

Adjusted R^2	0.864
# of Data Points	15,845
F-value	50,487.5
Prob>F	<0.0001
Root MSE	$1.64x10^{-3}$

Parameter Statistics

Intercept	Std. Error	$3.6x10^{-2}$		
	t-value	9.99	Prob > |t|	<0.0001
P_{LM6000}	Std. Error	$1.58x10^{-4}$		
	t-value	8.03	Prob > |t|	<0.0001
P^2_{LM6000}	Std. Error	$1.72x10^{-6}$		
	t-value	5.39	Prob > |t|	<0.0001

Region 4

Equation

$$\frac{dM_{CO2,LM6000}}{dt} = 2.72x10^{-2} + 1.88x10^{-3} P_{LM6000} - 9.207x10^{-6} \dot{P}_{LM6000} \quad [tonnes / \min]$$

Regression Statistics

Adjusted R^2	0.998
# of Data Points	447
F-value	88,330.9
Prob>F	<0.0001
Root MSE	$1.62x10^{-3}$

Parameter Statistics

Intercept	Std. Error	$2.72x10^{-2}$		
	t-value	122.72	Prob > |t|	<0.0001
P_{LM6000}	Std. Error	$4.48x10^{-6}$		
	t-value	420.07	Prob > |t|	<0.0001
P^2_{LM6000}	Std. Error	$1.66x10^{-6}$		S6
	t-value	-5.52	Prob > |t|	<0.0001

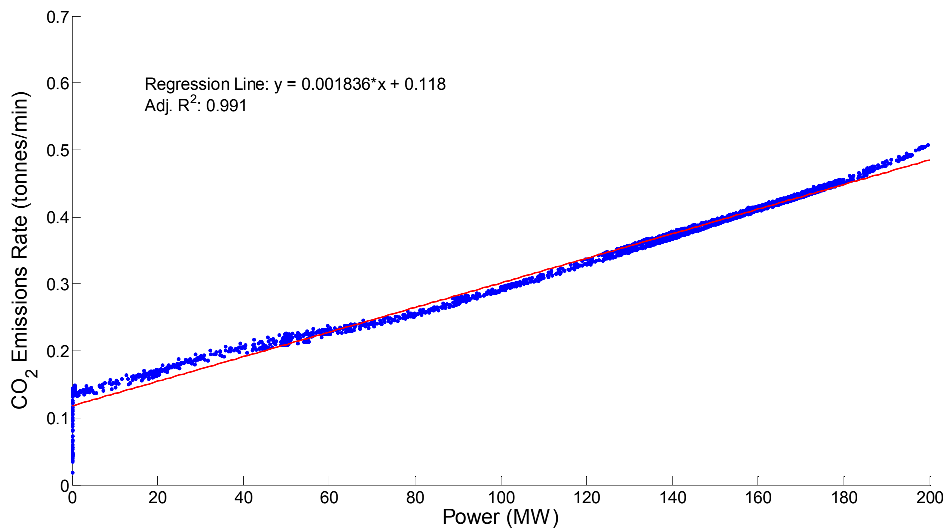

Figure 4-9 - CO_2 emissions rate for the 501FD turbines as a function of turbine output power (blue dots) and the linear regression model used to characterize the CO_2 emissions rate (red line). The linear regression equation is y = 0.00184x + 0.118 and has an adjusted R^2 value of 0.991.

Table 4-5 - 501FD Region CO2 Regression Analysis Results

Region 1

Equation $$\frac{dM_{CO2,501FD}}{dt} = 1.18x10^{-1} + 1.84x10^{-3}\,P_{LM6000} \quad [tonnes/\min]$$

Regression Statistics

Adjusted R^2	0.991
# of Data Points	6,501
F-value	711,368
Prob>F	<0.0001
Root MSE	7.29x10^{-3}

Parameter Statistics

Intercept	Std. Error	2.88x10^{-4}		
	t-value	416.07	Prob > |t|	<0.0001
P_{501FD}	Std. Error	2.16x10^{-6}		
	t-value	843.43	Prob > |t|	<0.0001

4.12.1.5 NO_x Approach

Available NO_x combustion control technologies are water (liquid or steam) injection systems and dry low-NO_x combustion designs (EPA, 1993). The LM6000 data were obtained from 45 MW turbines that injected steam into the combustion chambers, lowering flame temperatures to reduce NO_x. The 200 MW 501FD turbines used General Electric's Dry-Low NO_x (DLN) system of lean premixed combustion. The median nameplate size for all US natural gas turbines using Dry Low NO_x

control is 170 MW; using steam injection it is 80 MW. Thus, the turbines for which we have data are moderately representative.

In GE's Dry-Low NO_x systems, fuel is premixed with air to create a fuel-lean mixture that is burned in a two-stage process to reduce flame temperatures and residence times. At full generator output, GE's DLN operates at a mixture just richer than the flame blowout point of natural gas. As the generator load is reduced, less fuel is fed to the combustion chamber resulting in lower flame temperatures. As load is reduced further the flame blowout point is reached and GE's DLN system can no longer employ the fuel-lean premixed firing mode, and shifts to a diffusion flame where high flame temperatures are present. As a result, low NO_x emission rates are achieved in the power range of approximately 50% to 100% of nameplate capacity and NO_x emission rates an order of magnitude greater are observed in the power range of 0% to 50% (Davis and Black, 2000).

Taking the same approach used to model CO_2 emissions, we modeled NO_x emission rates as a function of power level and ramp rate (equations 4-20 – 4-23). For region 3, no satisfactory result could be derived and the mean of the data was used (standard deviation of 0.022). Figures 4-11 and 4-12 display the goodness of fit for each regression.

The 501FD NO_x data were divided into three regions: low power, medium power, and full power (labeled regions 1, 2, and 3, respectively). Equations 4-24 – 4-26 are the regression results for the 501FD data and figure 4-10 compares the regression results with the 501FD NO_x emission data. Adjusted R^2 values can be found in table 4-3 and detailed statistical information can be found in tables 4-6 and 4-7.

4.12.1.6 LM6000 NO_x Regression Results (in kg / min)

Region 1
$$\frac{dM_{NOx,LM6000}}{dt} = 1.31x10^{-1} + 6.62x10^{-2} P_{LM6000} - 3.89x10^{-3} \dot{P}_{LM6000} \quad (4\text{-}20)$$

Region 2
$$\frac{dM_{NOx,LM6000}}{dt} = 6.76x10^{-1} - 2.27x10^{-2} P_{LM6000} + 3.27x10^{-4} P_{LM6000}^{2} - 1.3x10^{-2} \dot{P}_{LM6000} + (\quad (4\text{-}21)$$

Region 3
$$\frac{dM_{NOx,LM6000}}{dt} = 2.68x10^{-1} \quad (4\text{-}22)$$

Region 4
$$\frac{dM_{NOx,LM6000}}{dt} = 8.35x10^{-2} + 7.53x10^{-4} P_{LM6000} - 3.85x10^{-3} P_{LM6000}^{2} \quad (4\text{-}23)$$

4.12.1.7 501FD NO_x Regression Results (in kg / min)

Region 1
$$\frac{dM_{NOx,501FD}}{dt} = 8.03x10^{-1} + 2.45x10^{-2} P_{501FD} - 3.49x10^{-4} P_{501FD}^{2} \quad (4\text{-}24)$$

Region 2
$$\frac{dM_{NOx,501FD}}{dt} = -9.48x10^{-1} + 6.12x10^{-2} P_{501FD} - 3.95x10^{-4} P_{501FD}^{2} \quad (4\text{-}25)$$

Region 3
$$\frac{dM_{NOx,501FD}}{dt} = 1.18x10^{-1} - 5.76x10^{-4} P_{501FD} + 4.1x10^{-6} P_{501FD}^{2} \quad (4\text{-}26)$$

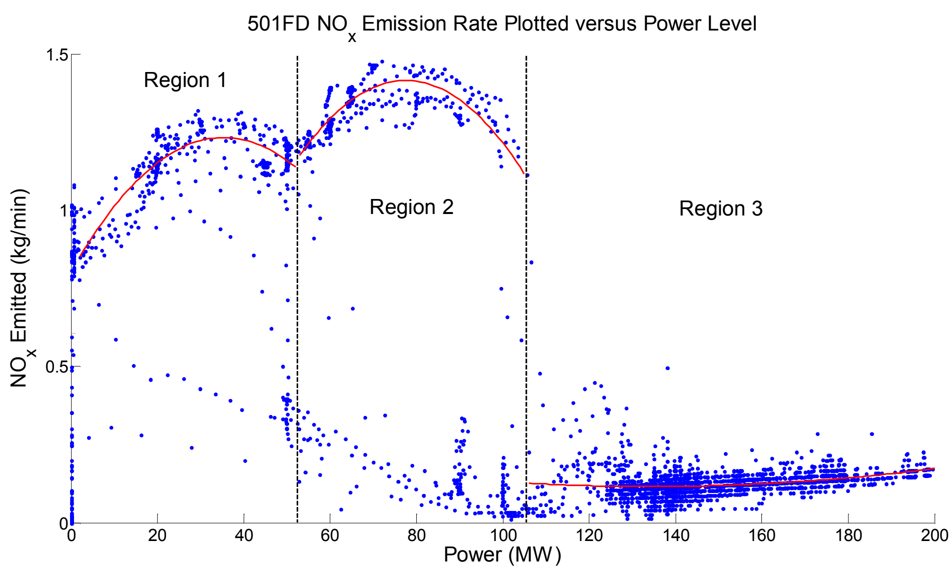

Figure 4-10 - 501FD NOx emissions data as a function of power (blue dots) and regression (red line). The emissions data were divided into three regions which were modeled independently of each other. This combined-cycle turbine is designed to produce low NOx only when operated at high power.

Table 4-6 - 501FD Region NO_x Regression Results

Region 1

Equation

$$\frac{dM_{NO_x,501FD}}{dt} = 8.03x10^{-1} + 2.45x10^{-2} P_{501FD} - 3.49x10^{-4} P_{501FD}^2 \quad [kg/\min]$$

Regression Statistics

Adjusted R^2	0.72
# of Data Points	463
F-value	723.12
Prob>F	<0.0001
Root MSE	$6.99x10^{-2}$

Parameter Statistics

Intercept	Std. Error	$6.99x10^{-3}$		
	t-value	124.45	Prob > $\lvert t \rvert$	<0.0001
P_{501FD}	Std. Error	$6.44x10^{-4}$		
	t-value	30.03	Prob > $\lvert t \rvert$	<0.0001
P_{501FD}^2	Std. Error	$1.18x10^{-5}$		
	t-value	-23.13	Prob > $\lvert t \rvert$	<0.0001

Region 2

Equation

$$\frac{dM_{NO_x,501FD}}{dt} = -9.48x10^{-1} + 6.12x10^{-2} P_{501FD} - 3.95x10^{-4} P_{501FD}^2 \quad [kg/\min]$$

Regression Statistics

Adjusted R^2	0.64
# of Data Points	562
F-value	489
Prob>F	<0.0001
Root MSE	$4.58x10^{-2}$

Parameter Statistics

Intercept	Std. Error	$7.26x10^{-2}$		
	t-value	-12.98	Prob > $\lvert t \rvert$	<0.0001
P_{501FD}	Std. Error	$2.0x10^{-3}$		
	t-value	30.47	Prob > $\lvert t \rvert$	<0.0001
P_{501FD}^2	Std. Error	$1.33x10^{-5}$		
	t-value	-29.49	Prob > $\lvert t \rvert$	<0.0001

Region 3

Equation

$$\frac{dM_{NO_x,501FD}}{dt} = 1.18x10^{-1} - 5.76x10^{-4} P_{501FD} + 4.1x10^{-6} P_{501FD}^2 \quad [kg/\min]$$

Regression Statistics

Adjusted R^2	0.28
# of Data Points	5,129
F-value	979.37
Prob>F	<0.0001
Root MSE	$1.02x10^{-2}$

Parameter Statistics

Intercept	Std. Error	$1.96x10^{-2}$		
	t-value	6.10	Prob > $\lvert t \rvert$	<0.0001
P_{501FD}	Std. Error	$2.52x10^{-4}$		
	t-value	-2.39	Prob > $\lvert t \rvert$	<0.0001
P_{501FD}^2	Std. Error	$7.98x10^{-7}$		
	t-value	5.24	Prob > $\lvert t \rvert$	0.0002

4.12.1.8 LM6000 Regression Analysis

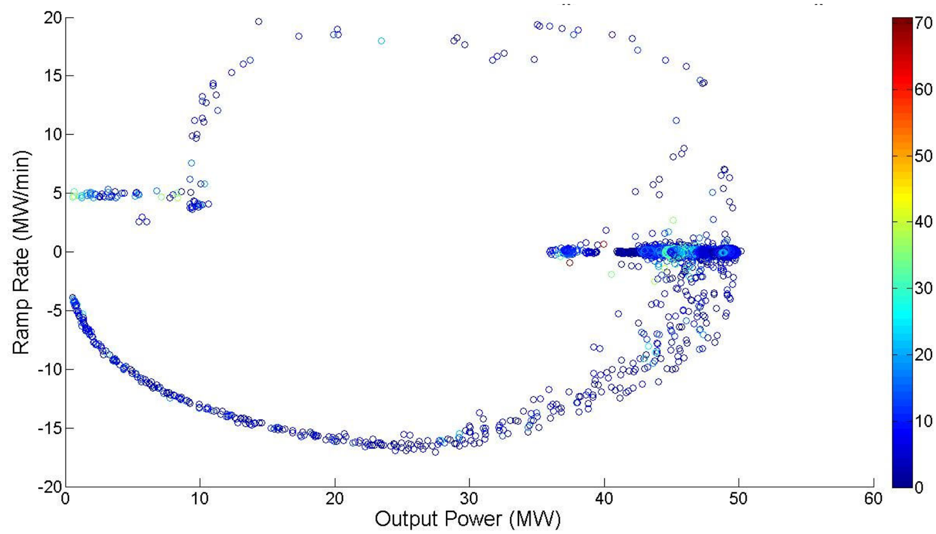

Figure 4-11 - Absolute percent error between NO_x emissions based on regressions and actual NOx emissions from LM6000 data set.

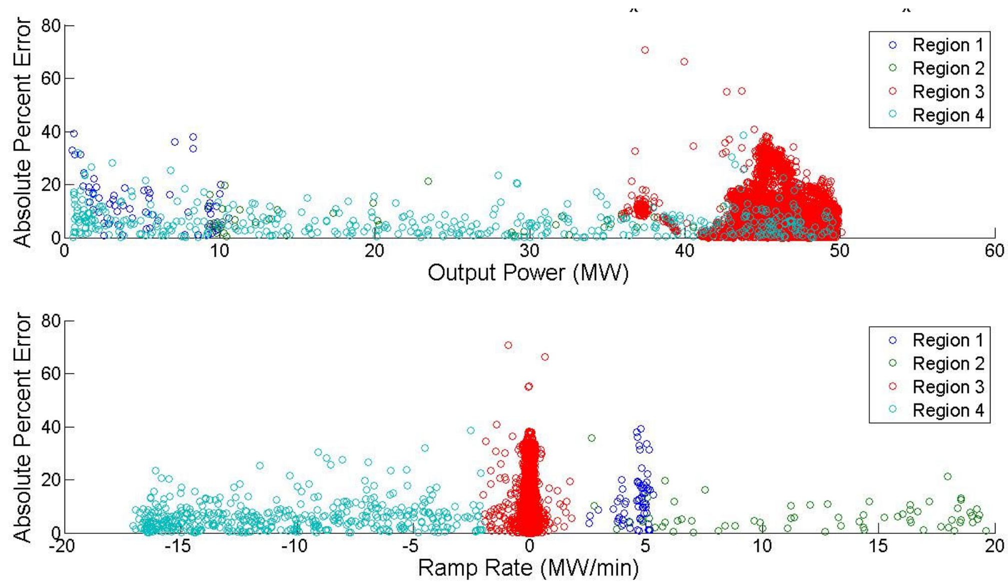

Figure 4-12 - Absolute percent error between calculated NO_x emissions based on regressions and actual NO_x emissions from LM6000 data set. Results are colored according to the regions (figure 4-6). Top: absolute percent error for each data point versus power level. Bottom: absolute percent error for each data point versus ramp rate.

Table 4-7 - LM6000 Region NO_x Regression Results

Region 1

Equation

$$\frac{dM_{NOx,LM6000}}{dt} = 1.31x10^{-1} + 6.62x10^{-2} P_{LM6000} - 3.89x10^{-3} \dot{P}_{LM6000} \quad [kg/\min]$$

Regression Statistics

Adjusted R^2	0.85
# of Data Points	134
F-value	159.56
Prob>F	<0.0001
Root MSE	$5.26x10^{-2}$

Parameter Statistics

Intercept	Std. Error	$6.99x10^{-3}$		
	t-value	13.64	Prob > |t|	<0.0001
P_{LM6000}	Std. Error	$1.6x10^{-3}$		
	t-value	11.77	Prob > |t|	<0.0001
R_{LM6000}	Std. Error	$2.48x10^{-3}$		
	t-value	13.18	Prob > |t|	<0.0001

Region 2

Equation

$$\frac{dM_{NOx,LM6000}}{dt} = 6.76x10^{-1} - 2.27x10^{-2} P_{LM6000} + 3.27x10^{-4} P_{LM6000}^2 - 1.3x10^{-2} \dot{P}_{LM6000} + 6.53x10^{-4} \dot{P}_{LM6000}^2 \quad [kg/\min]$$

Regression Statistics

Adjusted R^2	0.84
# of Data Points	65
F-value	83.56
Prob>F	<0.0001
Root MSE	$2.95x10^{-2}$

Parameter Statistics

Intercept	Std. Error	$3.96x10^{-2}$		
	t-value	17.13	Prob > |t|	<0.0001
P_{LM6000}	Std. Error	2.74x10-3		
	t-value	-8.27	Prob > |t|	<0.0001
P_{LM6000}^2	Std. Error	$4.81x10^{-5}$		
	t-value	6.83	Prob > |t|	<0.0001
R_{LM6000}	Std. Error	$4.85x10^{-3}$		
	t-value	-2.69	Prob > |t|	0.0094
R_{LM6000}^2	Std. Error	$2.18x10^{-4}$		
	t-value	2.99	Prob > |t|	0.004

Region 3

Equation

$$\frac{dM_{NOx,LM6000}}{dt} = 2.68x10^{-1} \quad [kg/\min]$$

Mean Statistics

Standard Deviation	0.0222	# of Data Points	15,844

Region 4

Equation

$$\frac{dM_{NOx,LM6000}}{dt} = 8.35x10^{-2} + 7.53x10^{-4} P_{LM6000} - 3.85x10^{-3} P_{LM6000}^2 \quad [kg/\min]$$

Regression Statistics

Adjusted R^2	0.94
# of Data Points	447
F-value	3,486
Prob>F	<0.0001
Root MSE	$1.67x10^{-2}$

Parameter Statistics

Intercept	Std. Error	$1.72x10^{-3}$		
	t-value	50.2	Prob > |t|	<0.0001
P_{LM6000}	Std. Error	1.91e-4		
	t-value	23.7	Prob > |t|	<0.0001
P_{LM6000}^2	Std. Error	3.89e-6		
	t-value	-3.71	Prob > |t|	0.0002

4.12.2 Regressions Constraints

4.12.2.1 LM6000 Regression Constraints

The LM6000 turbines were generally operated in a consistent manner (figures 4-4 – 4-6): initialized, ramped up quickly and held at or near full power, and ramped quickly down, and turned off. Thus, not all the power-ramp-rate control space is sampled in the data we obtained. We applied constraints to our LM6000 model to ensure the model turbine was operated in regions sampled by the actual data (green lines in figure 4-6).

Compensating for wind or solar power fluctuations in the simulations required some power and ramp rate combinations not situated on a constraint curve; we created an ensemble of samples from points on the constraint curves to match the desired combinations. We found that in doing so, the maximum error in the base load plant's output was 7.6% and the mean error was 1.6%. It is possible that our approach produces inaccurate results due to the incompletely sampled power-ramp-rate control space.

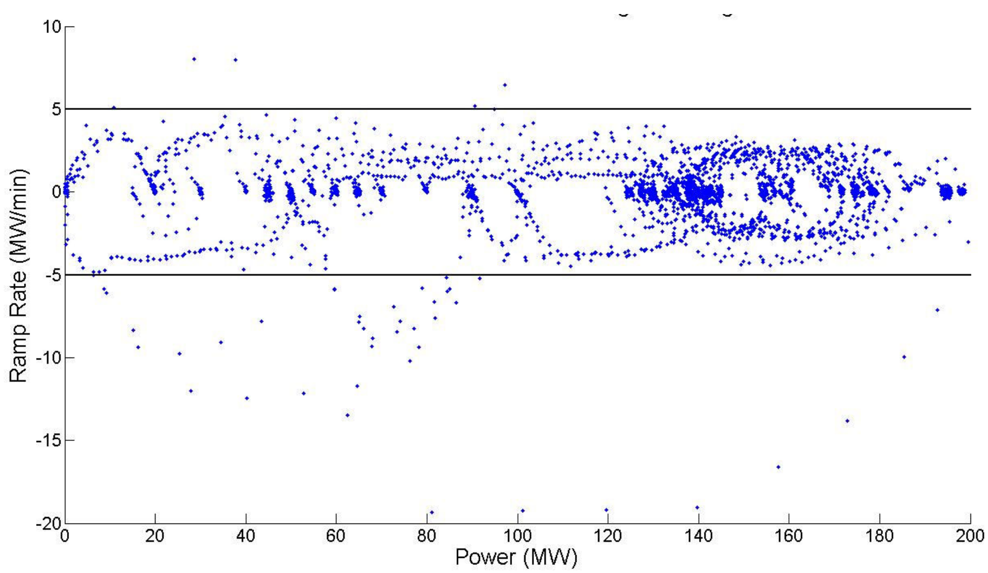

Figure 4-13 -501FD emissions data. The boundaries on the model's ramp rate, imposed by the populated data points in the control map, are shown. The 501FD was operated in a manner that sampled more points in its control map than the LM6000 and as a result the 501FD model is not as constrained as the LM6000 model.

The 501FD was cycled through its control space in a manner that sampled more points (figure 4-13) than the LM6000 turbines. As a result, the 501FD model is not as strictly constrained as the LM6000 model. The only constraints imposed on the 501FD model were limitations on the maximum and minimum ramp rates, set at 5 MW/min and -5 MW/min, respectively.

4.12.3 Profile Sensitivity Analysis Raw Data

The results of the model are dependent upon how much the gas turbine(s) ramp through their power range and at what power levels they are required to operate. Therefore, the results seen in table 4-1, obtained from using the full time series of the 5 data sets (see table 4-8), estimates only the emission reductions for the conditions that existed during the periods when the data were collected. Ideally, a significant number of high time-resolution independent power plant outputs would be used in our simulations. However we did not have access to such a data set, only to the 5 data sets described.

Table 4-8 - Wind and solar photovoltaic data sets from utility-scale sites used in the analysis. The maximum observed power of several of the power plants exceeded their nameplate capacity; in other cases the nameplate capacity was not reached during the period for which data were obtained.

Data set	Power plant type	Capacity factor based on nameplate wind or PV size	Normalized capacity factor based on maximum observed power	Resolution	Data set length
Eastern	Wind	0.07	0.12	1 second	240 hours
Northern Great Plains	Wind	0.57	0.59	10 second	15 hours
Central Great Plains	Wind	0.53	0.54	10 second	84 hours
Southern Great Plains	Wind	0.50	0.46	10 second	370 hours
Southwest	Solar PV	0.19	0.19	1 minute	732 days

For wind data, one could imagine generating theoretical wind data, subject to certain constraints, such as ensuring the appropriate frequency and phase characteristics (Apt, 2007; Curtright and Apt, 2008). Instead, we relied on the actual high time resolution data, creating smaller data subsets from the initial data thereby creating a large collection of data sets that represent a variety of variable power plant outputs. To create the smaller data sets, a sliding window 1,000 minutes in length was used to produce smaller data samples 1,000 minutes long. The Eastern wind plant data, recorded over a 10 day period, is 14,400 minutes in length and using the sliding window produced 13,401 data subsets. Each data subset differs from the preceding data subset by two data points. Therefore, there is a significant amount of correlation between the smaller data sets and it is this correlation that produces the lines, or tracks, seen in Figures 4-14 through 4-17.

For the solar PV data, each day that power was produced was used as a data subset. The solar data obtained was 732 days in length and thus produced 732 data subsets used in the profile sensitivity analysis.

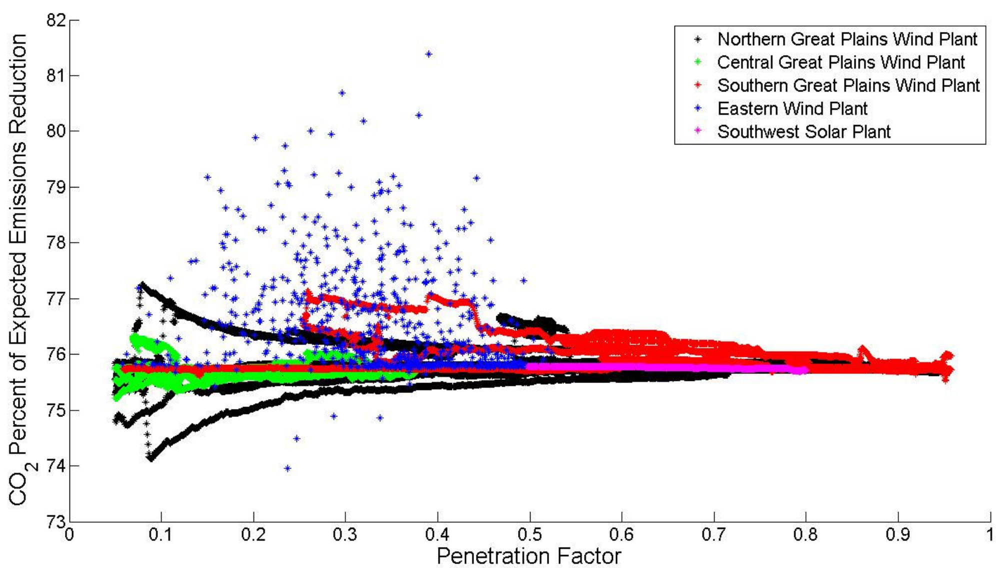

Figure 4-14 - 501FD CO_2 expected emissions reduction raw results from profile sensitivity analysis.

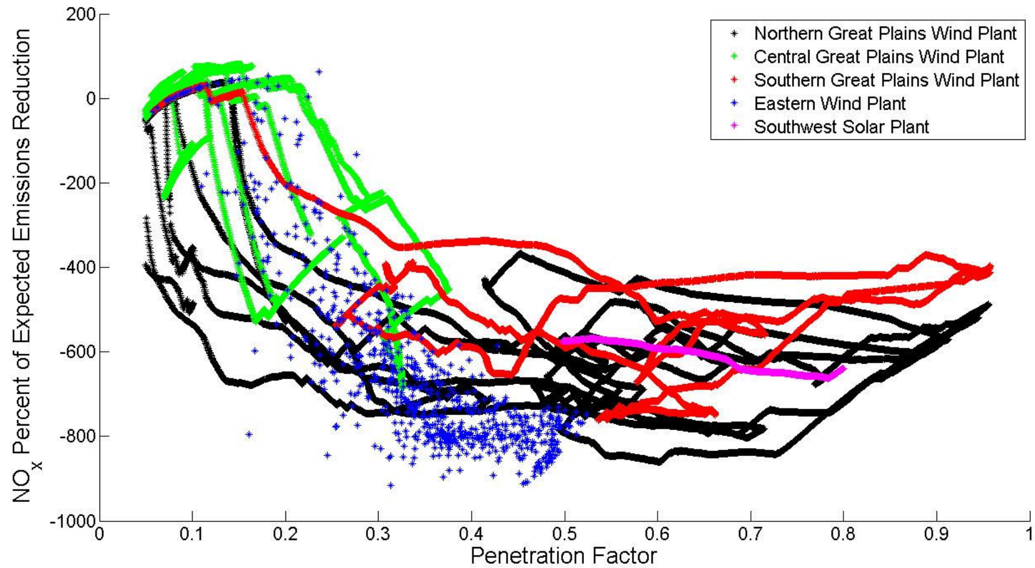

Figure 4-15 - 501FD NO_x expected emissions reduction raw results from profile penetration analysis.

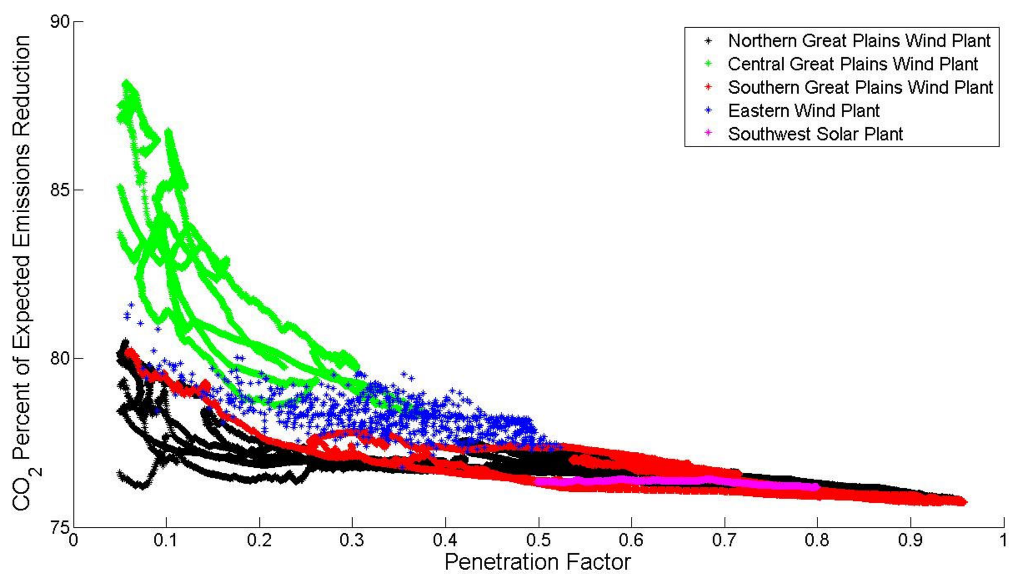

Figure 4-16 - LM6000 CO2 emissions reduction raw results from profile penetration analysis.

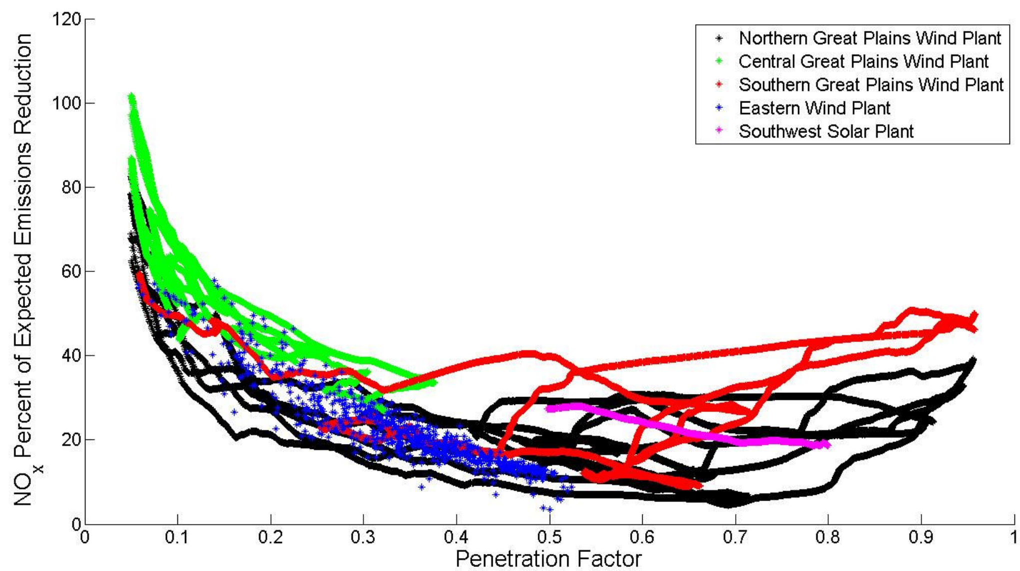

Figure 4-17 - LM6000 NOx expected emissions reduction raw results from profile penetration analysis.

4.12.4 Multiple Turbine Analysis

In order to investigate how emissions are affected by the penetration factor of wind, the constraint of pairing the wind plant with only one natural-gas turbine is relaxed. One to five natural-gas turbines were paired with the wind plant to produce a base load variable plant of size $n \cdot P$ MW, where n is the number of turbines and P is the power limit of the turbine. The fill-in power required is divided equally among the turbines and as a result the lower power limit of the turbines is P - P/n MW.

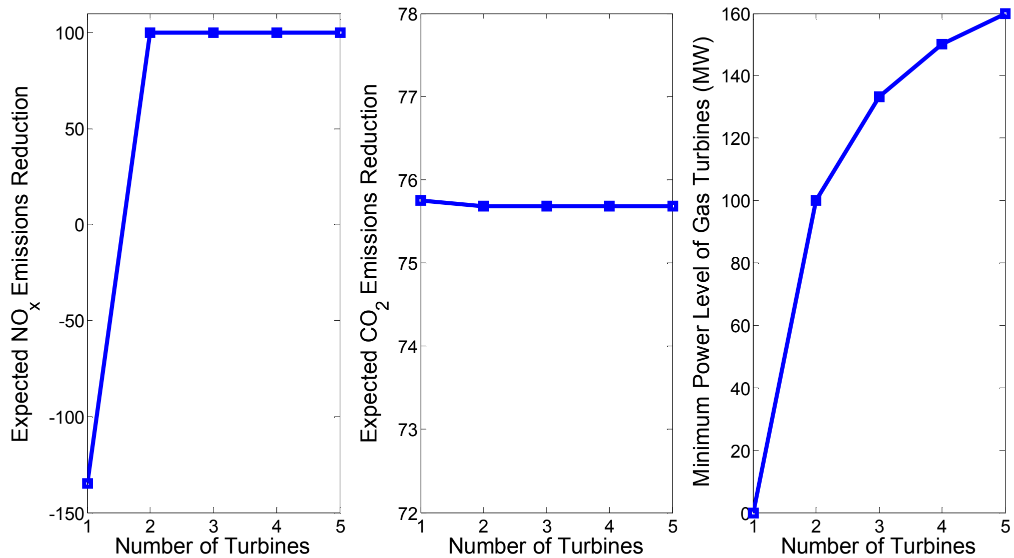

Figure 4-18 -501FD multiple turbine analysis using the Eastern wind data set. By pairing *n* 501FD turbines with a variable power plant, the lower power limit (P_{min}) of the turbines is P - P/*n* MW. For 2 or more turbines, P_{min} is greater than 50% of the 501FD's nameplate capacity and NO_x emissions are reduced according to expectations. If no attention is paid to P_{min}, NO_x emissions increase.

Figure 4-18 shows the results of the multiple turbine analysis for 501FD turbines using the Eastern wind data set. Limiting the minimum operating power level of the natural-gas turbine in the variable base load plant produces significantly better NO_x emissions performance. By limiting a 501FD to power regions of 50% of nameplate capacity or greater, the poor emissions performance region of GE's DLN system, where NO_x emissions are an order of magnitude higher, is avoided and emissions are displaced at effectively a linear rate and match expectations.

Chapter 5 - Conclusion

Utilities are striving to better understand wind power variability and its impact on their system. Results reported in this thesis are intended to help system operators understand the variability of large penetrations of wind power and how it affects their systems. Chapters 2 and 3 presented new methods to better characterize wind power variability and estimate its cost to a system. Chapter 4 estimated how wind power variability affects wind power's ability to displace emissions. Finally, we also discuss the implications of our results for policy makers and identify further work that should be completed.

5.1 Summary of Results

Chapter 2 presented a metric that better characterizes the variability of large penetrations of wind power. The variability of twenty interconnected wind plants is less than that of twenty individual wind plants when measured in the frequency domain with power spectrum analyses. We showed for the first time the reductions in variability that occur from interconnecting wind plants result from the spectrum of wind power departing from a Kolmogorov spectrum. The amount of smoothing (or departure from a Kolmogorov spectrum) is a predictable function of frequency, correlation coefficient, nameplate capacity ratio, and the number of interconnected wind plants. Reductions in variability diminish as more wind plants are interconnected as only 4 wind plants need to be interconnected to achieve 87% of the reductions in variability produced by interconnecting 20 wind plants. Yearly wind power production is likely to vary, and have year-to-year variations about half that observed nationally for hydropower.

Chapter 3 presented a cost metric capable of estimating the variability cost of individual wind plants and valuing reductions in power variability. The cost metric divided the energy produced by a wind plant into hourly energy components and 15-minute load following energy and capacity components. In order to create an unbiased metric, each hourly energy component was set at a level that minimized the cost of the four 15-minute load following components.

Wind plants with higher capacity factors have lower variability costs (roughly half of lower capacity factor wind plants) and cost a system less to integrate. In 2008, the mean variability cost for 20 wind plants in ERCOT was $8.73 per MWh with a standard deviation of $1.26 per MWh. In 2009, the mean variability cost was $3.90 per MWh with a standard deviation of $0.52 per MWh. The substantial reduction in cost was largely due to decreased ancillary service prices (natural gas prices declined significantly in 2009). The relative ranking of wind plants based on variability costs is dependent on the wind power produced from the wind plants and not on ancillary service prices. Interconnecting 20 wind plants reduced the variability costs of ERCOT's 20 wind plants by approximately half (a mean savings of $3.76 per MWh).

Chapter 4 presented a wind + gas baseload power plant model that estimated how effective wind power is at displacing CO_2 and NO_x emissions. Carbon dioxide emissions reductions from a wind (or solar PV) plus natural gas system are likely to be 75-80% of those presently assumed by policy makers. Using multiple generators improves the CO_2 emission efficiency of a wind + gas system by 3-15% for wind penetration levels of 5 to 95%. Nitrous oxide reduction from such a system depends strongly on the type of NO_x control and how it is dispatched. For the best system we examined, NO_x reductions with 20% wind or solar PV penetrations are 30-50% of those expected. For the worst, emissions are increased by 2-4 times the expected reductions with a 20% RPS using wind or solar PV.

5.2 Future Work

The methods and results presented in Chapters 2-4 have answered many questions but have left a few unanswered that should be resolved by future research in this field. In Chapter 2, we observed a difference between using real wind power data versus simulated wind power data in the frequency domain. The PSD of forty interconnected modeled 1.5 MW GE turbines located throughout the Great Plains and Midwest did not depart from a Kolmogorov spectrum as the PSD of twenty interconnected wind plants did. It is important to resolve this discrepancy because wind integration studies rely on simulated wind power data and their results may be inaccurate if simulated wind power data does not behave in the same manner as real wind power data.

The methods presented in Chapter 2 should be applied to a system's net variability (wind + load variability). It is unclear how wind power and load interact and Chapter 2 provides a method for system operators to measure how their net variability changes as more wind power is added. In the wind industry many believe a system's net variability will be less variable than its wind power due to the interaction of wind power with load. The methods presented in Chapter 2 are ideally suited to answer this question.

In addition, researchers or system analysts should estimate and model the departures from a Kolmogorov spectrum for the following cases:

- Wind plants spread over a larger area than west Texas
- Net wind power capacities greater than the 1 GW
- Wind power located in different regions

By doing so, system operators can obtain a better understanding of how wind plant correlation coefficients, capacities, and location determine their systems net wind power variability.

In addition, the slope at which the magnitude of a system's wind power PSD depends on frequency (defined as β in Chapter 2) is a better metric to define wind power variability than current metrics (such as energy or capacity penetration levels). For example, in Chapter 2 we analyzed 1

GW of wind power capacity in ERCOT and 1.5 GW of wind power capacity in BPA in 2008. Even though BPA had a greater amount of wind power capacity, we observed BPA had a β greater than ERCOT, indicating BPA's wind power is more variable than ERCOT's wind power[9]. As a result, system planning and operation charts should be developed where a system can determine how ancillary service requirements, generation capacity levels, and ramp rate resources are needed for given β levels of wind energy. System planners would then have a better idea of how much wind power to build and where to build it to achieve the least adverse affect on their systems.

In Chapter 3, regulation costs were not estimated due to a lack of high time-resolution wind power data sets. In addition, forecast error and unit-commitment costs were not estimated. Future work should expand our cost metric to estimate how much regulation, unit commitment, and forecast error add to a wind plant's integration costs. The resulting cost estimates should be compared to the results of the large integration studies to ensure the cost metric produces similar results.

In Chapter 4, the baseload wind + gas power plant model indicated variability adversely affects the emission efficiency of fossil-fuel generators but a more extensive analysis of the emissions performance of a system's generator fleet needs to be completed in order to have a clear picture of how wind power will displace emissions, particularly NO_x and SO_x emissions. If a more detailed study is undertaken, how the type of generator and the type of NO_x mitigation technology affects the results of NO_x emission displacement should be examined. The results of such an analysis can be used to provide a more accurate method to estimate the emissions displaced by wind power. In addition, system operators could identify dispatch scenarios that maximize the displacement of NO_x emissions.

---

[9] This is because all of BPA's wind plants are located in the Columbia River Gorge and their outputs are likely highly correlated with each other.

Finally, gas turbine manufactures should investigate creating a generator(s) suited to compensate for wind power variability. The generator would have better emissions efficiencies over larger power and ramp rate ranges. This could possibly be achieved easily through the utilization of firing modes not commonly used in today's gas turbines or it could be more complicated and require redesigning combustion chambers. A potential market could develop in the next decade for such a technology when the aggressive growth of wind energy begins could conflict with stricter generator emission limits.

5.3 Policy Implications

Wind plants pose two problems to system operators. The first is they are a variable source of power and system operators have been going through great efforts to determine how they will integrate significant penetrations of variable power. The second is the best wind sites are primarily located far from load centers in areas with little to no transmission capacity. System operators are currently analyzing if they should construct billions of dollars worth of long transmissions lines to encourage wind plant development in wind rich regions.

Electricity systems will not be able to mitigate wind power variability simply by interconnecting more wind plants to their system. It is true a system of interconnected wind plants exhibit less variability than the individual wind plants it is composed of, but the majority (~87%) of the reductions in variability are achieved by interconnecting 4 to 6 wind plants together. All but one of the electricity systems in the United States currently have more than 6 wind plants interconnected to each of their systems (the southeast is the exception). As a result, there will likely be little benefit, in terms of mitigating wind power variability, in interconnecting additional wind plants. This is true from a cost perspective as well.

Additionally, we have provided system operators with a regression model capable of estimating how much their wind power variability is reduced as their future penetration of wind energy increases. By better understanding how the variability injected into their system changes as more wind plants are built, system operators can better understand what assets they will need to have to compensate for the injected variability.

The benefit of interconnecting distant wind plants is adding higher capacity factor wind plants to a system. Higher capacity factor wind plants are more profitable and they cost a system less to integrate. But transmission lines are expensive while wind integration costs are not. The reductions in wind power variability, from a system's cost perspective, are not enough to justify significant investments in transmission lines. For example, ERCOT would be willing to extend a transmission line a maximum of 2 miles based on the benefit an additional wind plant would provide in reducing ERCOT's wind integration costs. Based on this, system operators should determine if it is better to incentivize the development of wind plants in poor wind resource areas located close to load centers instead of building long transmission lines to encourage the development of wind plants in wind rich resource areas.

System operators will have to decide if they want to recover wind integration costs ex-ante or ex-post. By recovering integration costs ex-ante, systems can provide wind plants with more certainty on how much they will have to pay over the course of a year. Wind plants could also pay more or less than what it actually cost to integrate their power into a system. By recovering costs ex-post, wind plants will pay each year what it actually cost to integrate their power into a system. Unfortunately, doing so would inject a significant amount of uncertainty would into wind plant financial pro formas and would make it harder for wind plants to obtain financing.

As a result, if electricity systems follow the precedent set by BPA and recover integration costs of wind power through tariffs levied on wind plants, they should consider a capacity factor based tariff indexed to the price of electricity that recovers integration costs ex-ante. Systems should offer a reduced tariff to wind plants that actively mitigate their variability to encourage the development of market based solutions. If system planners can identify wind plants in their interconnection queues with the highest capacity factors they could take an active approach to decrease their integration costs by giving priority to these projects. Wind plants should also be given priority in the interconnection process if they implement flexible technologies to mitigate their variability costs.

Finally, the results shown in Chapter 4 indicate that at large scale variable renewable generators may require that careful attention be paid to the emissions of compensating generators to minimize additional pollution. If careful attention is not paid, emission allowance prices could increase substantially. Finally, on a time scale compatible with RPS implementation, design and market introduction of generators that are more appropriate from an emissions viewpoint to pair with variable renewable power plants may be feasible.